IMPROVING FLOW STRUCTURE AND NATURAL CONVECTION WITHIN FIN SPACINGS OF PLATE FIN HEAT SINKS

A THESIS SUBMITTED TO
GRADUATE SCHOOL OF NATURAL AND APPLIED SCIENCES
OF
MIDDLE EAST TECHNICAL UNIVERSITY

BY

MEHMET ERDEM ÖZET

IN PARTIAL FULFILLMENT OF THE REQUIREMENTS
FOR
THE DEGREE OF MASTER OF SCIENCE
IN
MECHANICAL ENGINEERING

SEPTEMBER 2015

Approval of the thesis:

IMPROVING FLOW STRUCTURE AND NATURAL CONVECTION WITHIN FIN SPACINGS OF PLATE FIN HEAT SINKS

submitted by **MEHMET ERDEM ÖZET** in partial fulfillment of the requirements for the degree of **Master of Science in Mechanical Engineering Department, Middle East Technical University** by,

Prof. Dr. M. Gülbin Dural Ünver _____
Dean, Graduate School of **Natural and Applied Sciences**

Prof. Dr. R. Tuna Balkan _____
Head of Department, **Mechanical Engineering**

Assoc. Prof. Dr. İlker Tarı _____
Supervisor, **Mechanical Engineering Dept., METU**

Examining Committee Members

Assoc.Prof. Dr. Almıla Güvenç Yazıcıoğlu _____
Mechanical Engineering Dept., METU

Assoc. Prof. Dr. İlker Tarı _____
Mechanical Engineering Dept., METU

Asst. Prof. Dr. F. Nazlı Dönmezer Akgün _____
Mechanical Engineering Dept., METU

Asst.Prof. Dr. Özgür Bayer _____
Mechanical Engineering Dept., METU

Assoc. Prof. Dr. Cemil Kocar _____
Nuclear Engineering Dept., Hacettepe University

Date: 07.09.2015

I hereby declare that all information in this document has been obtained and presented in accordance with academic rules and ethical conduct. I also declare that, as required by these rules and conduct, I have fully cited and referenced all material and results that are not original to this work.

Name, Last name: Mehmet Erdem Özet

Signature:

ABSTRACT

IMPROVING FLOW STRUCTURE AND NATURAL CONVECTION WITHIN FIN SPACINGS OF PLATE FIN HEAT SINKS

Özet, Mehmet Erdem
M.S., Department of Mechanical Engineering
Supervisor: Assoc. Prof. Dr. İlker Tarı
September 2015, 134 Pages

The main objectives of this thesis are to numerically investigate the previously observed recirculation zones and longitudinal vortices that occur in low fin height plate finned horizontal heat sinks and to improve the flow structures and heat transfer in these zones using various approaches with the help of simulations performed using commercially available CFD software. The approaches used for improvements are replacing the outer most fins with higher ones, introducing gaps on the length of the fins in various patterns, and introducing interstitial fins of different shapes within the channels among the plate fins. Starting with a validated model of the original low height plate fin heat sink and making the geometric modifications without altering the solution strategy, newer models that do not require experimental validation are obtained. The original model and the newer models are used in a series of simulations with related parametric analyses. The performances of the newly introduced heat sink geometries are compared with the performance of the original low height plate fin heat sink using the simulation results. Among these alternatives the one performing the best is selected as an optimal solution to the recirculating flow problem observed in the low height plate fins.

Keywords: Natural Convection, Horizontal Plate Finned Heat Sink, Computational Fluid Dynamics, Flow Improvement

ÖZ

PLAKA TİPİ ISI ATICILARDA AKIŞ YAPISININ VE DOĞAL TAŞINIMIN ARTTIRILMASI

Özet, Mehmet Erdem
Yüksek Lisans, Makina Mühendisliği Bölümü
Tez Yöneticisi: Doç. Dr. İlker Tarı
Eylül 2015, 134 Sayfa

Bu tezin amaçları, önceki çalışmalardaki kısa kanatçıklı plaka tipi ısı atıcılarda görülen resirkülasyon bölgeleri ve boylamsal girdapları numerik yöntemler ile incelemek ve akış yapısı ile ısı transferini çeşitli yaklaşımlarla, ticari bir Hesaplamalı Akışkanlar Dinamiği yazılımı ile artırmaya çalışmaktır. İyileştirme için yapılan yaklaşımlar: dıştaki kanatçıkları yükseltmek, kanatçıklar boyunca çeşitli şekillerde boşluklar oluşturmak ve kanatçıkların arasındaki kanallara çeşitli şekillerde başka kanatçıklar yerleştirmektir. Daha önceden doğrulanmış orijinal kısa kanatçıklı plaka tipi ısı atıcı modelinde, çözüm stratejisini değiştirmeden ısı atıcı geometrisinde geometrik değişimler yapılmış ve deneysel doğrulamaya ihtiyaç duymayan yeni modeller oluşturulmuştur. Orijinal model ve yeni oluşturulan modeller ilgili parametrik analizler ile simulasyonlarda kullanılmıştır. Yeni oluşturulan ısı atıcıların performansları, orijinal modelin performansları ile simulasyon sonuçları kullanılarak karşılaştırılmıştır. Oluşturulan bu alternatifler arasında, resirkülasyonlu akış yapısı görülen kısa plaka tipi kanatçıklara en uygun çözümü sunan model seçilmiştir.

Anahtar Kelimeler: Doğal Taşınım, Kanatçıklı Isı Atıcılar, Hesaplamalı Akışkanlar Dinamiği, Akış Arttırımı

To my parents

Gülsüm Özet

Ahmet Özet

ACKNOWLEDGEMENTS

I would like to thank to Assoc. Prof Dr. İlker Tarı for his endless support and encouragement.

I would like to thank Aydan for her support and love.

I also would like to express my gratitudes to my parents Gülsüm Özet and Ahmet Özet for their belief in me.

TABLE OF CONTENTS

LIST OF TABLES

TABLES

LIST OF FIGURES

FIGURES

LIST OF SYMBOLS

A	Area, m^2
A_b	Base Area, m^2
A_{wet}	Wet Area, m^2
d	Base plate thickness, m
Gr	Grashof number
h	Convection heat transfer coefficient, $W/(m^2K)$
H	Fin height, m
L	Fin length, m
m_{fins}	Mass of the fins, kg
$m_{Heat\ Sink}$	Mass of the heat sink, kg
N	Number of fins
Nu	Nusselt number
q''	Total heat flux rate, W/m^2
q''_{conv}	Convection heat flux, W/m^2
q''_{rad}	Radiation heat flux, W/m^2
Q_{conv}	Convection heat transfer rate, W
Q_{in}	Heater input power, W
Q_{rad}	Radiation heat transfer rate, W
Q_{Total}	Total heat transfer rate, W
Ra	Rayleigh number
S	Fin spacing, m
S_{opt}	Optimum Fin Spacing, m
t	Fin thickness, m
T_{mean}	Average temperature, ºC
W	Heat Sink width, m

CHAPTER 1

INTRODUCTION

1.1 Motivation

Heat dissipation in electronics cooling is an important issue. Generated heat by the electronic components needs to be managed, because the unwanted heat may decrease the system performance or may cause the failure of the system. Approximately 55% of the failures in electronic devices are related to thermal management problems [1] .

The performance of electronics is dependent on the processor speed. However the more processing tends to increase the heat generated by the electronics. In order to maintain a reliable operation, heat has to be rejected out of the system in an efficient way.

Although many systems are cooled via forced convection systems since they offer higher heat dissipation rates, natural convection cooling has many advantages. Main ones are; it requires lower weight and less space compared to forced convection heat transfer. In addition, forced convection heat transfer is more complex, more expensive and less reliable compared to natural convection heat transfer.

To improve the heat dissipation rates by natural convection cooling that is inherently low due to lower heat transfer coefficients, enhanced surfaces are being used. Using fins is one of the easiest ways of enhancing the heat transfer. It is well known that increasing wet area leads to higher heat dissipation rates. Rectangular plate fins are

the most popular ones because of their ease of manufacture, high effectiveness and simplicity.

There are two main orientations for using the Rectangular Plate Finned Heat Sink which are the vertical orientation and the horizontal orientation. Although many studies showed that the vertical orientation is more effective than the horizontal orientation in most of the cases, sometimes it is necessary to use the horizontal orientation due to the design constraints. Therefore studies have to be performed for improving the efficiency of the horizontal heat sinks as well as the vertical heat sinks.

The efficiency of a heat sink depends on many parameters. One of the important measures affected from these parameters is the flow characteristics in the heat sink. There have been many studies conducted in this area observing flow characteristics as explained in Section 1.2. Recirculating-flow zones have been reported in many of these studies. Within the recirculation zones, local heat flux reduces and the overall heat transfer performance of the heat sink is negatively affected.

The miniaturization is the trend in electronic design for solving space and weight problems such as the ones in aerospace applications. Thermal design problem needs to be on the same way as the electronic design since thermal design is one of the factors of limiting the packaging of the design. For this reason the motivation of this study is to try different methods to regulate the flow in low height heat sink and examine their effect on flow and heat transfer characteristics.

1.2 Literature survey

There has been plenty of work conducted on the subject of horizontal heat sinks. Elenbaas conducted experimental studies [2] within the subject of Free Convection with channels and plates in experimental and semi empirical basis.

Starner and McManus [3] have done experimental work on free convection heat transfer from Rectangular Fin Arrays in 1962. They used four different sets of heat sinks. The dimensions of the heat sink are given in Table 1 and an illustration of heat sink and dimension parameters is given in Figure 1.

Table 1 Starner-McManus Experimental Cases [3]

Set No	L (in)	W (in)	H (in)	S (in)	T (in)	N
1	10.0	5.0	0.5	0.25	0.040	17
2	10.0	5.0	1.5	0.25	0.040	17
3	10.0	5.0	0.25	0.25	0.040	17
4	10.0	5.0	1.00	0.313	0.040	14

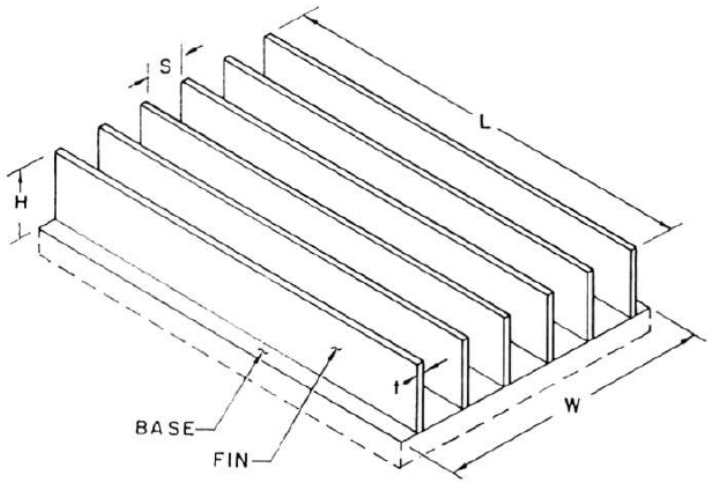

Figure 1 Fin Array Configuration of Starner –McManus [3]

Three different orientations had been examined; vertical, 45 degrees, and horizontal. For the horizontal configuration it was observed as in Figure 2, Set 3 yielded the higher heat transfer coefficients. Also it has been observed that for the ends closed case it did not differ from the ends open case. However for set 2, preventing the end flow reduced heat transfer rate by 50%. In set 2 they observed an up-down flow pattern in the heat sink as in Figure 3.

They resulted that vertical orientation is better for best heat transfer rate for parallel plate finned heat sinks. The heat transfer rate depends greatly on the geometry of the heat sink. Also, for horizontal heat sink configuration the end flow affects the heat transfer rate strongly.

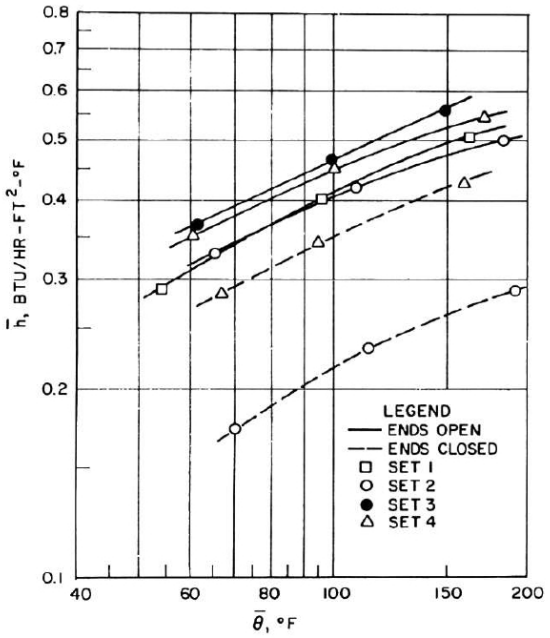

Figure 2 Average Convection Coefficients as a Function of Temperature Difference - Horizontal Case [3]

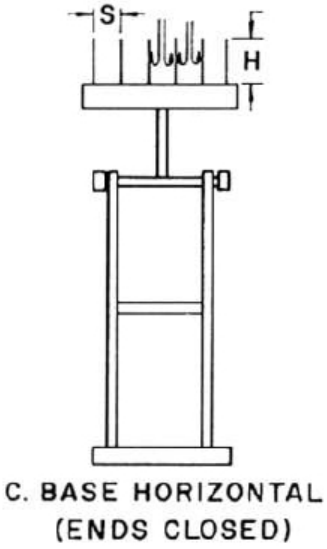

Figure 3 Up-Down Flow Illustration [3]

Another experimental work which has been done by Harahap and McManus [4] . In this work two different sets of Horizontal Rectangular Fin Arrays had been used.

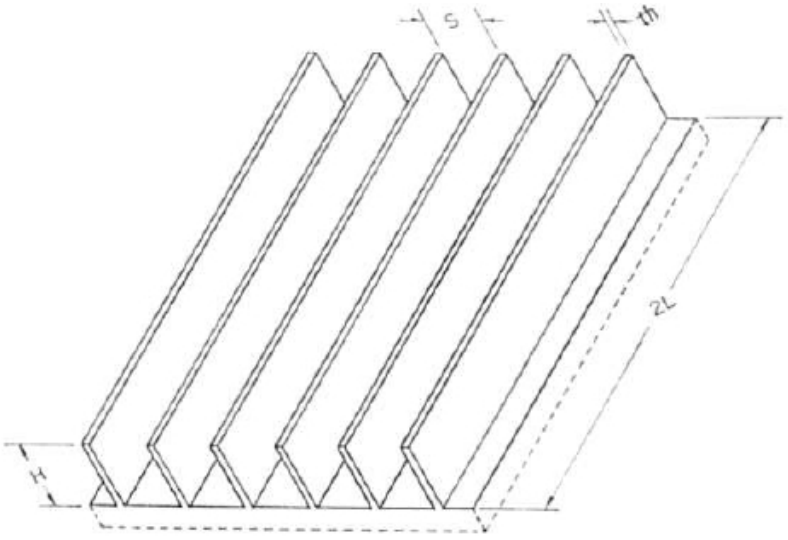

Figure 4 Fin-Array Configuration [4]

Table 1(a) Dimensions of fin arrays (2L5-series)

Set No.	2L, in.	H, in.	S, in.	th, in.	n
I-2L5	5.0	0.250	0.250	0.050	33
II-2L5	5.0	0.500	0.250	0.050	32
III-2L5	5.0	1.500	0.250	0.050	33
IV-2L5	5.0	1.000	0.313	0.050	28

Table 1(b) Dimensions of fin arrays from (5) (2L10-series)

Set No.	2L, in.	H, in.	S, in.	th, in.	n
I-2L10	10.0	0.250	0.250	0.040	17
II-2L10	10.0	0.500	0.250	0.040	17
III-2L10	10.0	1.500	0.250	0.040	17
IV-2L10	10.0	1.000	0.313	0.040	14

Figure 5 Dimensions of Sets [4]

In this study flow visualization has been performed via smoke injection. The findings about the flow pattern are as follows. The main observation was there were three different types of flow from the heat sink.

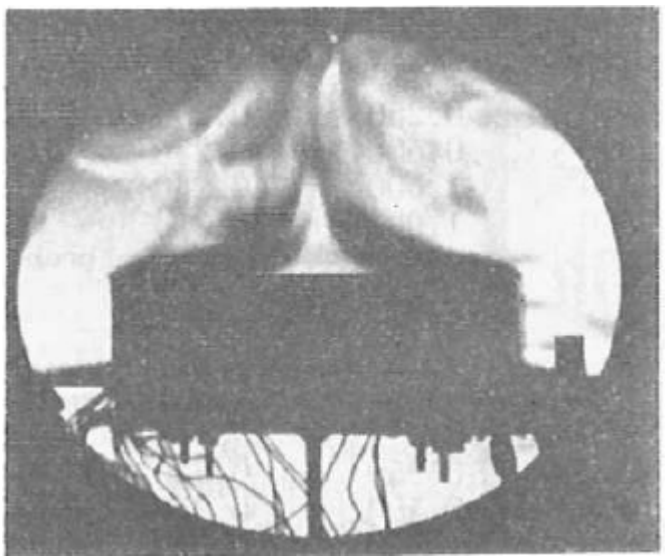

Figure 6 Partial schlieren of fhe single chimney flow. Horizontal knife edge; set III-2L5, power input: 92.0 watts. [4]

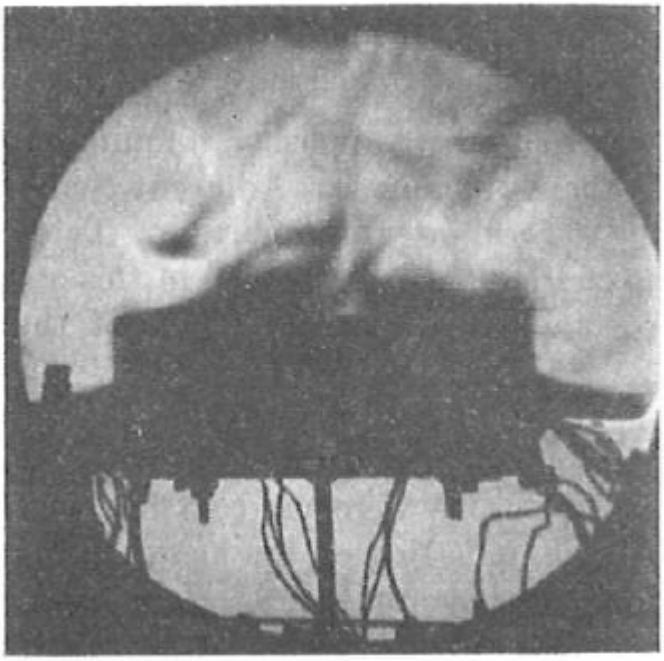

Figure 7 Partial schlieren of the single chimney flow. Horizontal knife edge; set IV-2L5, power input: 84.0 watts.[4]

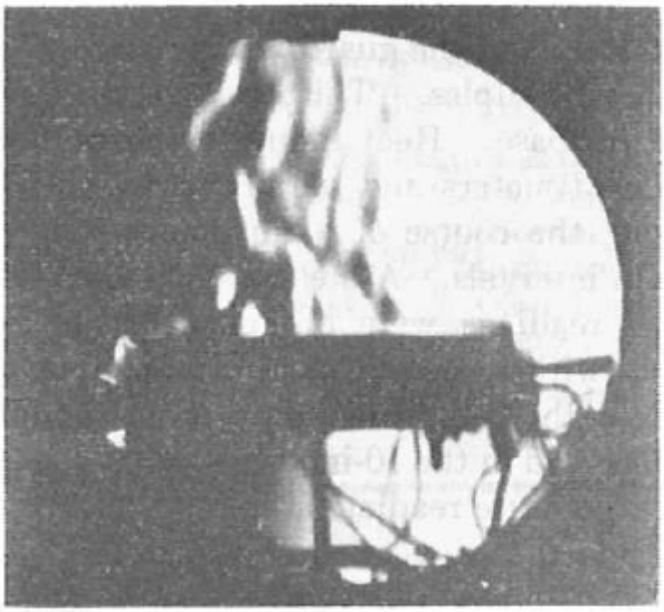

Figure 8 Partial schlieren of the sliding chimney strip flow.Vertical knife edge; set II-2L5, power input: 42.0 watts.[4]

Figure 6 shows a typical single chimney flow the flow from each side coalesces in the middle to form a single chimney. Area below the chimney had been investigated and resulted that it occupies recirculation zone the air in this region was seen to be long residency. Figure 7 shows the case IV-2L5 which has a disturbed chimney flow. With further lowering of the fin height, as was the case with the shallow sets I-2L5 and II-2L5 the single chimney broke into several smaller chimneys. These chimney strips were observed to be sliding back and forth along the longitudinal direction. Figure 8 shows the chimney strip flow associated with set II-2L5. This flow pattern had been explained in [4] as, since the low fin height reduces the mass flow rate entering into the channel, fluid become sufficiently heated for upward flow in the channels before coming to middle of the heat sink.

The results show that single chimney flow governed cases posses higher heat dissipation rates and sliding chimney flow cases has low performance heat transfer

characteristics. Also Harahap and McManus [4] proposed a correlation for Nu for the cases which they had conducted experiments.

Jones and Smith [5] conducted an experimental study for further analysis. The fin temperature has been assumed as constant and the length of the fins is not a variable in the experimental analysis. They proposed a simpler correlation for the heat transfer and investigated optimum fin spacing of the fins case. By the correlation, Fin Spacing has been suggested as the prime geometric variable.

Fitzroy [6] conducted a study to examine the effects of fin spacing for the maximum rate of natural convection heat transfer from vertically placed fins in the laminar flow regime. A correlation has been found which relates the ratio of average heat transfer coefficient based on fin spacing to vertical heat transfer heat coefficient.

Mobedi and Yüncü [7] conducted a numerical study which involves code development for solving Navier-Stokes equations using vorticity-vector potential approach. The flow mechanism has been investigated and effects of the geometrical parameters on heat transfer coefficient have been determined. Fin spacing has found to have significant effect on the type of flow and heat transfer coefficient. According to this study fin height did not have a significant effect on heat transfer besides increasing H leads to increasing of the heat transfer area. Two different flow has been observed in narrow fin spacing air enters from open ends moves along the channel and flows out from the central portion of the channel. In this type of flow velocity component through the fin spacing is negligible and flow is two dimensional. In wide fin spacing, air can also enter into the channel from middle part between the fins, turn 180 degrees at the base and move upward along fin height.

Anbar and Yüncü [8] conducted an experimental study on horizontal heat sinks with 15 different sets with varying fin geometries also Q_{in} is a parameter in the study. They found out that for a specific Q_{in} there is an optimum H and S value for

maximizing heat transfer. A correlation was proposed with a function of H, S and N values.

Baskaya et al. [9] conducted a numerical study on horizontal rectangular fin arrays. It has been concluded only changing two parameters on heat sink design does not provide optimum results. Every geometric parameter has an effect on heat transfer performance. The main findings were heat transfer increases with increasing H, and decreasing L hence H/L. In addition S_{opt} for different configurations has been obtained.

Suryawanshi et al. [10] conducted an experimental study in unconventional way. In the heat sink configurations where single chimney flow pattern occurs; in the bottom middle section a stagnant zone occurs. This part does not contribute much to the heat transfer. For this reason they used notched fin arrays in order to force the flow to stagnant zones and enhance the heat transfer. Fin spacing, heater input, and percentage of area removed in the form of inverted notch are the parameters. Heat transfer coefficients rises up to 53% in notched fin arrays and single chimney flow pattern is retained in Notched Arrays with a wider chimney zone which has been thought to be the reason of heat transfer enhancement.

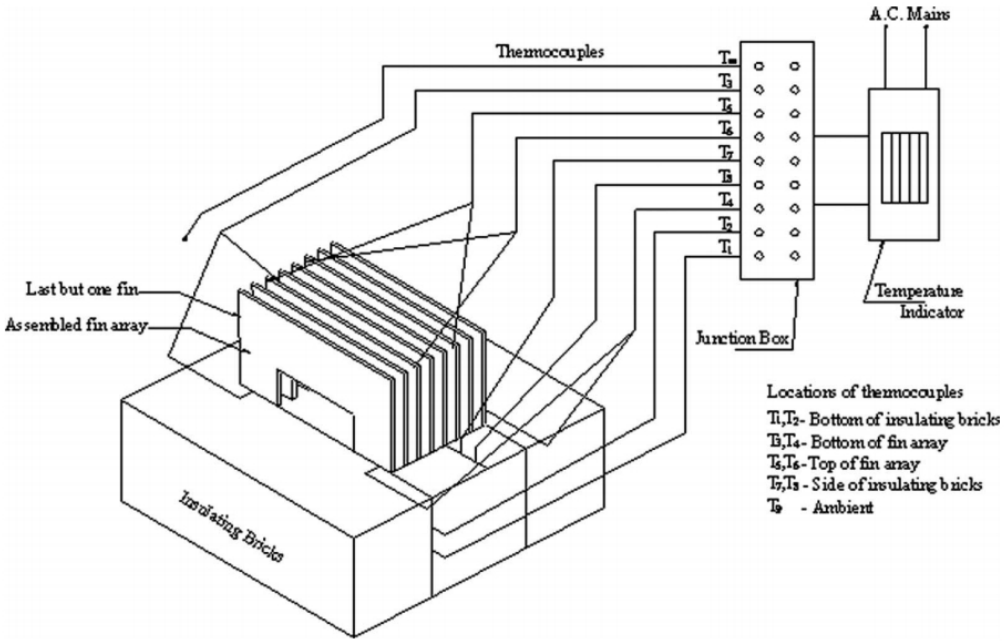

Figure 9 Experimental Setup with Notch Arrays of [10]

Wong and Huang [11] conducted a numerical study using the commercial software FLUENT. They have investigated 3 different lengths and variety of height and spacing. In this study they solved the horizontal plate finned heat sink problem on unsteady conditions and they have observed the heat transfer rate per unit base area Q/A_b decreases with increasing L and decreasing H. In this study flow has been taken as incompressible laminar flow and radiation has been ignored. The results of this study shows that increasing L tends to enhance oscillating sliding chimney flow where increasing S weakens it due to increasing mass flow rate in the channel. The time-averaged overall convection heat transfer coefficients are larger for high and short fin arrays, due to the stronger buoyancy and thinner boundary layers.

Huang et al. [12] conducted a numerical study. In this work base of the heat sink has been perforated in order to provide air flow to the stagnant zones of the heat sink. By this method the heat transfer coefficients has been observed to have been increased by a factor of 1.43-2.77 in this study.

Yalcin et al. [13] conducted a numerical study to examine the effects of shrouded fin arrays on heat transfer performance. The effects of clearance between fins and shroud, fin geometric parameters have been investigated. Optimum fin geometry and clearance between fins and shroud has been suggested.

Dogan et al. [14] conducted a numerical study to analyse the effect of various fin geometries on the heat transfer characteristics. They analyzed six different fin shapes in this study. The inspection of flow patterns and temperature contours has indicated that the most important factors affecting heat transfer coefficient are: the size of air flow inlet area of the fin channel, the size of the region through which heated air leaves the fin channel, and the presence of air recirculation regions of low velocity. This study shows that there are more advantageous fin shapes other than rectangular fins.

A numerical study has been conducted by Dialameh et al. [15] for horizontal rectangular plate finned heat sinks. Finite Volume Model solver has been used to solve flow and energy equations. The study has been done for short fin lengths of 128 different fin geometries. Two different kinds of flow has been observed; for the fin arrays with $H/L>0.24$ and $S/L<0.2$, air can only enters into the channel from the fin end regions. However, for lower values of $H/L<0.24$ and higher values of $S/L>0.2$, air can also enter into the channel from the middle parts between fins. For the second type of flow, heat transfer coefficient is smaller than the first one. From the study it has been seen that fin thickness does not affect the heat transfer characteristics considerably. Besides that, it has been shown that natural convection heat transfer coefficient increases with increasing temperature differences and fin spacings and decreases with fin length. For maximum heat transfer, optimum value of fin spacing was obtained to be $S=7mm$ for fin arrays with $H/L<0.24$. Based on all computations two correlations are proposed to predict average Nusselt number of an array of fins based on non-dimensional parameters, Ra, H/L, S/H and H/t, using the fin spacing as a characteristic dimension for two ranges of Ra number.

Dake and Majdalani [16] conducted an experimental study using different shapes of vortex generators for forced convection heat transfer in heat sinks. Their work was about examing the flow characteristics of vortex generators and they concluded that: the flat shape provides the most stable structure. The trapezoidal design induces the most oval shaped vortices with the spacing being a function of the width of the fin tip. The curved shape tends toward smaller faster rotating vortices with separating rotational centers. The double delta design provides the least productive vortices exhibiting small outer diameters and widely spaced centers. It has been proven in this study that vortices generated by a triangular vortex generator mounted at the entrance to a fin channel may be controlled as to the shape and fill characteristics of the channel. These parameters provide a means to potentially enhance the heat transfer from the heat sink fins to the surrounding air.

Yang et al. [17] conducted an experimental study on the performance of vortex generators in force cooled heat sinks. They concluded that the enhancement using VG mounted in a heat sink are relatively effective when the flow is in the developing region whereas they become quite ineffective in developed region especially when the fin pitch is small or operated at a lower frontal velocity. In summary of the results, it was concluded that augmentation via various fin patterns like interrupted or vortex generator is quite effective only at the developing region or at a large fin pitch(>1.8mm). The conventional enhanced fin patterns lose their superiority at the fully developed region of the flow.

Tari and Mehrtash [19] conducted a numerical study where they have conducted analyses for horizontal and inclined heat sinks. Correlations have been proposed for both cases. In this study they have observed longitudinal vortices and recirculating flow regions in low height plate finned heat sink. In Figure 11, speed contours above the baseplate of three different heat sink geometries can be seen. For the 5 mm fin height an X shaped flow had been reported where recirculating flow regions occurred.

1.3 Objective

The motivation of this study arises from another study conducted in the literature. In Tari and Mehrtash [19] , natural convection from horizontal and inclined plate finned heat sinks has been analysed by a commercially available CFD software and reported. Verification procedure has been done with number of correlations which arises from experimental studies in the literature. Geometry of the heat sink which is a conventional plate finned heat sink's geometry can be seen in Figure 10. The parameters that has been changed in [19] besides the orientation of the heat sink are listed as follows:

- 250 and 340 mm for the heat sink length *L,*
- 25, 50, 75, 100 and 125 W for the heat input *Qin*,
- 11, 12, 13, 14, 15, and 16 for the number of fins spanning the width
- corresponding to the fin spacing (*S*) values of 14.7, 13.09, 11.75, 10.62,
- 9.64, and 8.8 mm, respectively.
- 5, 15, and 25 mm for the fin height *H*.

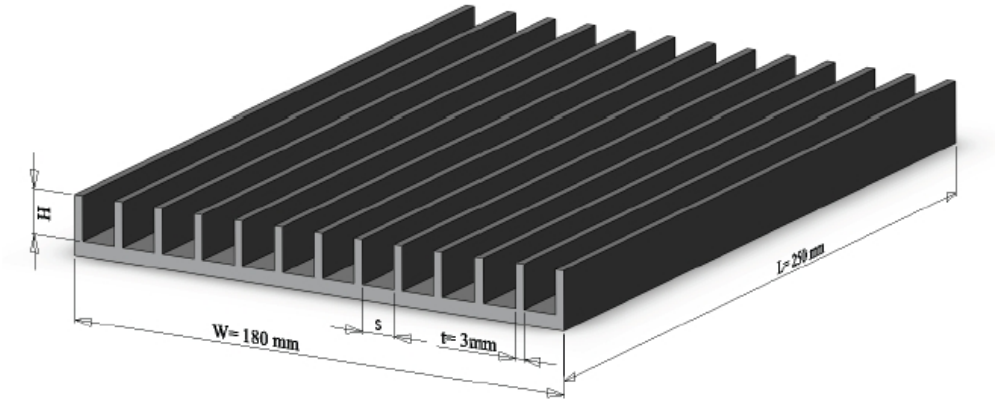

Figure 10 Heat Sink Model [19]

With the help of different configurations of heat sink analyses, correlations have been proposed which has been shown to be in good accordance with the other correlation in the literature. In addition, an observation related to low fin height horizontal plate fin heat sink with

- L=250 mm
- W=180 mm
- S=11.75 mm
- N=13
- Q_{in}=125 W

parameters had been made: in Figure 11: speed contours above 2 mm of the base plate can be seen for 3 horizontal plate finned heat sink with 3 different fin heights of H=25 mm, H=15 mm and H=5 mm can be seen. It was observed that flow in most of the parts for 5 mm height finned heat sink is stagnated before coming to the middle of the heat sink. In the middle channels, flow from the end of the fins can reach to the middle of the heat sink but the channels on the side of the heat sink did not have an effective flow. This situation leads to heat transfer inefficiency.

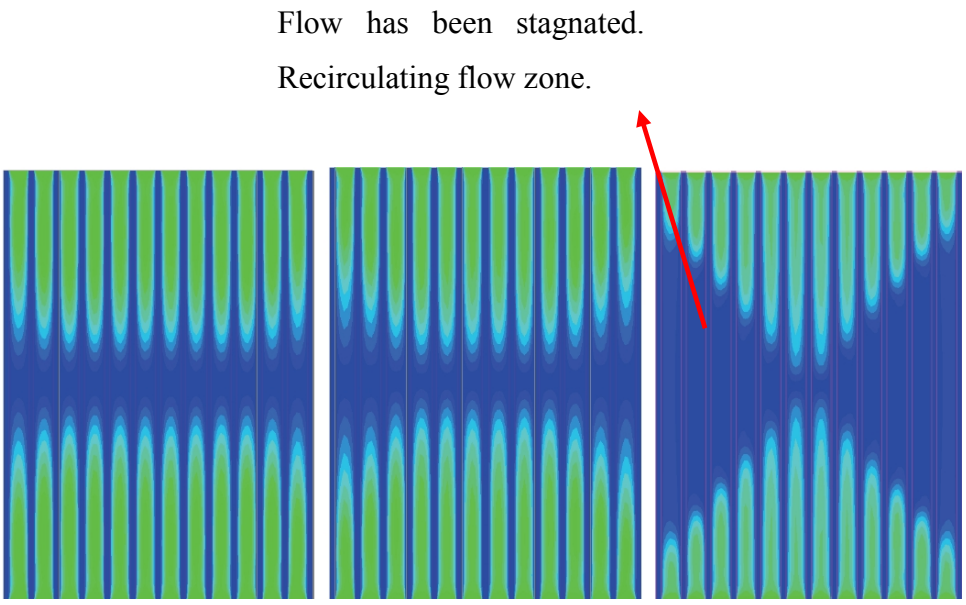

Figure 11 Speed contours for the upward facing horizontal heat sinks of 25, 15 and 5 mm fin heights (from left to right) for Q_{in}=125 W and L=250 mm, and S=11.75 mm, W=180 mm ,obtained at 2 mm above the baseplate surface. Vertical lines are the fins with 3 mm thickness. Darker colors (blue) show slower speeds [19]

Observation of Figure 12 also makes a good understanding of the flow situation in this case. This figure shows the chimney flow structures at the mid planes of the heat sink. The heat sink above which has 15 mm fin height appears to have regular buoyancy type of flow and therefore having single chimney structure. On the other hand the figure below which has 5mm fin height exhibits longitudinal vortices and this makes the buoyancy flow not to perform to dissipate the heat. The heat transfer rate is thought to be affected by this kind of flow and the objective of this thesis is to prevent the longitudinal vortices structured and recirculating flow zones to occur and by this way increasing the heat transfer rate of the heat sink.

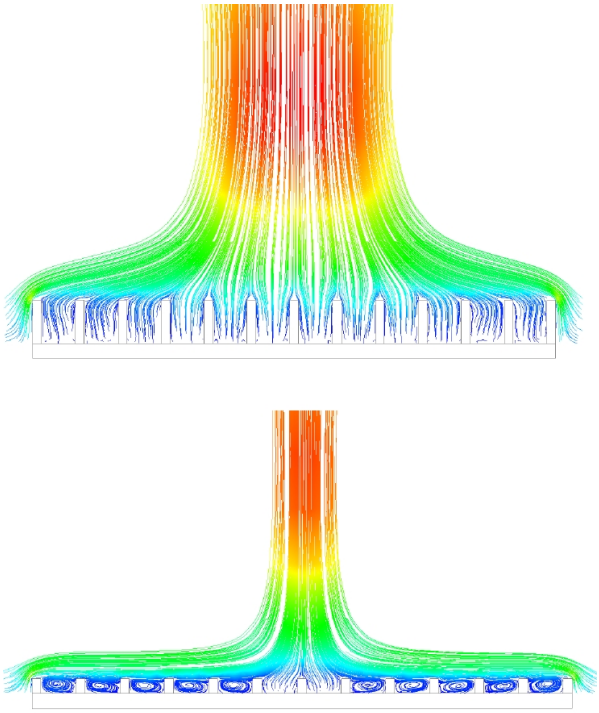

Figure 12 Chimney flow structures at the mid-planes of the upward facing horizontal heat sinks with 15mm and 5mm fin heights. Q_{in}=125 W, L=250 mm, and S=11.75 mm. [19]

Present study aims to analyze different methods and observe the effects on heat transfer of this special case. In the further chapters various methods which were assumed to regulate the flow will be explained. In this study mainly four different methods have been implemented to the model to regulate the flow.

- X Shaped Mixing Gaps Case
- Disturbance in Channels Case
- Middle Gap Case
- High End Fins Case

The results and explanations of these cases are explained in further chapters of this thesis.

CHAPTER 2

BASE CASE PROBLEM

This study's objective is to improve the flow pattern and heat transfer of the special case which Tari and Mehrtash observed in [19]. The numerical model which had been created by Tari and Mehrtash [19] had been verified by other correlations in the literature and experimental study of [20]. This study uses the same numerical model of [19] because of its verification and being in good accordance with the correlations in literature. Therefore in order to analyse different configurations of heat sink for this study; the first step should be modelling the exact case of [19]. In this chapter the definition of model properties will be given and reasoning behind these properties will be explained. Finally the created numerical model will be compared with the results of [19].This study has been done with the commercially available software ANSYS Icepak.

2.1 Model Setup

The same computational model which had been used in [18] and [19] has been used. The computational domain is 3000x3000x3000mm. The model is installed in a cube filled with air. The reason for using these dimensions is, in [18] an experimental study of [20] had been used for verification purposes. In order to simulate the laboratory conditions of [20], this domain had been used. Since a non-conformal mesh had been used for modelling of the problem, the room's computational cost is not so high due to the low mesh number of the coarse mesh domain.

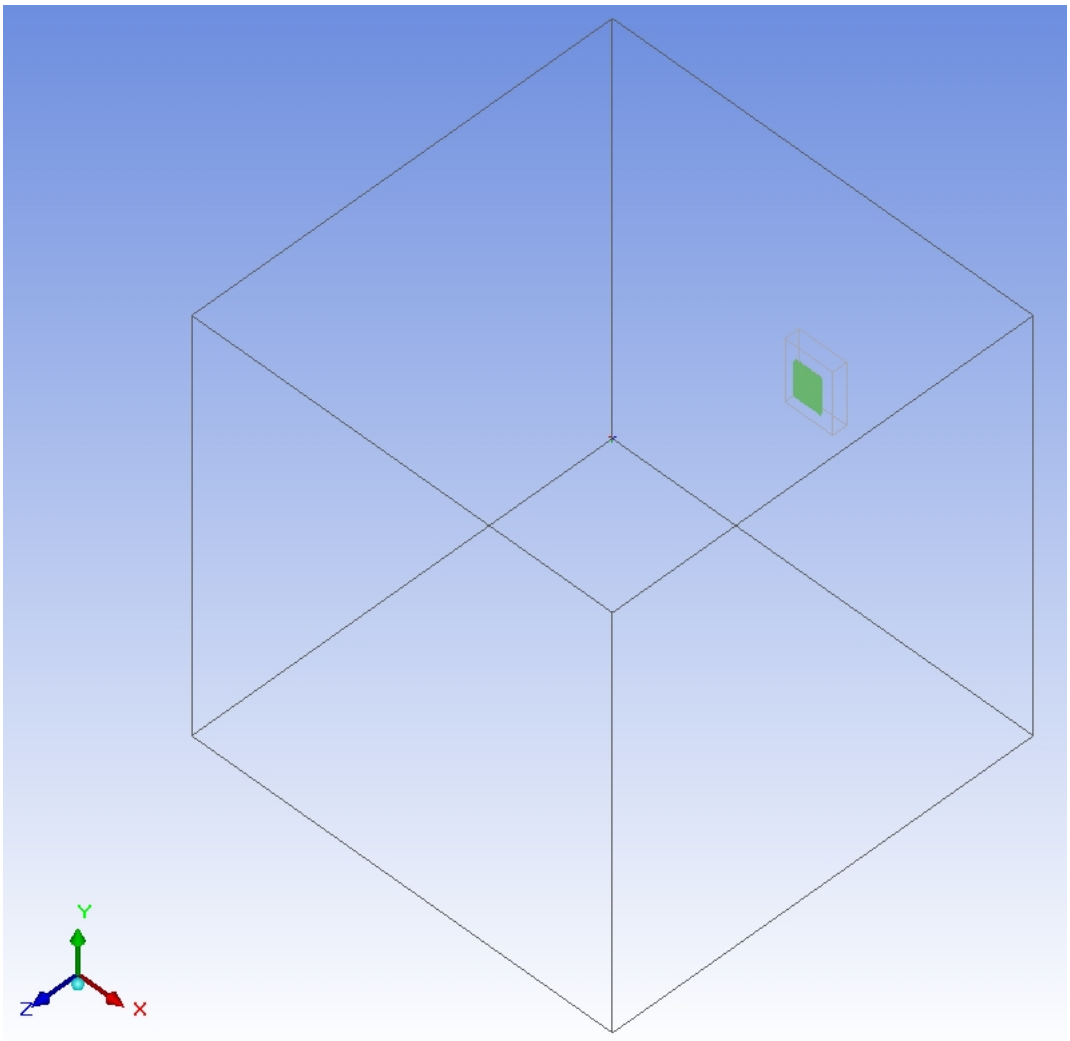

Figure 13 Entire Model (*g* is in –z direction)

The model consists of four different elements,

- Aerated Concrete Block
- Heater Plate
- Plate Finned Heat Sink
- Cabinet

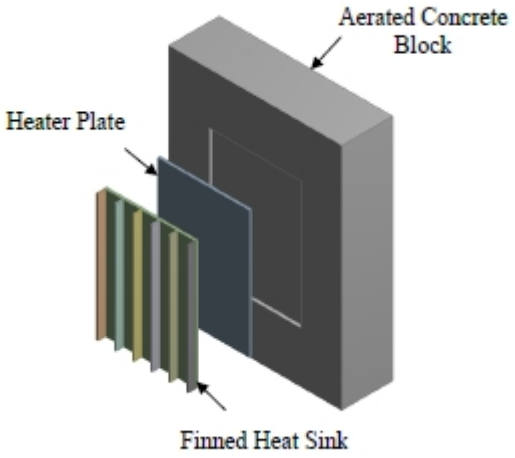

Figure 14 Schematic View of the Model [18]

Figure 14 shows the schematic of the model of cooling assembly installed in the cabinet. The heater plate is installed into the aerated block concrete. Heat sink is installed on the heater plate. This model has been created in [18] because verification of the study in [18] has been conducted with the experimental work of [20]. The experimental assembly of [20] can be seen in Figure 15. As it can be seen a heater plate is installed in an aerated concrete block and the heat sink is installed on top of it. The reason for installing heater plate into the aerated concrete block in [20] is to preserve the input power for the heat sink.

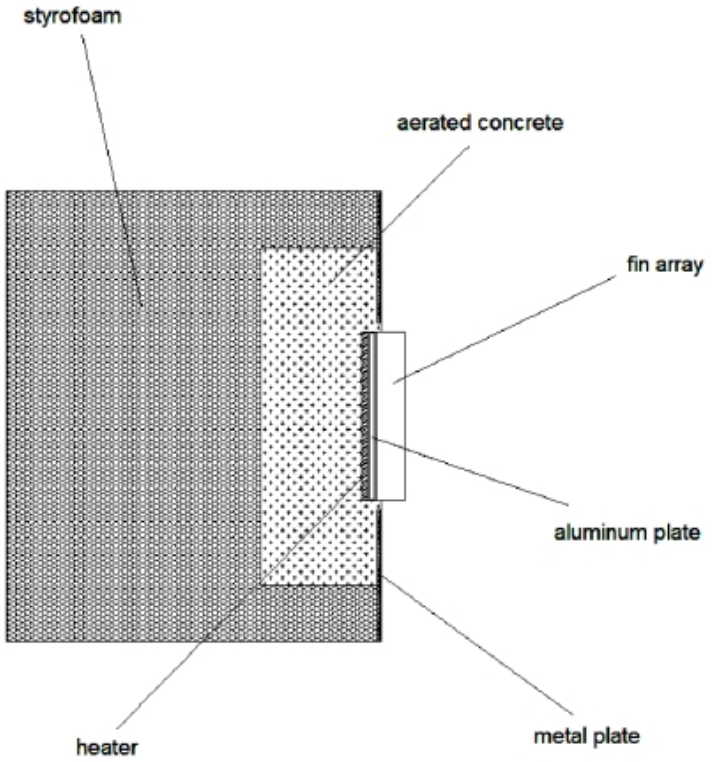

Figure 15 Experimental Assembly of [20]

Table 2: Dimensions of the models' elements

Dimensions (mm)	
Heater	180x250x5
Concrete Block	340x450x100
Heat Sink	180x250x5
Computational Domain (Cabinet)	3000x3000x3000

Throughout this study, the dimensions of the heat sinks will be the same as shown in Table 2 and Table 3 also the heater power is taken as constant as Q_{in}=125 W for simulating the case in [19] unless otherwise specified.

The case which identifies a conventional plate finned heat sink with the dimensions of Table 2 and Table 3 with Q_{in}=125 W will be named as "Base Case" throughout this study.

Table 3 Dimensions of the Heat Sink

Dimensions (mm)	
Fin Height (H)	5.00
Fin Length (L)	250
Fin Spacing (S)	11.75
Fin Thickness	3.00
Number of Fins	13
Width	180

2.2 Material Properties

The same materials of [18] have been used in this study. The material properties are given in Table 4.The materials of the model in [18] has been chosen in order to simulate the experimental study of [20]. In order to preserve the heat that is generated by the source, an aerated concrete block which has very low conductivity has been used. Aluminum has been used for the heater plate and heat sink because of high thermal conductivity properties despite its low emissivity. The radiation for the concrete block and heater plate has not been calculated therefore their emissivity values have been taken as zero.

Table 4 Material Properties of the Setup

Part Name	Material Type	Conductivity (W/m*K)	Specific Heat (J/kg*C)	Emissivity	Surface Roughness (mm)
Concrete Block	Aerated Concrete	0.15	1000	0.0	-
Heater Base Plate	Aluminum	130	900	0.0	-
Heat Sink	Aluminum	130	900	0.2	0.02

2.3 Meshing

One of the most important aspects of a CFD study is using an appropriate mesh. Too coarse meshing can make the solution inaccurate and too fine meshing may result in high computational cost. In this study non-conformal mesh had to be used because the domain is too large although the interest of the study occupies a small volume. Therefore non-conformal mesh had been used as in [19] in order to have accurate results in interest of study and lowering the computational effort.

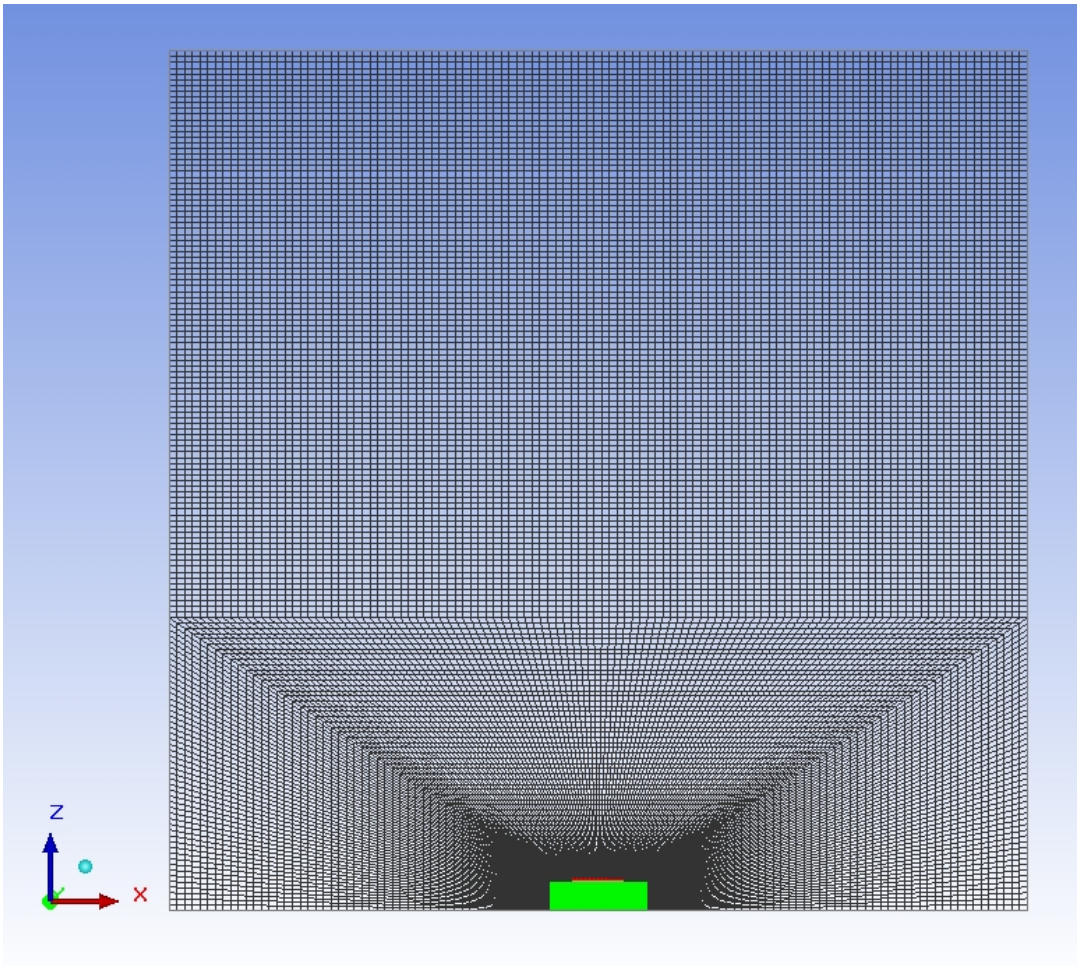

Figure 16 Mesh of entire domain; for the cooling assembly fine mesh has been used and for the domain coarse mesh has been used

Since the most important part of this study is to observe flow around and inside the heat sink, very fine mesh around the fins had been implemented in this study. This study involves flow pursuing around the fins in some cases. Therefore fine mesh is implemented on the fins with fluid interactions to have better boundary layer development. More detailed information can be obtained from Appendix A.

Mesh refinement studies had been conducted in [18,19]. Since this study uses the same model in [18,19], an additional mesh refinement study has not been done. In

[18,19] mesh with 1685832, 2834264 and 4077608 cells had been analyzed. And the mesh with 2834264 cells had been chosen because it yielded results matching to the finer mesh solution. Same mesh parameters of [18,19] have been used in this study. More detailed information about the mesh refinement can be found in [18].

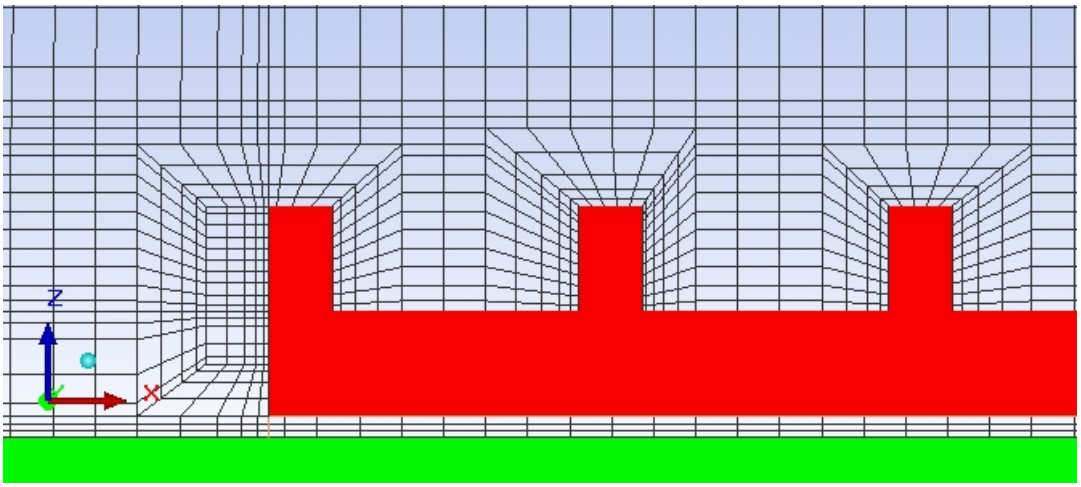

Figure 17 Finer mesh around fins gradual increase of mesh size around the fins can be seen in order to implement boundary layer development

2.4 Solver Details

Since a pre-verified model of [19] has been used in this study the solver details are the same as [19].

- Working fluid has been chosen as air at 20^{o}C. Since this study used the experimental study of [20] to validate the model air at room temperature had been chosen in [18].
- Flow regime has been assumed as turbulent and Zero Equation Turbulence Model has been used in this study. Since the flow structure that can be seen in Figure 12 shows longitudinal vortex structured flow characteristics; turbulent flow solver is appropriate for this study.

- The temperature of the walls of the cabinet has been set as constant at 20^{O}C.
- Radiation heat transfer is included and Surface to Surface model has been used. In heat transfer performance of the naturally cooled heat sinks radiation also plays an important role in heat transfer. Therefore radiation is included in this study.
- Ideal gas law has been assumed as the Gas Dynamics model and gravitational acceleration has been used as 9,80665 m/s^2 in –z direction. Since the temperature difference is high; using ideal gas law model instead of the boussinesq model has been advised.
- The cases are solved for steady state conditions.
- Contact resistances have been taken as zero.
- 2nd order discretization schemes have been chosen for Pressure, Momentum and Temperature in order to get more accurate results.
- Number of maximum iterations is 500.
- Under relaxation factors has been chosen as
    - Pressure 0.3
    - Momentum 0.3
    - Temperature 1.0
    - Viscosity 1.0
    - Body Forces 1.0
- Convergence Criteria has been chosen as follows
    - Flow 10^{-3}
    - Energy 10^{-7}

2.5 Verification of the used model

The model of [18,19] has been pre-verified with the experimental work of Yazicioglu [20] . Also as explained in [18] it has been verified with different Empirical Nusselt Number Correlations in literature via the Plate Model and Parallel Two Plates model. Therefore the CFD model that has been used in this study has been taken from a pre-verified model from [18] and in this case a separate verification has not been

conducted for this study since the same model has been used. More detailed information about the verification of the model can be found in [18].

The pre-verified model [18,19] analyses simple conventional plate finned heat sinks. In Icepak, creating simple conventional heat sinks is possible with "Create Heat Sink" command. This study analyses unconventional heat sink models therefore in this study "Create Heat Sink" GUI command has not been used. All of the heat sinks have been created by defining blocks. This situation led to minor result changes around 1% as it can be seen in Table 5.

Table 5 Comparison of This Study and Tari and Mehrtash [19]

Case	T_{mean} Heatsink Base (^oC)	Q_{rad} Heatsink (W)	Q_{Total} Heatsink into fluid (W)	Q_{conv} Heatsink (W)
Tari and Mehrtash [19]	173,17	26,53	95,60	69,07
Base Case	174,28	26,82	95,37	68,55
% Deviation	0,64%	1,12%	0,23%	0,76%

2.6 Governing Equations

The governing equations which will be solved by Finite Volume Method with ANSYS Icepak are given below.

The Conservation of Mass Equation:

$$\frac{\partial}{\partial} + \nabla.(\rho\vec{v}) = 0 \tag{1.1}$$

where ρ is the fluid density and $\vec{v}$ is velocity vector.

The Conservation of Momentum Equation

$$\frac{\partial}{\partial}(\rho\vec{v}) + \nabla.(\rho\vec{v}\vec{v}) = -\nabla \quad + \nabla.(\tilde{\tau}) + \rho\vec{g} + \vec{F} \tag{1.2}$$

Where $\tilde{\tau}$ is the stress tensor and $\vec{g}$ is the gravitational accelaration. $\vec{F}$ is the term that is defining the source terms that may be occur from the resistances, sources and etc..

$\tilde{\tau}$ can ben defined as:

$$\tilde{\tau} = \mu\left[(\nabla\vec{v} + \nabla\vec{v}^{T}) - \frac{2}{3}\nabla.\vec{v}I\right] \tag{1.3}$$

where μ is the dynamic viscosity of the fluid.

The Conservation of Energy Equation

$$\frac{\partial}{\partial}(\rho h) + \nabla.(\rho h\vec{v}) = \nabla.[(k + k_t)\nabla \ ] + S_h \tag{1.4}$$

Where h is the sensible enthalpy and S_h is the volumetric heat generation.

2.7 Results

The model was implemented for the case mentioned in the previous sections. The visualization of the simulation results can be seen in Figure 18. The same speed contours in Figure 11 (from [19]) were observed in the results of the re-created model, as it can be seen in Figure 18.

The numerical results of Base Case study described in this chapter can be seen in Table 6. Sample Calculations procedure can be found in Appendix B.

Table 6 Results of the Base Case

Case Name	T_{mean} Heatsink Base (°C)	Q_{Total} Heatsink into fluid (W)	Q_{rad} Heatsink (W)	Q_{conv} Heatsink (W)	q" (W/m²)	q" conv (W/m²)	q" rad (W/m²)
Base Case	174,28	95,37	26,82	68,55	1186,36	852,69	333,67

Blue Zones: Recirculating Flow Zones

Green Zones: Flow in Channels

Flow stagnation points in the channels

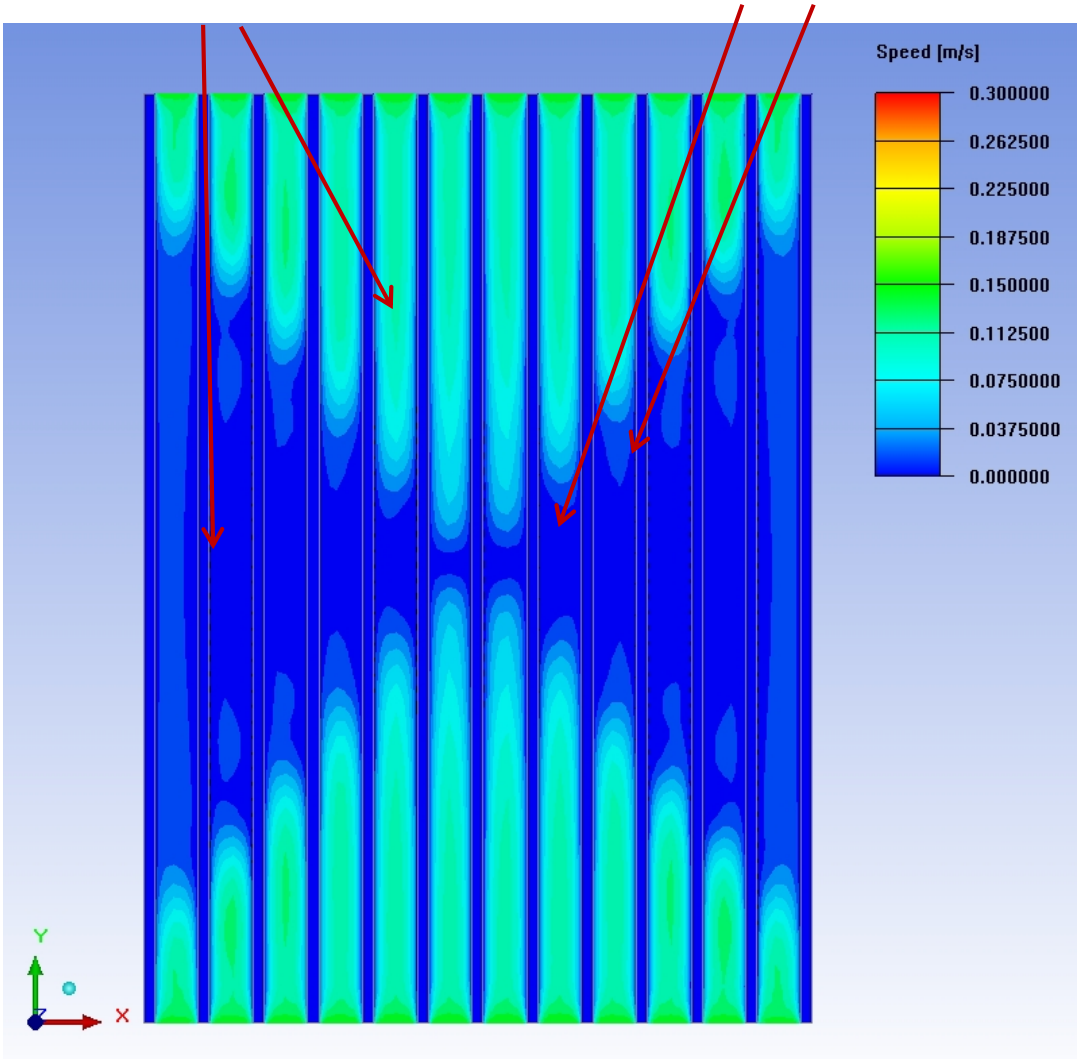

Figure 18 Speed Contours above 2 mm of the base plate of Base Case

Figure 18 shows the speed contours of Base Case. The discussion of this figure is important because this figure clearly explains the flow structure. Throughout this thesis comparison of different cases will be conducted based on this figure. The speed scale will be the same for all speed contour figures which will be minimum 0 and maximum 0.3 m/s. As it can be seen on Figure 18 the blue zones exhibit zero or very low speed values which means that the flow is mostly not present there. The points which the speed becomes zero or green contour turns blue mean that flow is stagnated in the channel. The blue zones will be called as recirculating flow zones because the air in those zones are recirculating slowly.

2.8 Radiation Heat Transfers of Elements

The used model assumes that concrete block does not radiate to its surroundings in [19] therefore this study follows the same approach. Since this study uses the pre-verified model of [19] it has to be identical. In addition, this study is about the heat transfer properties of the heat sink therefore there is no need to compute the radiation heat transfer of the concrete block. For these reasons the emissivity value of the concrete block has been taken as 0. The small differences between the results presented in Table 7 are due to slightly different mesh formed in the present study when the heat sink geometry is defined as a compound of individual plate fins and the heat sink base as opposed to the single heat sink block in Tari and Mehrtash [19]. The new geometry definition was necessary to make the further modifications and additions to the heat sink.

Table 7 Comparison of the results with both radiation settings

Case	T_{mean} Heatsink (^{O}C)	Q_{rad} Heatsink (W)	Q_{total} Heatsink (W)	Q_{rad} Concrete (W)
Ref [19]	173,17	26,53	95,60	0,00
Ref [19] with aerated concrete block radiating	167,14	24,71	92,27	10,25
Base Case with same radiation properties of [19]	174,28	26,82	95,37	0,00
Base Case with aerated concrete block radiating	164,96	24,13	93,13	9,87

CHAPTER 3

ENHANCEMENT TRIALS

Throughout this study, different alterations of the base case geometry will be analysed based on different assumptions for the reason of the recirculating flow zone observed in Tari and Mehrtash [19]. The assumptions for the tried geometries and the results will be explained for each case. Mainly 4 different cases will be shown in this chapter.

- X Shaped Mixing Gaps Case
- Disturbance in Channels Case
- Middle Gap Case
- High End Fins Case

3.1 X Shaped Mixing Gaps Case

The main motivation of this work is to provide fresh air to recirculating flow zones of Figure 11. The first trial is cutting mixing gaps on the plate fins where the flow stagnates in each channel in order to provide fluid transfer to recirculating flow zones.

The hypothesis of this method is air to be moved from flowing zones to recirculating flow zones by its own momentum between the channels. In the base case, the air in the channels of the heat sink stagnates at different y points. So the hypothesis for this case is air to be move to non flow channels from the flowing channels. An illustration of the hypothesis can be seen in Figure 19.

In the numerical study five different sizes of mixing gaps have been analyzed. As it can be seen in Figure 20 mixing gaps with a width of G has been implemented on the fins of the heat sink.

- G=3 mm mixing gaps
- G=5 mm mixing gaps
- G=10 mm mixing gaps
- G=15 mm mixing gaps

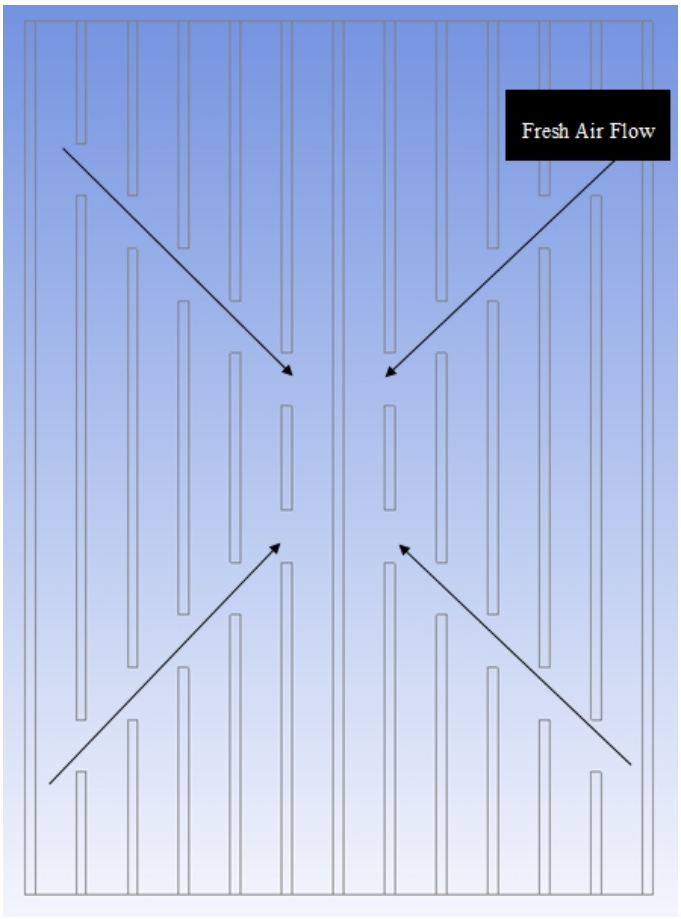

Figure 19 X Shaped Mixing Gaps hypothesis

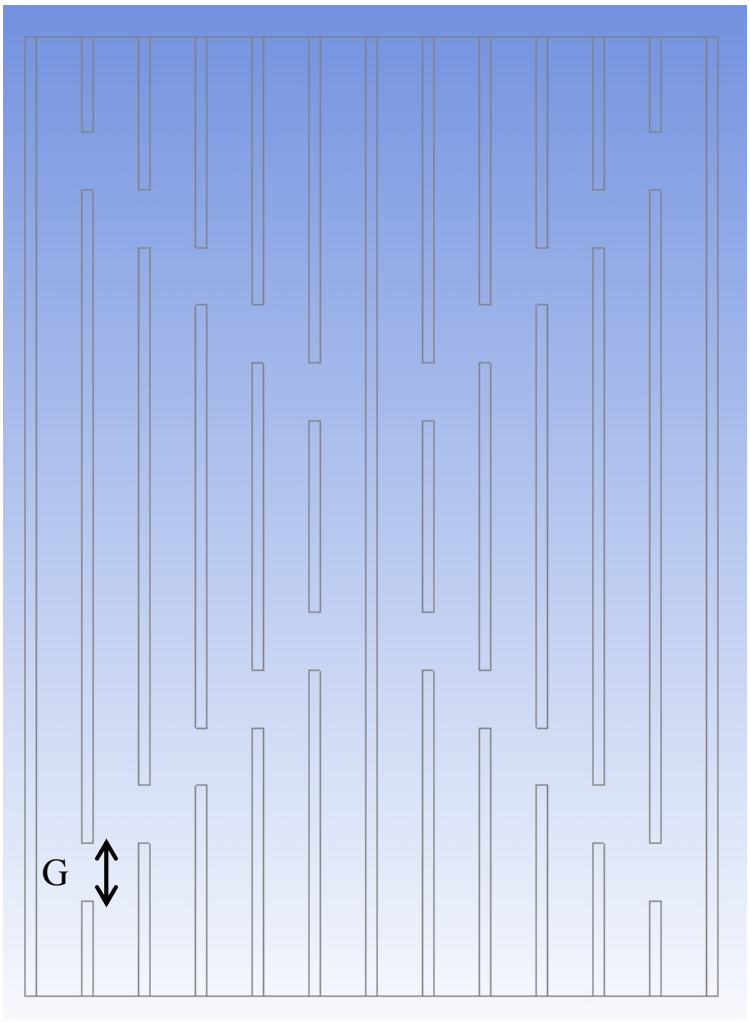

Figure 20 Illustration of Gap Size in X Shaped Mixing Gaps Case

3.1.1 Results of X Shaped Gaps Case

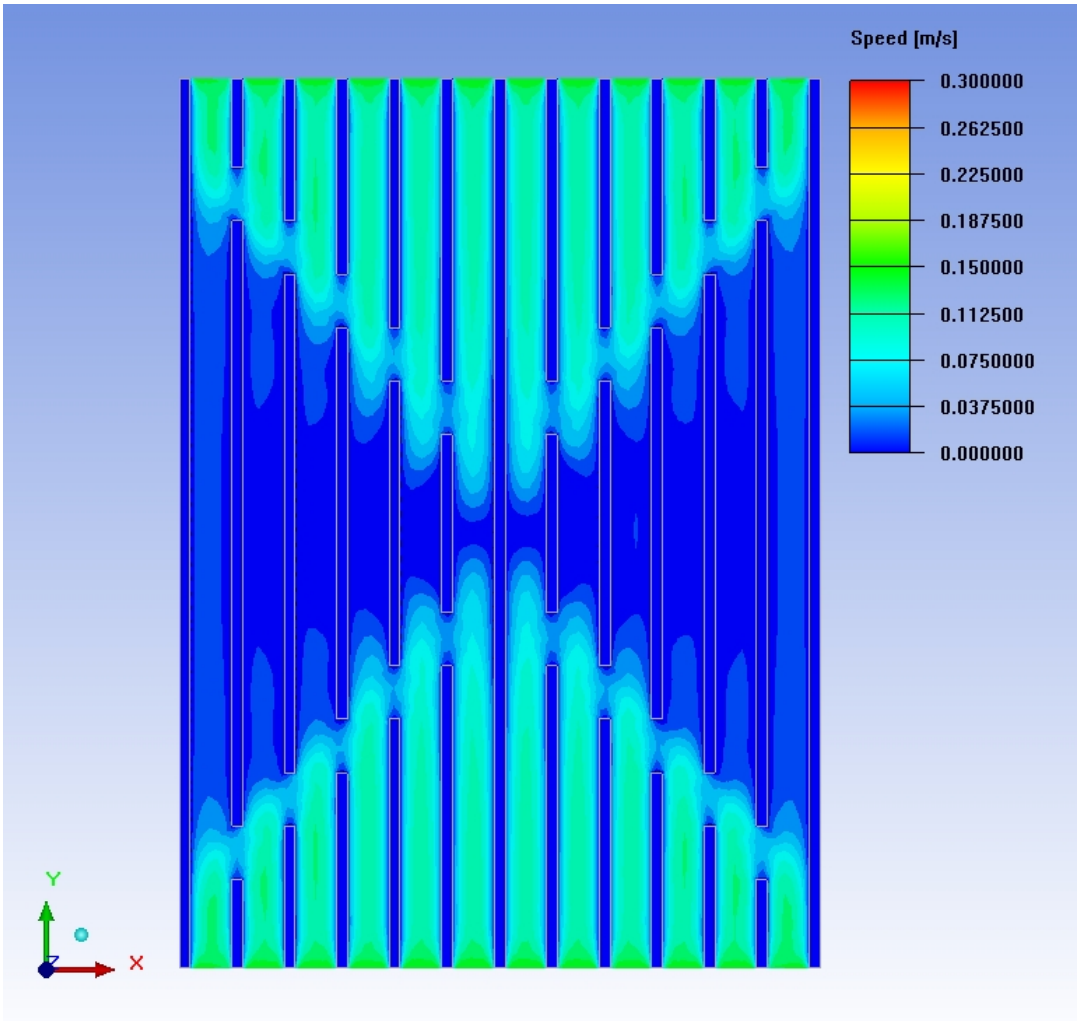

Figure 21 Speed contours above 2 mm of the base plate of G=15mm X Shaped Mixing Gaps Case

Figure 21 shows the velocity contours above 2 mm of heat sink base with G=15mm X shaped mixing gaps case. It has been observed from the figure that the cutting gaps

did not contribute to the flow. Also from Figure 22 through Figure 24 shows that this hypothesis did not affect the flow characteristics as it has been assumed. Another observation for these analyses has been made is for the G=15 mm case fluid is present in the gaps on the other hand for the other cases fluid seemed to be absent in the gaps.

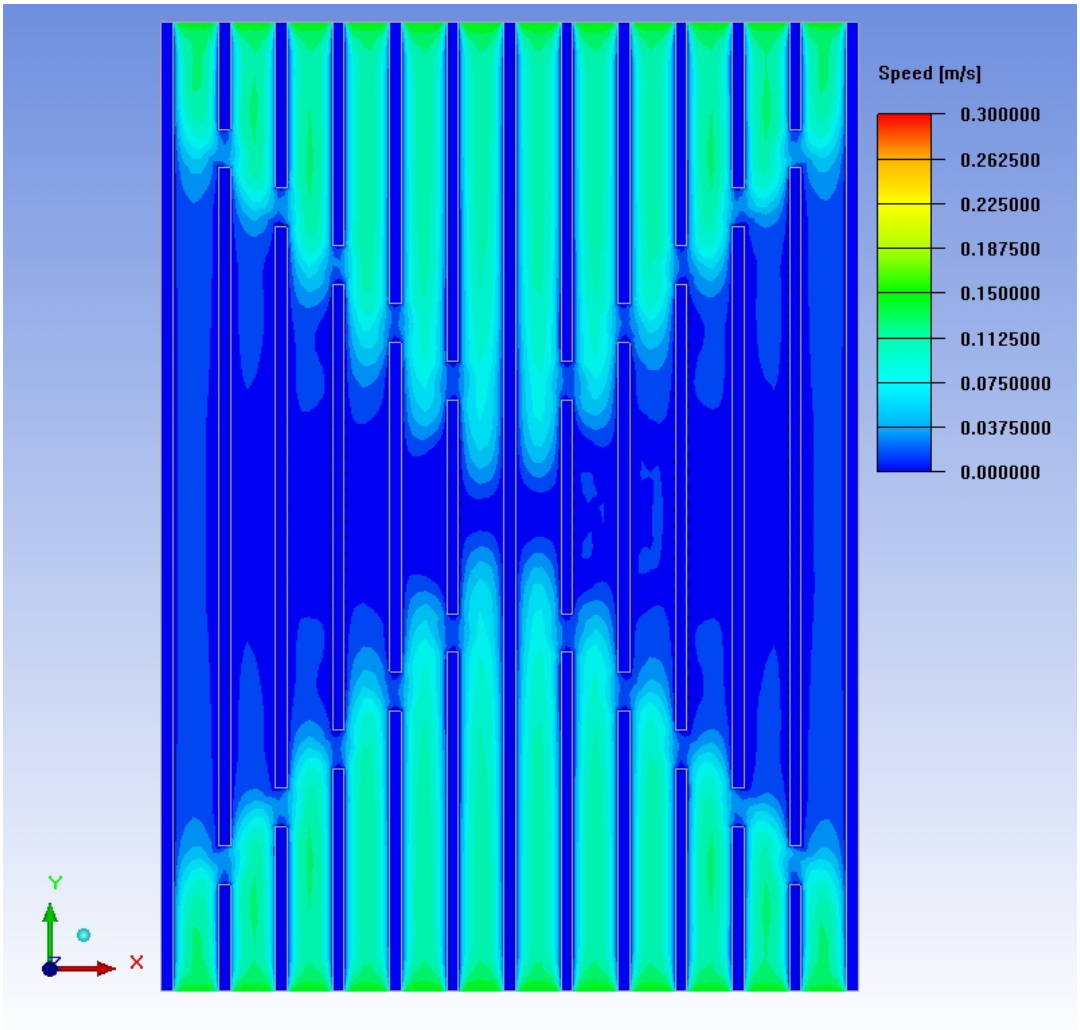

Figure 22 Speed contours above 2 mm of the base plate of G=10mm X Shaped Mixing Gaps Case

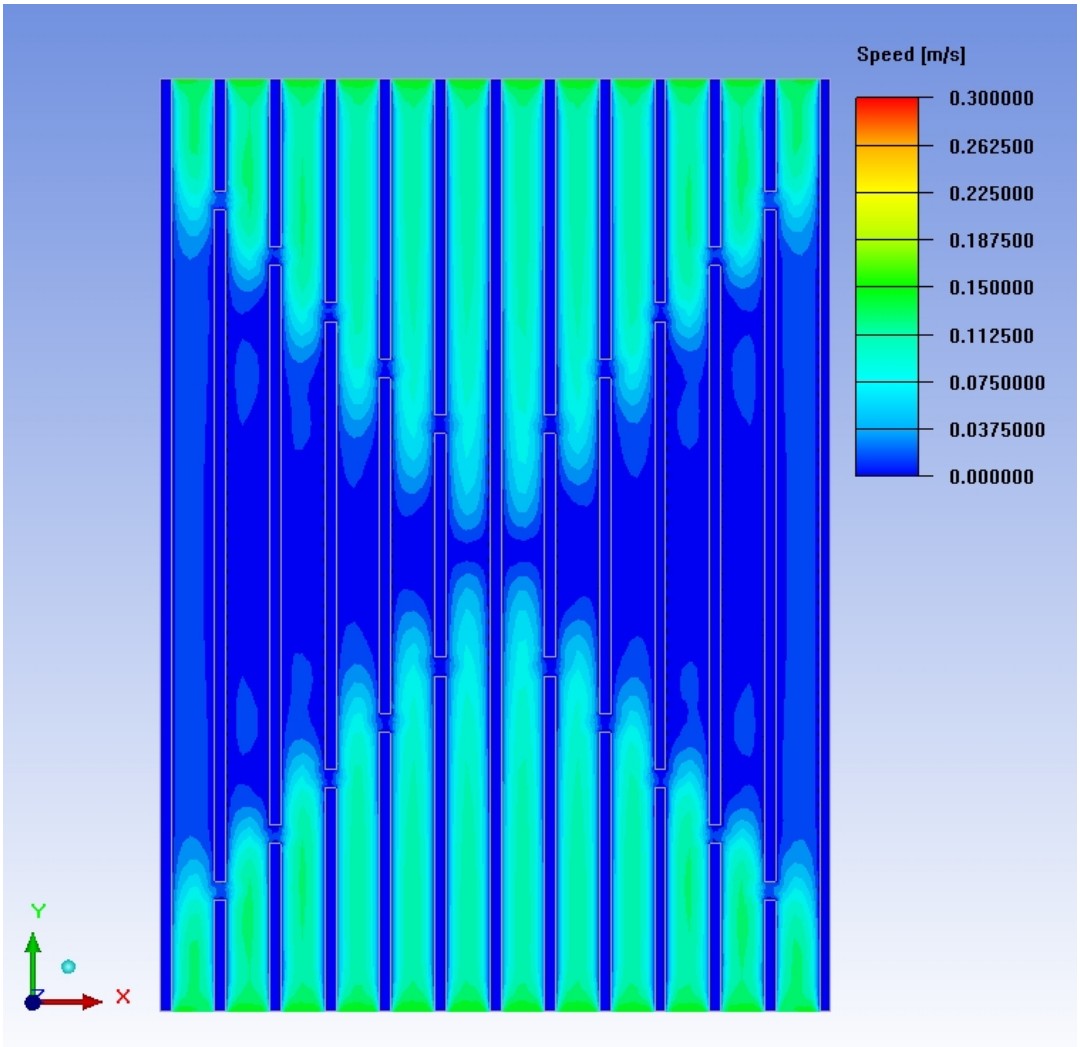

Figure 23 Speed contours above 2 mm of the base plate of G=5mm X Shaped Mixing Gaps Case

Observing through the figures of speed contour figures of X shaped mixing gaps case from Figure 21 to Figure 24 and comparing them with the Figure 18 which is the speed contours of the Base Case shows that the flow structure has not been affected by the mixing gaps. The reason why this solution is not successful will be explained in Section 3.4 and in Chapter 4 Conclusion.

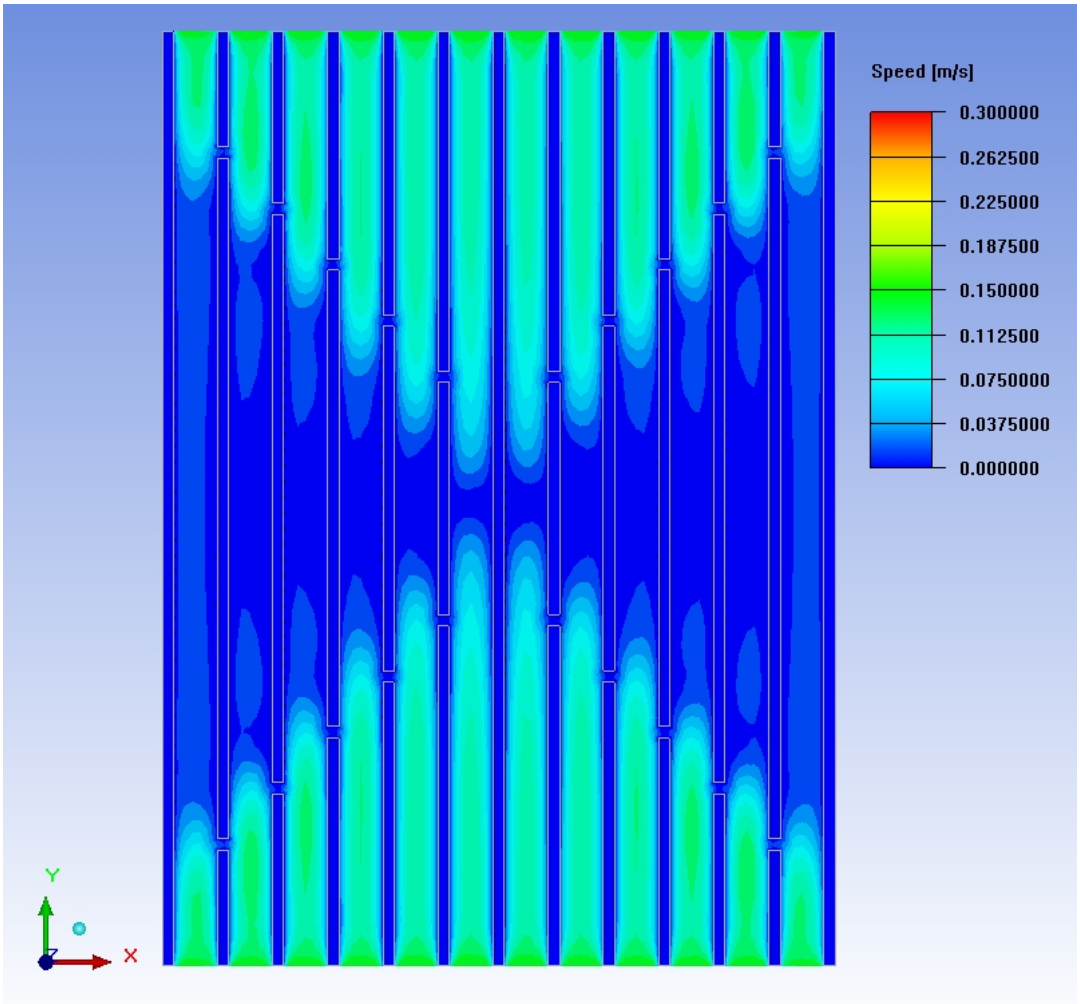

Figure 24 Speed contours above 2 mm of the base plate of G=3mm X Shaped Mixing Gaps Case

Table 8 X Shaped Mixing Gaps Case Results

Case Name	T_{mean} Heatsink Base (^oC)	Q_{Total} Heatsink into fluid (W)	Q_{rad} Heatsink (W)	Q_{conv} Heatsink (W)	q" (W/m^2)	q" $_{conv}$ (W/m^2)	q" $_{rad}$ (W/m^2)
Base Case	174,28	95,37	26,82	68,55	1186,36	852,69	333,67
G=3mm X Shaped Mixing Gaps Case	174,72	95,20	26,97	68,22	1184,17	848,62	335,55
G=5mm X Shaped Mixing Gaps Case	173,76	95,41	26,63	68,78	1192,75	859,81	332,93
G=10mm X Shaped Mixing Gaps Case	174,25	95,28	26,53	68,75	1206,28	870,42	335,86
G=15mm X Shaped Mixing Gaps Case	174,62	95,26	26,42	68,84	1221,44	882,72	338,71

Inspecting Table 8; it can be concluded that this case did not contribute to heat transfer characteristics. There are only slight variations in the values. One interesting finding about this case is despite the reduction in wet area of the heat sink the solutions yielded nearly the same values.

Calculation procedure for the values can be found in Appendix B.

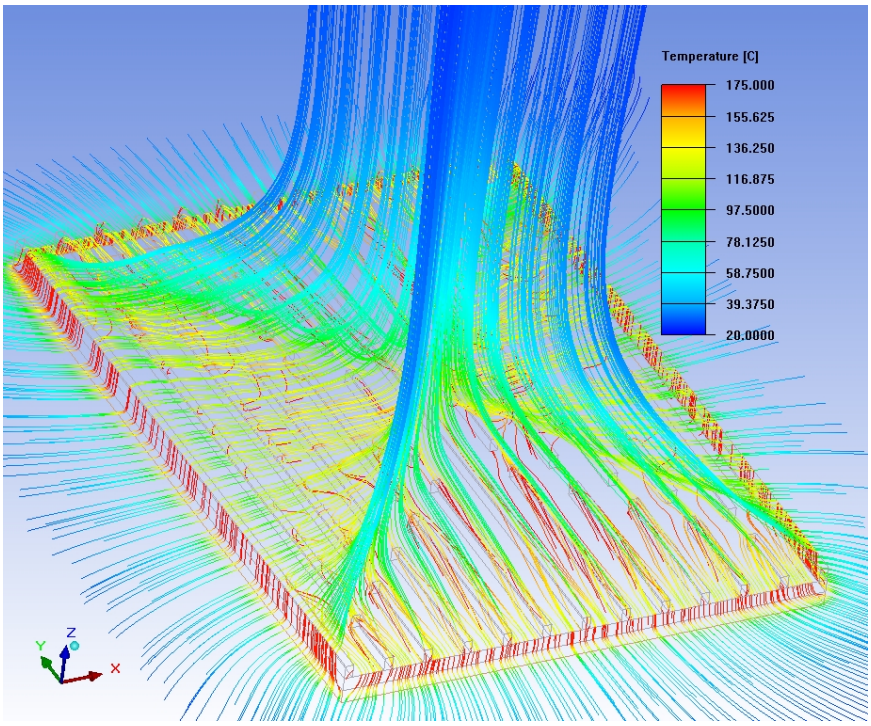

Figure 25 Pathlines of the G=15mm X Shaped Mixing Gaps Case with coloring based on temperature

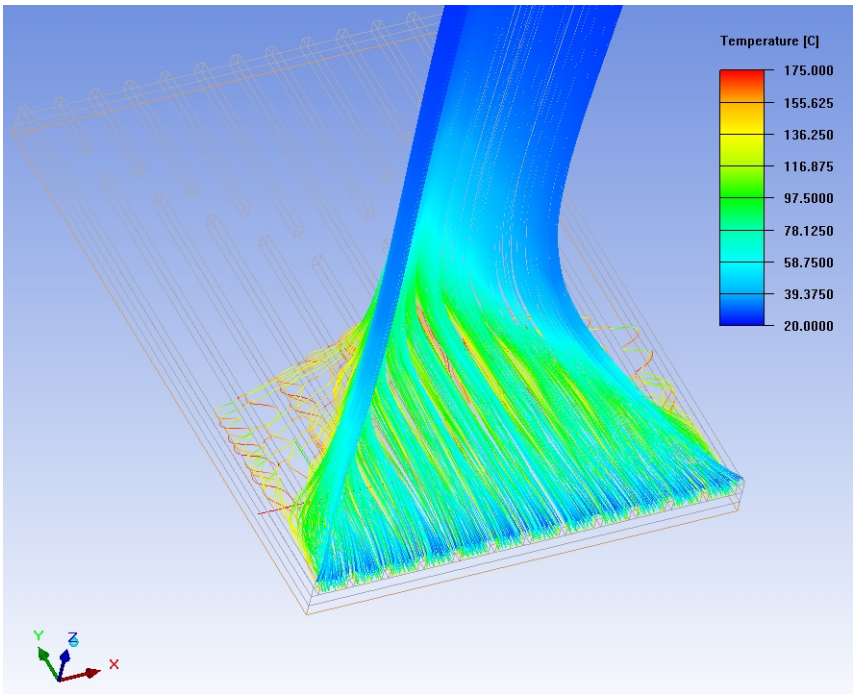

Figure 26 Pathlines of air entering into the channels of the heat sink in the G=15mm X Shaped Mixing Gaps Case with coloring based on temperature

Figure 25 and Figure 26 shows the pathlines of the G=15mm X shaped Mixing Gaps Case. Observing the figures it can be observed that flow still has vortex structured flow within the heat sink. Also it has been observed that a wide chimney flow structure occurs for these cases.

In addition to the 4 analyses an additional run has also been conducted in which for the G=5 mm X shaped mixing gaps case, additional gaps also has been implemented on the outmost fins. As it can be seen on Figure 27; gaps has been also cutted on the outmost fins.

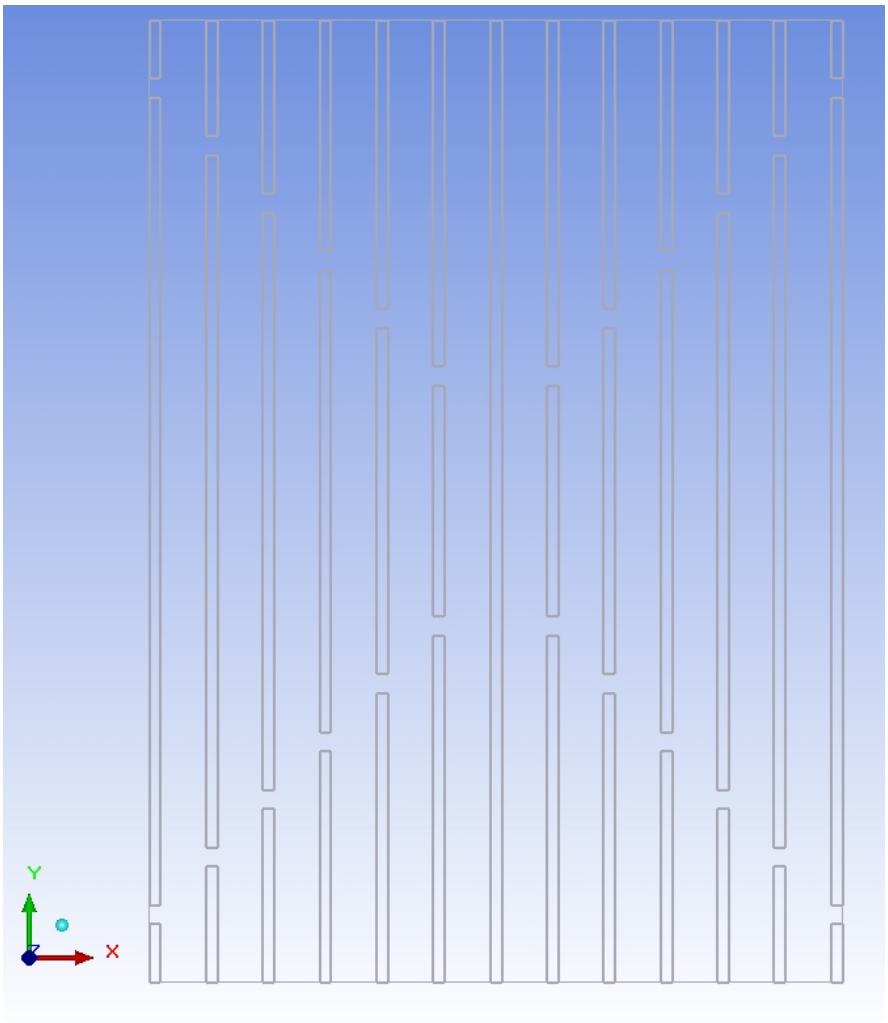

Figure 27 G=5mm X Shaped Mixing Gaps Case (Outmost fins included)

By this way air has been assumed to move into the flow stagnation points from outside of the heat sink to the recirculating flow zones and therefore by the fresh air provided to the flow in the channels it has been thought that recirculating flow zones will vanish.

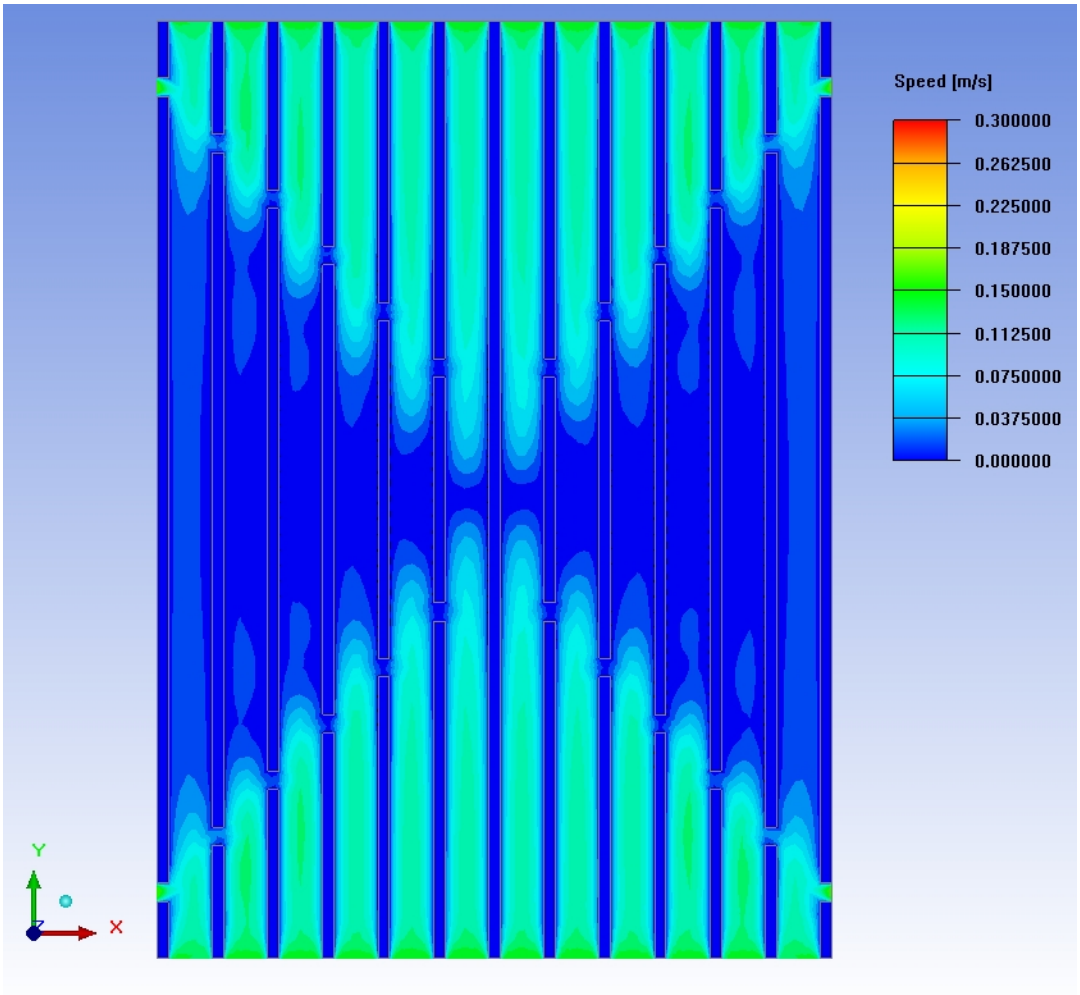

Figure 28 Speed contours above 2 mm of the base plate of G=5mm X Shaped Mixing Gaps Case (Outmost fins included)

However examining Figure 28 shows that even cutting gaps into outer fins did not provide air to recirculating non-flow zones although air entering into heat sink from the gaps on outmost fins can be seen. Table 9 shows that this solution did not change the heat transfer characteristics of the heat sink. This was expected from the Figure 28 since this figure shows that the flow structure did not change.

Table 9 X Shaped Mixing Gaps Case results with the cut on outmost fins case included

Case Name	T_{mean} Heatsink Base (°C)	Q_{Total} Heatsink into fluid (W)	Q_{rad} Heatsink (W)	Q_{conv} Heatsink (W)	q" (W/m^2)	q" $_{conv}$ (W/m^2)	q" $_{rad}$ (W/m^2)
Base Case	174,28	95,37	26,82	68,55	1186,36	852,69	333,67
G=3mm X Shaped Mixing Gaps Case	174,72	95,20	26,97	68,22	1184,17	848,62	335,55
G=5mm X Shaped Mixing Gaps Case	173,76	95,41	26,63	68,78	1192,75	859,81	332,93
G=10mm X Shaped Mixing Gaps Case	174,25	95,28	26,53	68,75	1206,28	870,42	335,86
G=15mm X Shaped Mixing Gaps Case	174,62	95,26	26,42	68,84	1221,44	882,72	338,71
G=5mm X Shaped Mixing Gaps Case (Outmost fins included)	174,23	95,26	26,76	68,50	1193,88	858,50	335,38

3.2 Middle Gap Case

3.2.1 Entire Gap in the Middle

Another improvising hypothesis was to force the fluid flow via gaps in the middle part of the heat sink to obtain a distributed flow zone, preventing the vortices to occur and enhancing heat transfer in the heat sink.

Figure 18 which is the speed contour figure above 2mm of the heat sink base shows that there are recirculating flow zone in the middle part of the chimney. These parts do not contain cooling fluid therefore the wet area of the heat sink decreases. From the X Shaped Gaps Case in which gaps also been cutted on the outmost fins showed that transferring fluid from the sides of the heat sink is possible. As illustrated in Figure 29 the reasoning behind this case is that the air from the sides entering into heat sink within the gaps cutted in middle part of the heat sink.

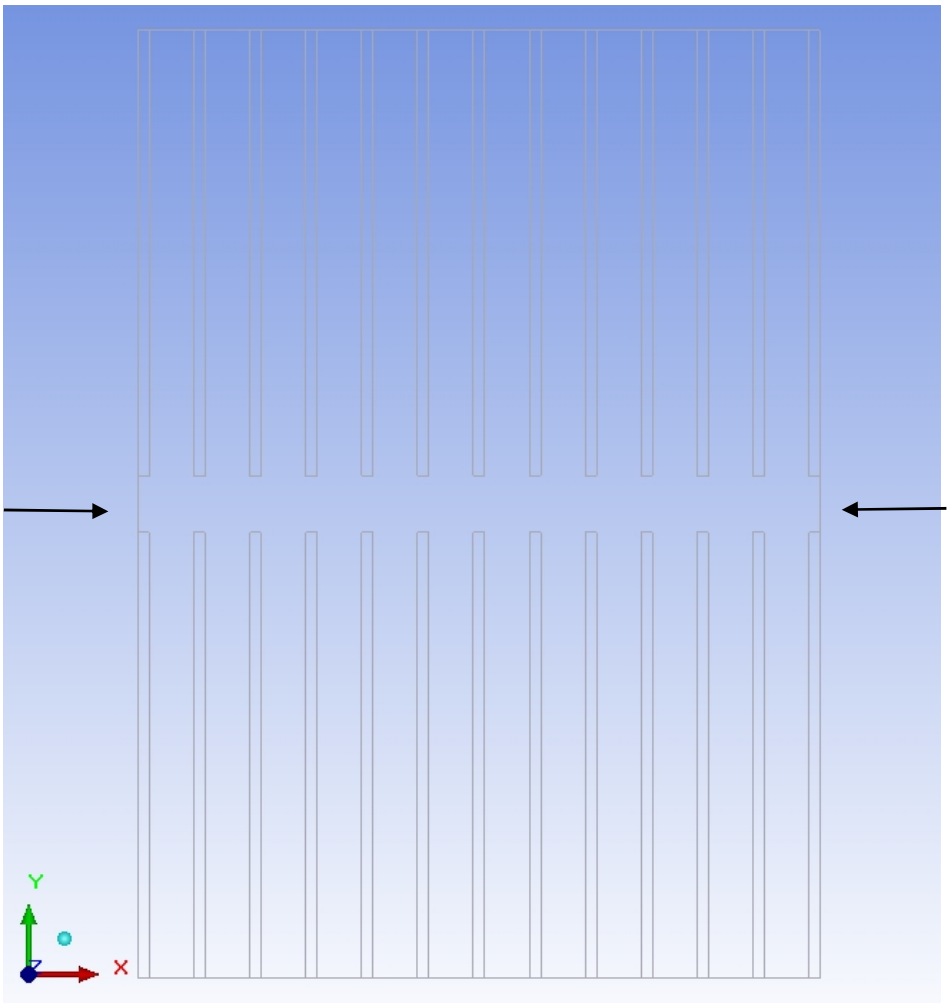

Figure 29 G=15 mm Middle Gap Case hypothesis

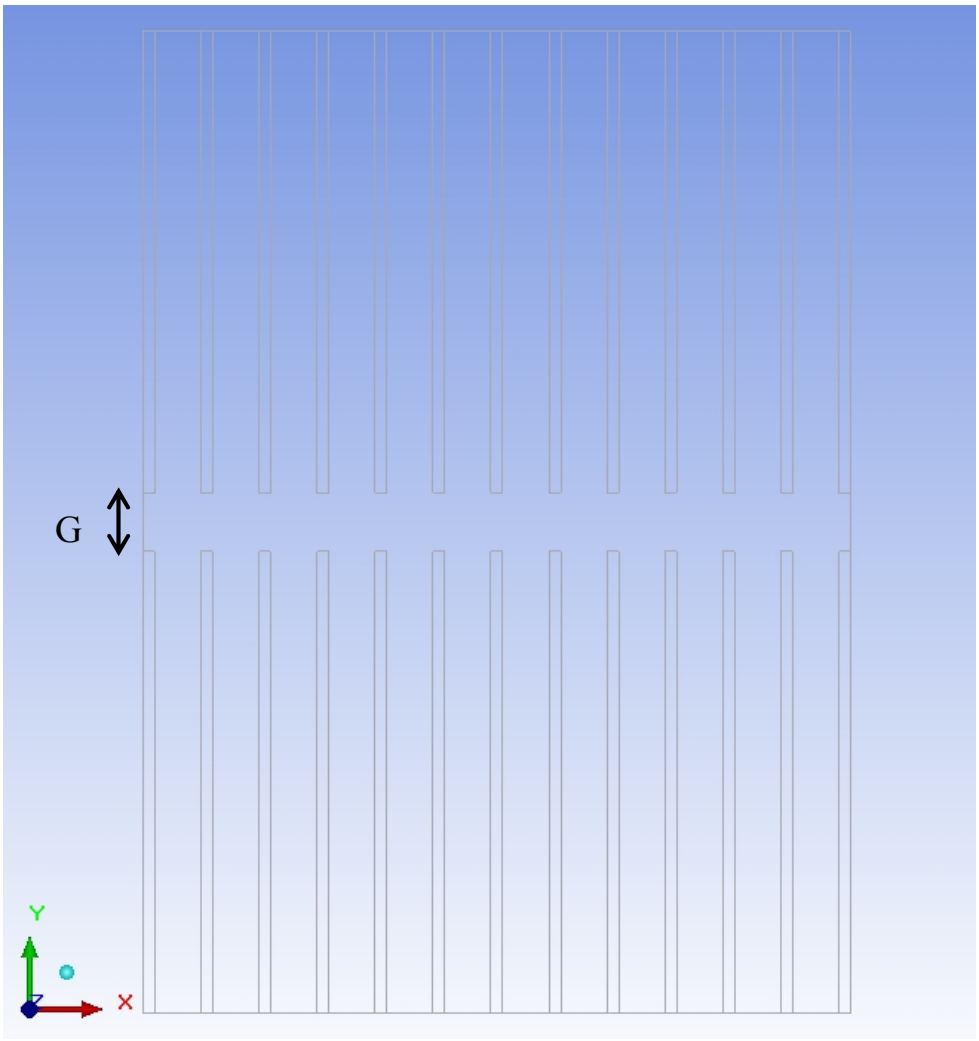

Figure 30 Illustration of Gap Size in Middle Gap Case

In this study the middle of the heat sink has been cut in order to diminish non- flow recirculating flow zones via lateral flow.

6 different sizes of cut have been analyzed.

- G=5 mm
- G=10 mm
- G=15 mm

- G=20 mm
- G=25 mm
- G= 30 mm

The results are discussed in the next chapter.

3.2.2 Results of Entire Middle Gap Case

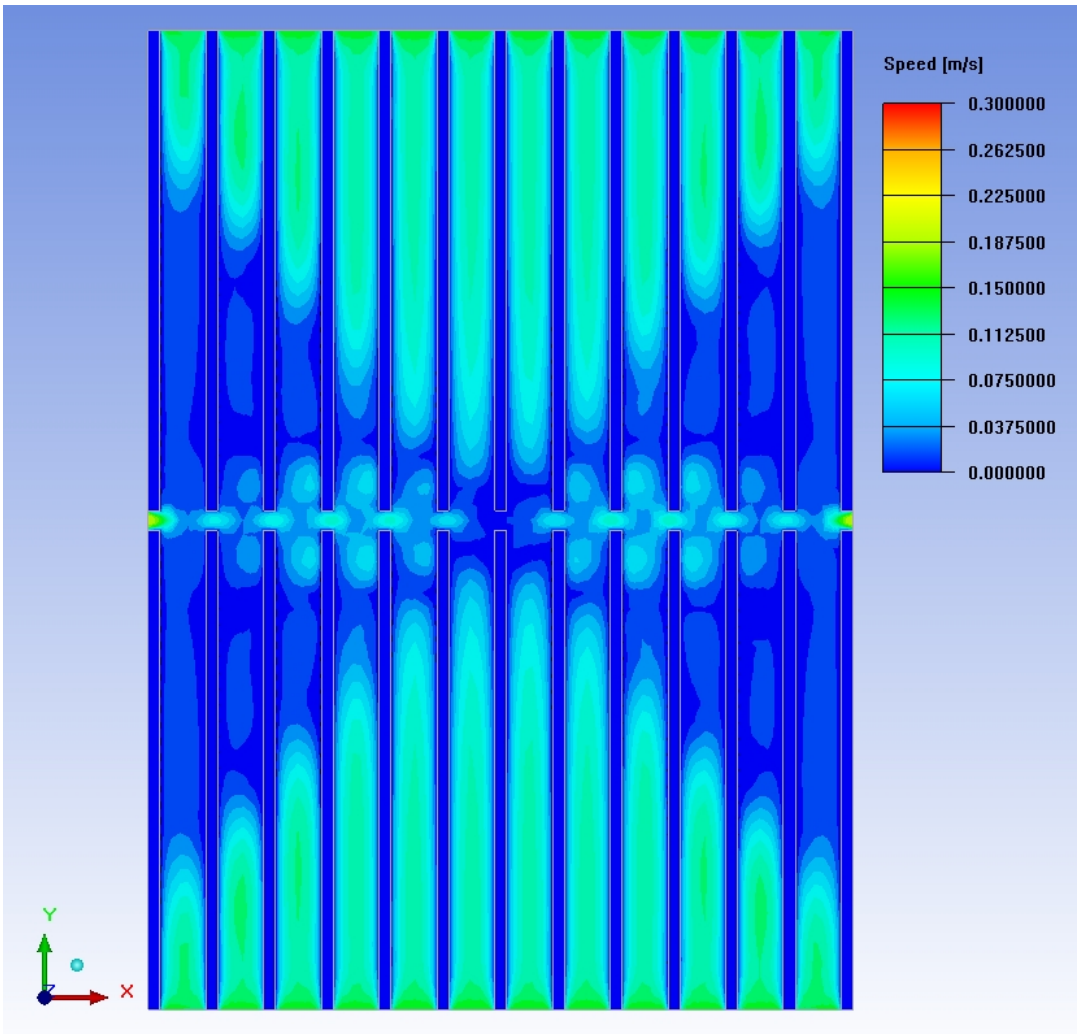

Figure 31 Speed contours above 2 mm of the base plate of G=5mm Middle Gap Case

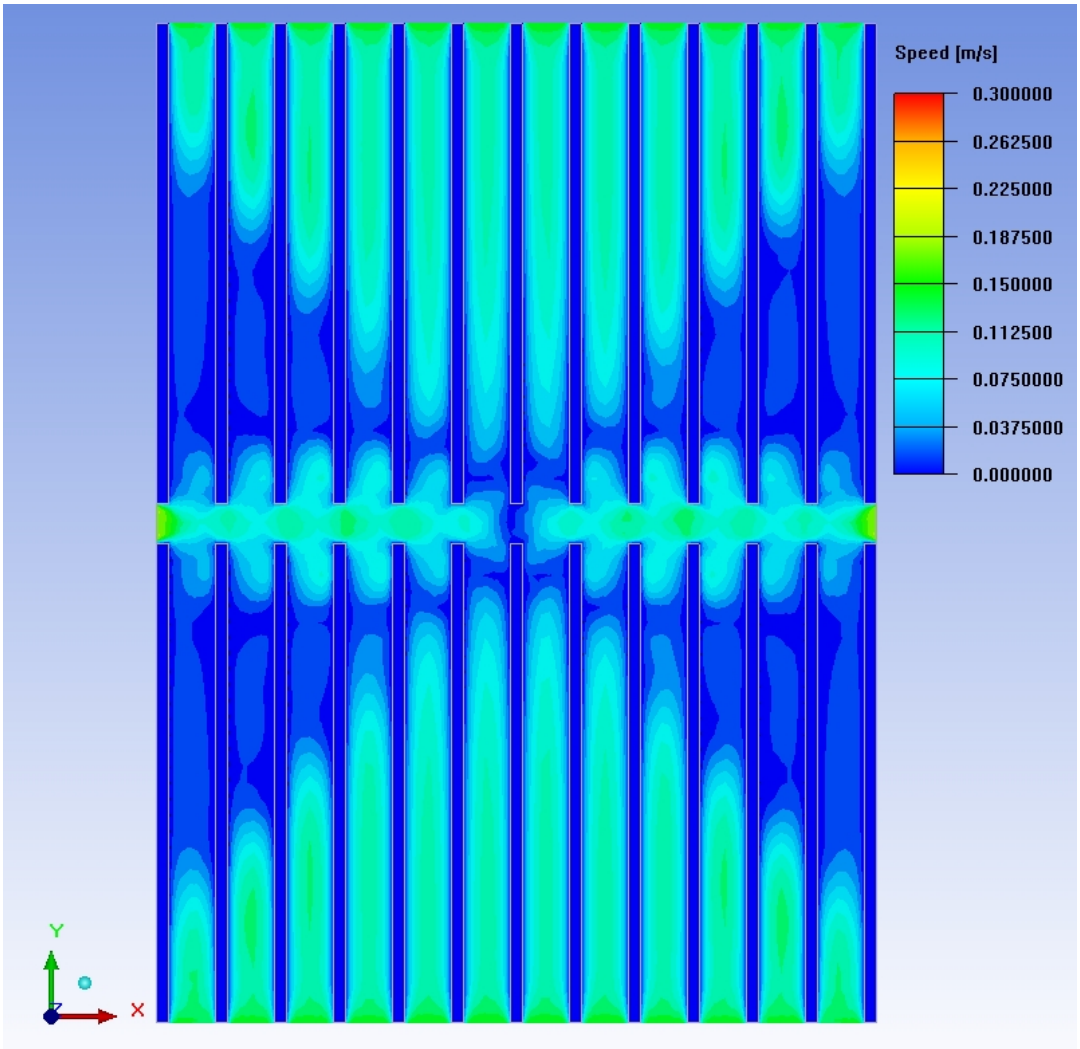

Figure 32 Speed contours above 2 mm of the base plate of G=10mm Middle Gap Case

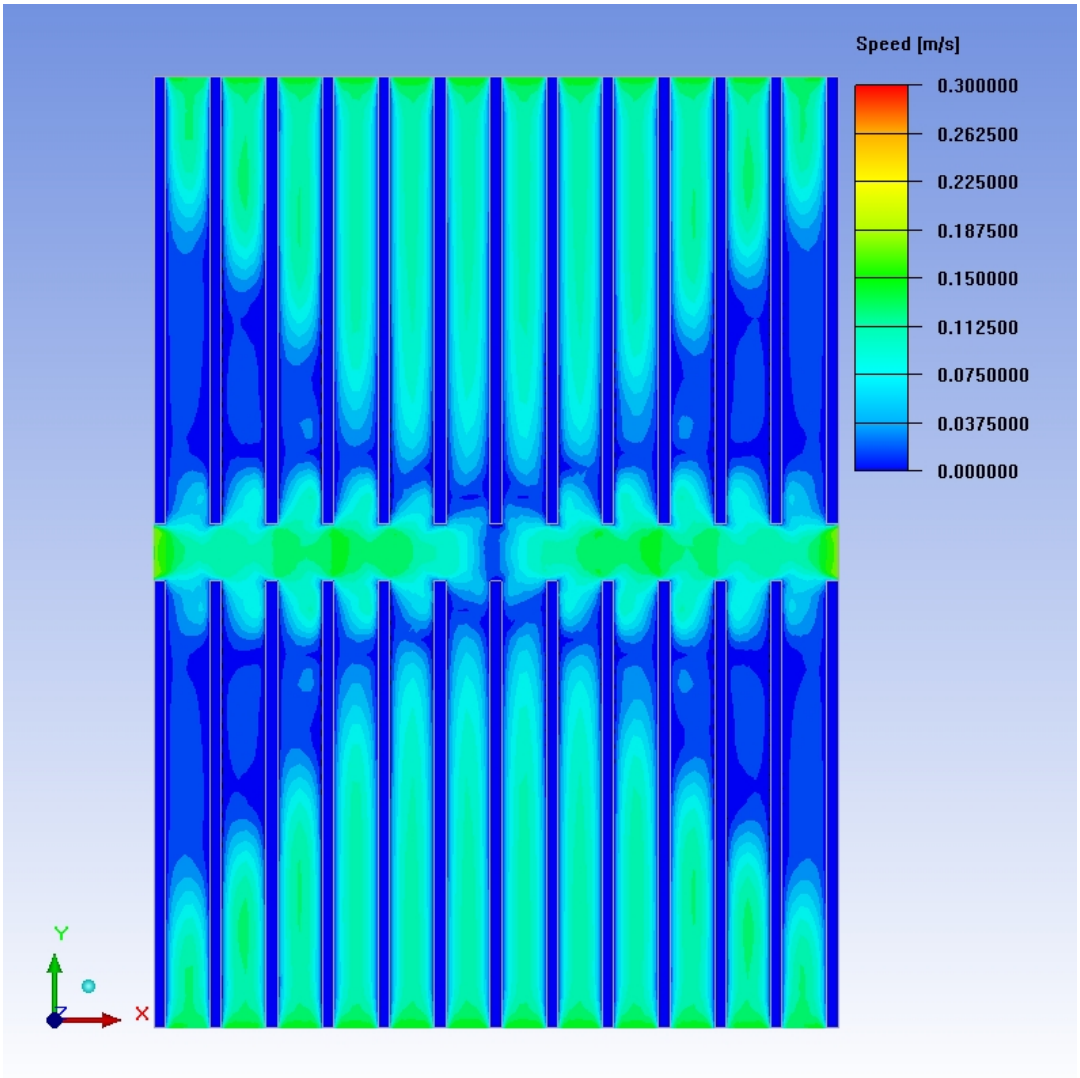

Figure 33 Speed contours above 2 mm of the base plate of G=15mm Middle Gap Case

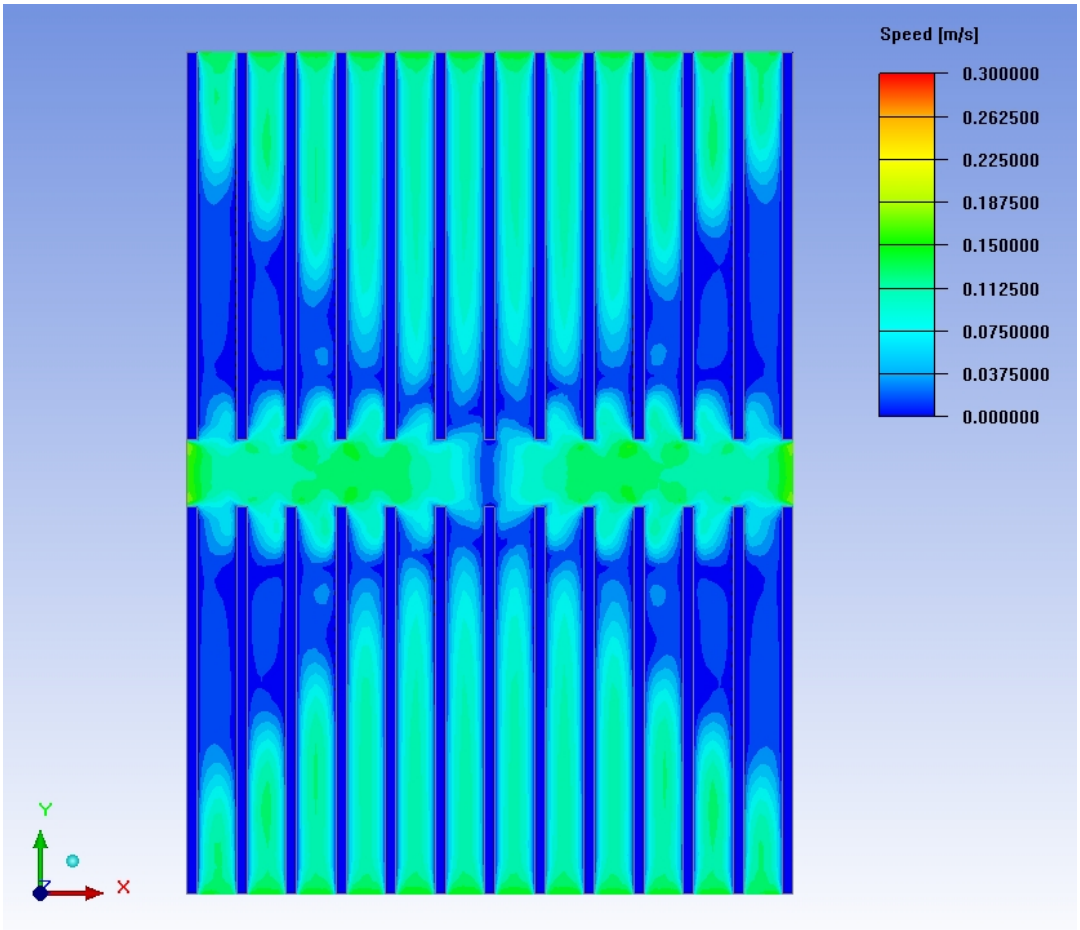

Figure 34 Speed contours above 2 mm of the base plate of G=20mm Middle Gap Case

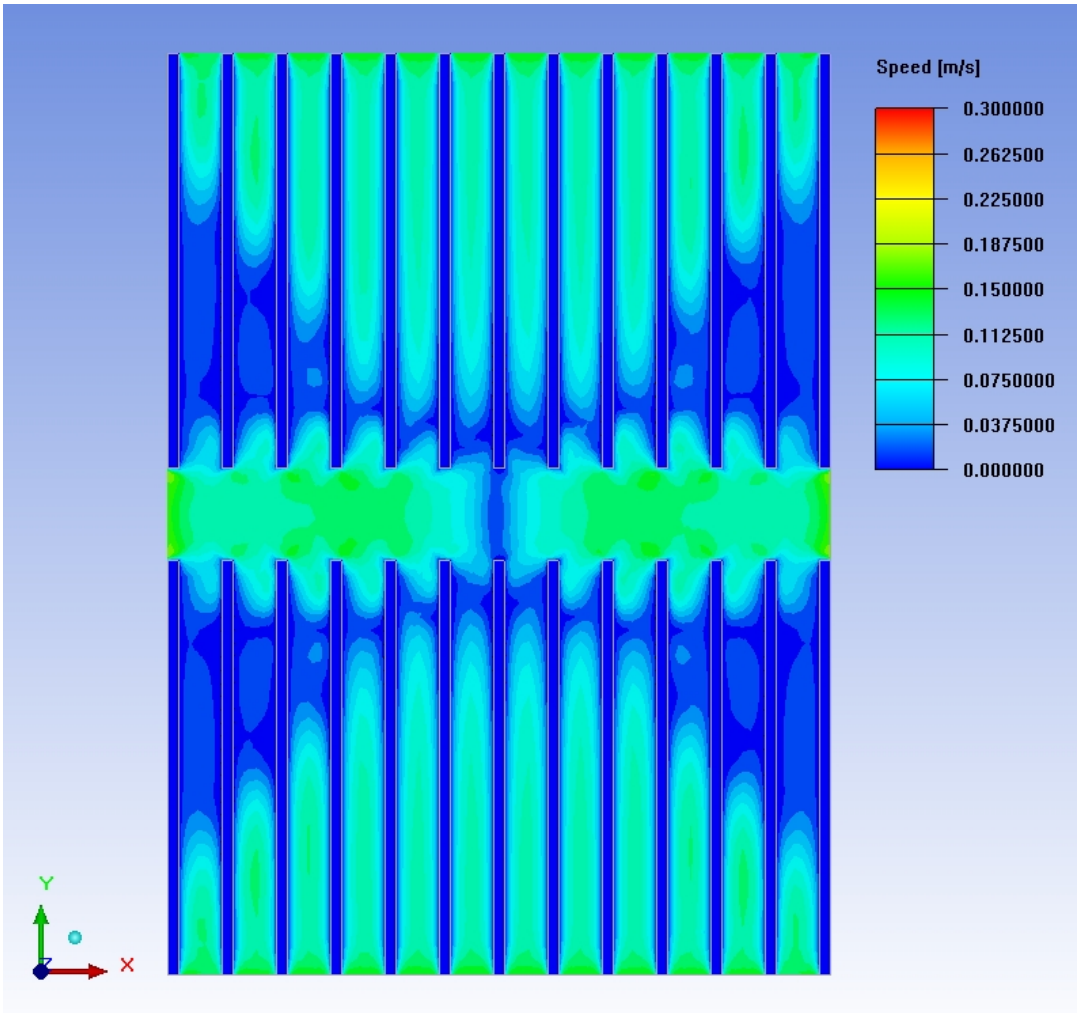

Figure 35 Speed contours above 2 mm of the base plate of G=25mm Middle Gap Case

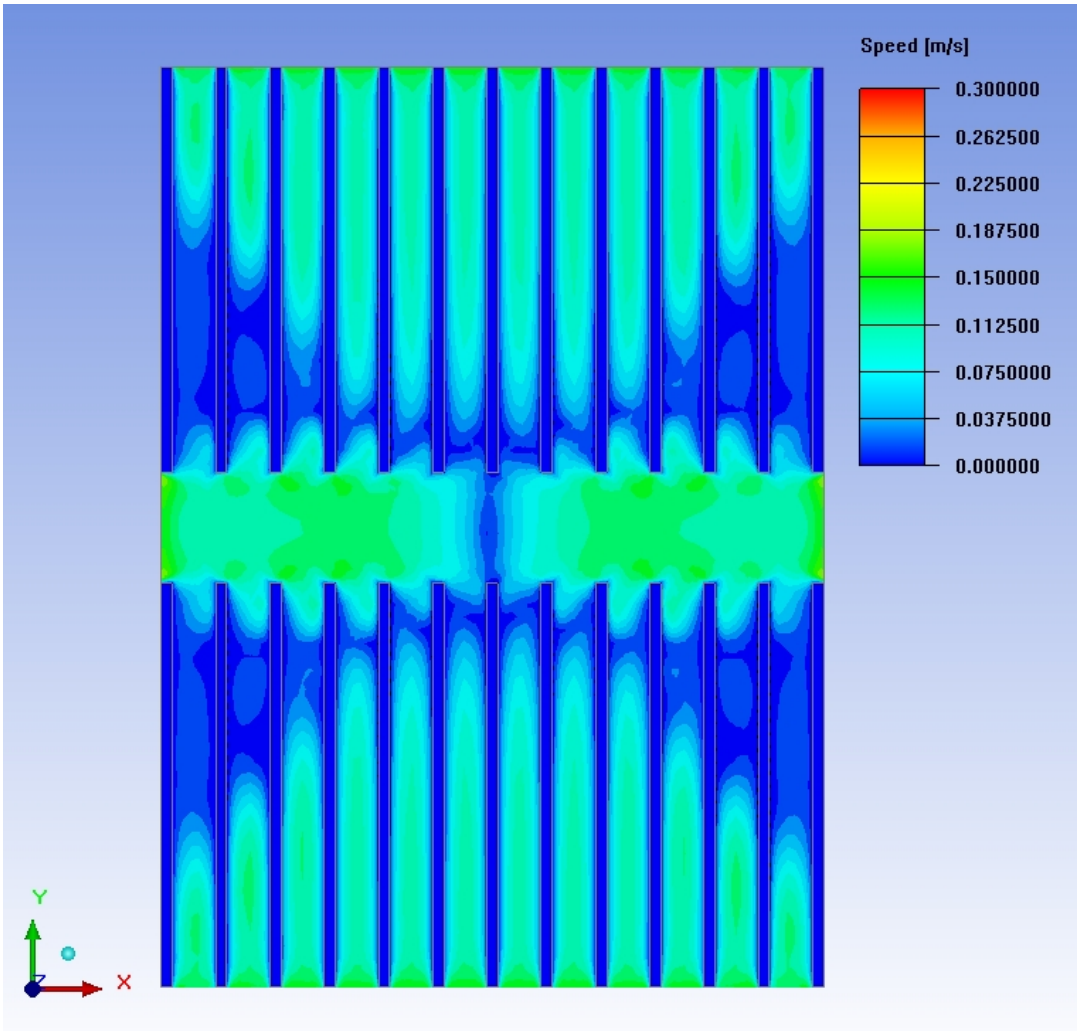

Figure 36 Speed contours above 2 mm of the base plate of G=30mm Middle Gap Case

Examining the speed contours from Figure 33 through Figure 36 it has been seen that recirculating flow zones are still not hindered completely although there is some distribution from the middle gap part. The middle gaps make it possible for the air to come inside the channels but they are not distributed to recirculating flow zones completely. The former blue parts which did not have convection cooling; can now be cooled via convection by the help of the air entering from the sides of the heat sink. Increasing the gap size increases the base area cooled by convection. But on

the other hand the fin area decreases. The optimum value for the gap size can be seen in Table 10. 25mm and 20 mm gap size gave similar values for the temperature of the base plate but when gap size has been increased to 30 mm the base temperature value increased. By looking at these results optimum value for the gap size can be stated as G=20 mm or G=25 mm.

Table 10 Results of the Middle Gap Case

Case Name	T_{mean} Heatsink Base (°C)	Q_{Total} Heatsink into fluid (W)	Q_{rad} Heatsink (W)	Q_{conv} Heatsink (W)	q" (W/m^2)	q" $_{conv}$ (W/m^2)	q" $_{rad}$ (W/m^2)
Base Case	174,28	95,37	26,82	68,55	1186,36	852,69	333,67
G=5 mm Middle Gap Case	170,94	95,92	25,87	70,05	1194,17	872,06	322,11
G=10 mm Middle Gap Case	168,70	96,32	25,02	71,30	1205,95	892,68	313,27
G=15 mm Middle Gap Case	168,30	96,39	24,77	71,62	1213,75	901,83	311,92
G=20 mm Middle Gap Case	167,80	96,48	24,49	72,00	1224,97	914,15	310,94
G=25 mm Middle Gap Case	167,76	96,48	24,36	72,12	1235,16	923,30	311,86
G=30 mm Middle Gap Case	168,95	96,25	24,55	71,70	1242,56	925,63	316,93

Heat sink base temperature has been reduced by up to 6,5 °C in 25 mm middle gap case. As expected from the speed contours figures, convection heat transfer has been increased. Also total heat transfer rate has been increased by distributing flow to

recirculating flow zones although the wet area has been reduced. The reduction in Q_{rad} values can be explained by reduction in area and temperature values.

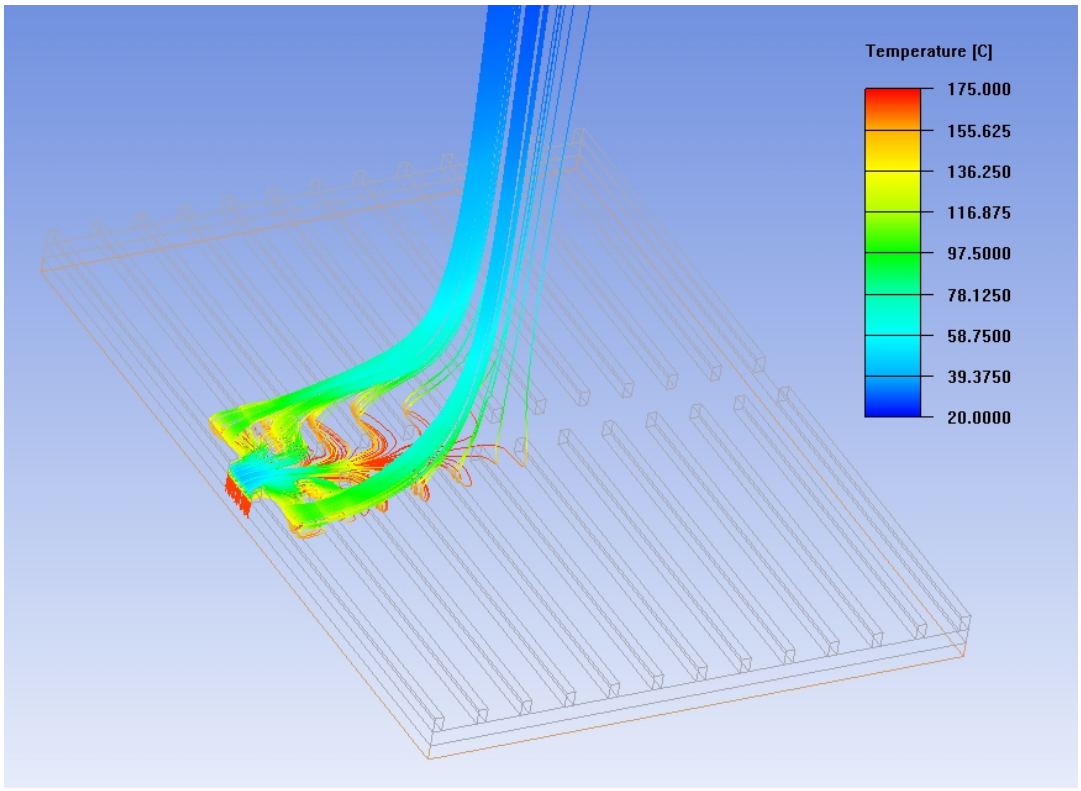

Figure 37 Fluid pathlines entering into heat sink through the left middle gap in G=15mm Middle Gap Case

Examining Figure 37 explains the increase in convection heat transfer and reduction in base temperature. Additional air coming from the sides of the heat sink distributes to a small region of recirculating flow zones. These parts did not contain fluid in Base Case so by letting the air to cool formerly flow stagnated parts increased convection heat transfer rate. The air coming from the sides, first distributes into flow hindered zones and when they gain enough energy to rise via increasing its temperature, they join the chimney flow structure.

3.2.3 Partial Cut Case

Observing the flow visualizations of middle gaps case showed that the air from the sides enters to heat sink from the gaps cut in the middle of the fins. Another analysis has been made in order to observe the effects of middle cuts in the middle fins to see if the flow in channels would distribute to the non flow zones without the help of the air which is entering into the heat sink from the gaps on the sides. As it can be seen in Figure 38 and Figure 39 the 11 fins in the middle 7 fins in the middle have been cut.In order to choose an optimum gap size 15mm middle gaps have been implemented on the heat sink.

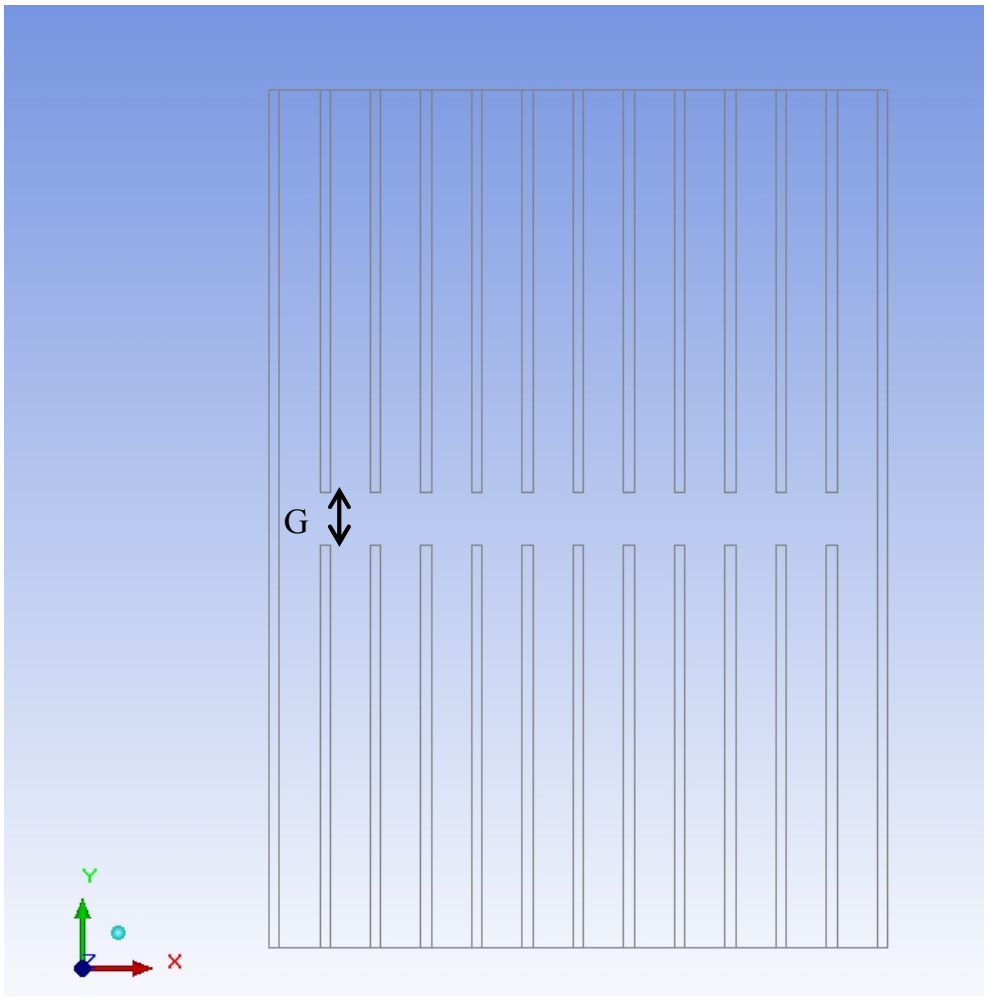

Figure 38 G=15 mm Partial Middle Gap Case (11 fins cut)

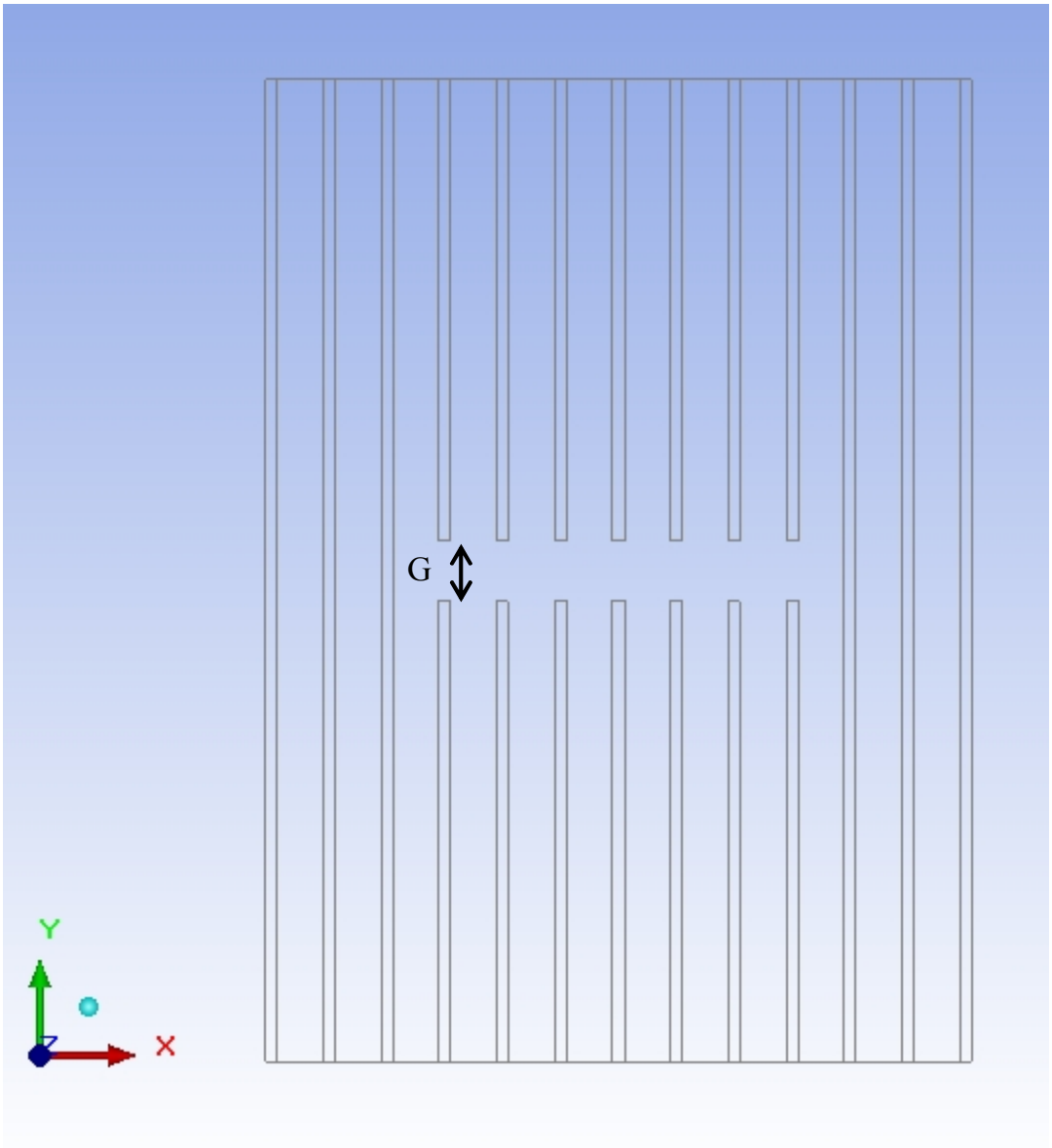

Figure 39 G=15 mm Partial Middle Gap Case (7 fins cut)

3.2.4 Results of Partial Middle Gap Case

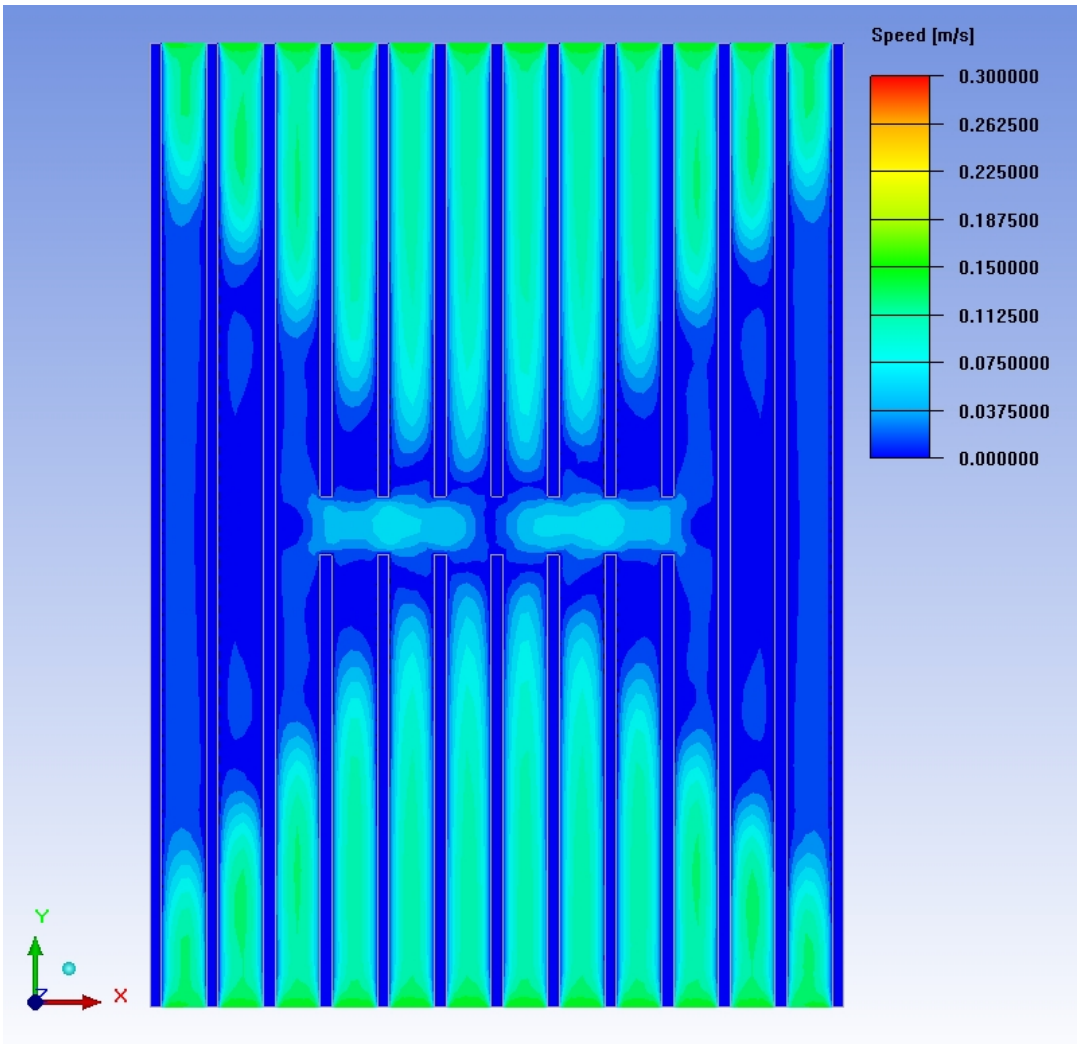

Figure 40 Speed contours above 2 mm of the base plate of G=15mm Partial Middle Gap Case (7 fins cut)

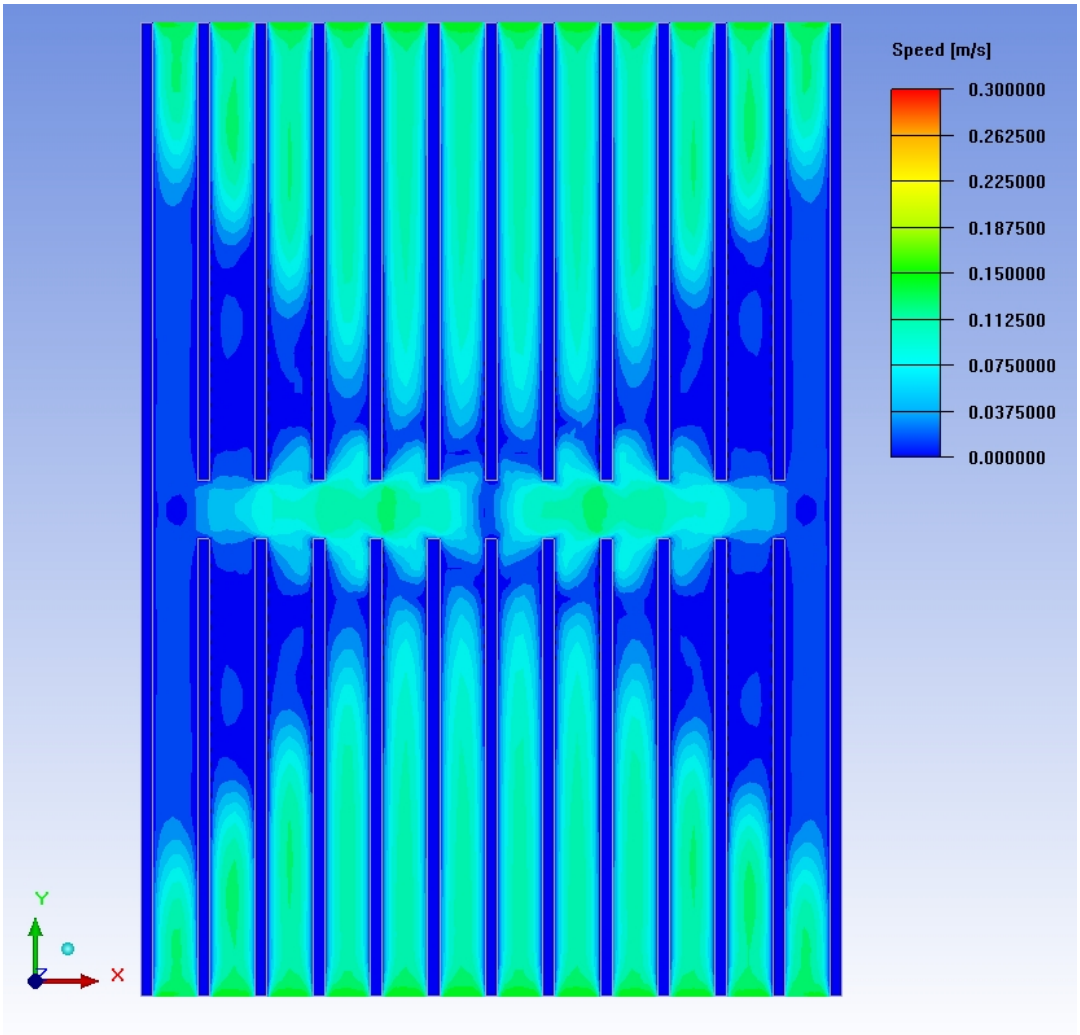

Figure 41 Speed contours above 2 mm of the base plate of G=15mm Partial Middle Gap Case (11 fins cut)

From Figure 40 and Figure 41 it is observed that partial middle gap method makes the distribution in the channels but only a small region is affected by this solution. At first the source of the fluid in the middle parts seems like the flow in the channels. However examining Figure 42 which shows the pathlines of air entering to heat sink channels shows that the middle flow which is seen in Figure 40 and Figure 41 does not arise from the flow in heat sink channels; examining Figure 43 shows that the flow which is present in the middle of the heat sink arises from flow entering to heat sink from the sides of the heat sink. The air first enters to heat sink zone and descends

and rises again when its temperature increases. This situation also led to increase in convection heat transfer.

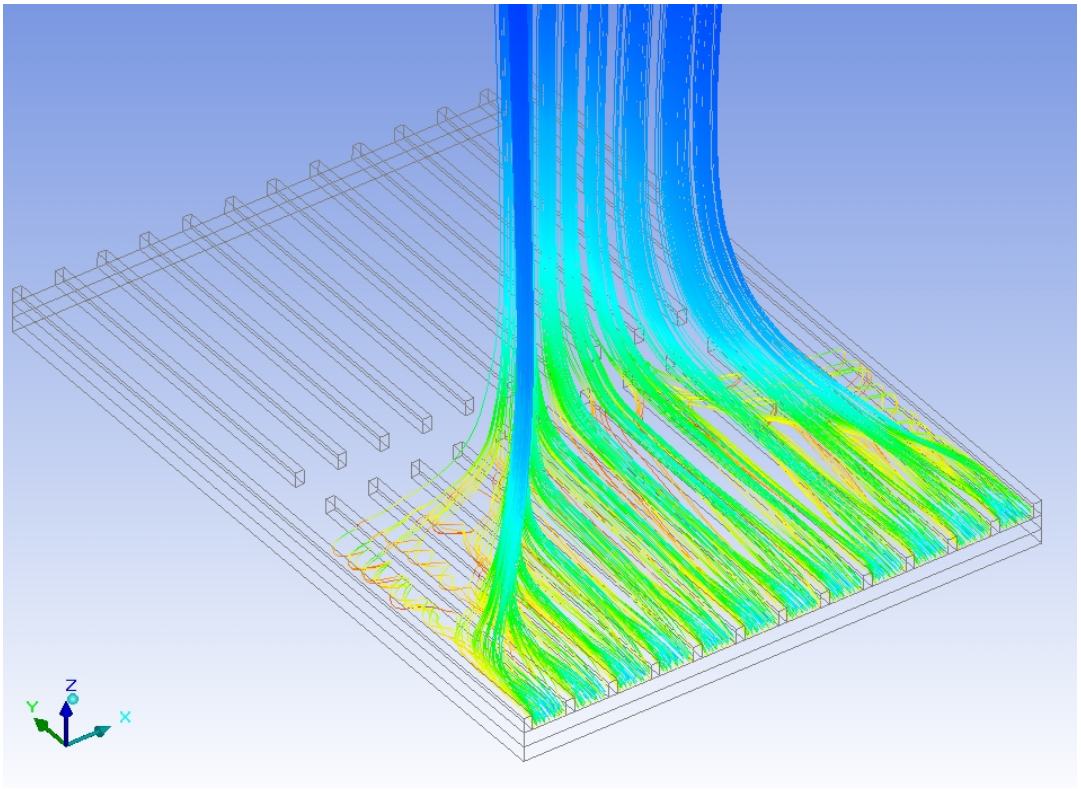

Figure 42 Pathlines of air entering into the channels of the heat sink in the G=15mm Partial Middle Gap Case(11 fins cut) with coloring based on temperature

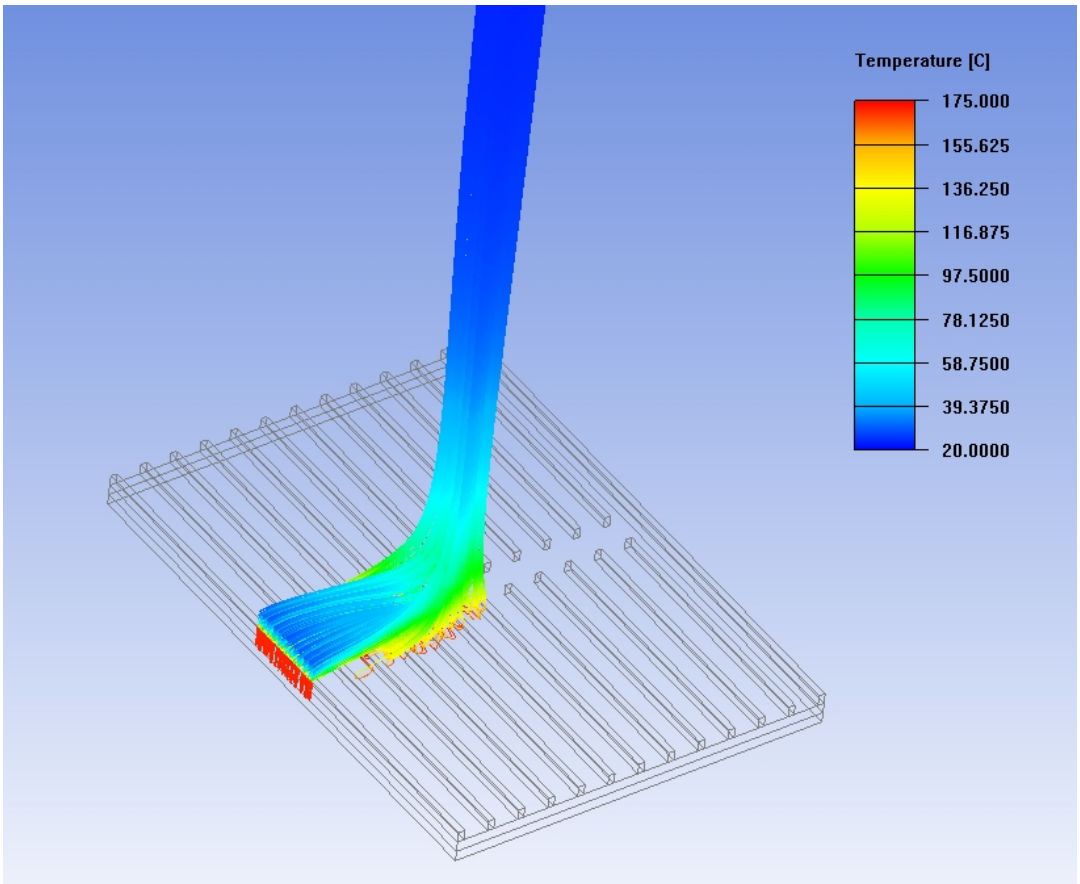

Figure 43 Pathlines of air entering from the left side of the heat sink in G=15mm Partial Middle Gap Case coloring based on temperature of the fluid(11 fins cut)

Table 11 shows the results of this solution and it can be seen that this solution reduced the T_{mean} of Heat Sink base slightly but not as much as Entire Middle Gap Case. Since the entire middle gap case provides more wet areas than partial middle gap case these comparation results have been expected. Convection heat transfer has been increased by 1.6 W compared to Base Case in Middle Gap in 12 fins case. The reduction in Q_{rad} is being explained by reduction in area and surface temperature.

Table 11 Results of Middle Gap Case and Partial Middle Gap Case

Case Name	T_{mean} Heatsink Base (^oC)	Q_{Total} Heatsink into fluid (W)	Q_{rad} Heatsink (W)	Q_{conv} Heatsink (W)	q" (W/m^2)	q" $_{conv}$ (W/m^2)	q" $_{rad}$ (W/m^2)
Base Case	174,28	95,37	26,82	68,55	1186,36	852,69	333,67
5 mm Middle Gap Case	170,94	95,92	25,87	70,05	1194,17	872,06	322,11
10 mm Middle Gap Case	168,70	96,32	25,02	71,30	1205,95	892,68	313,27
15 mm Middle Gap Case	168,30	96,39	24,77	71,62	1213,75	901,83	311,92
G=20 mm Middle Gap Case	167,80	96,48	24,49	72,00	1224,97	914,15	310,94
G=25 mm Middle Gap Case	167,76	96,48	24,36	72,12	1235,16	923,30	311,86
G=30 mm Middle Gap Case	168,95	96,25	24,55	71,70	1242,56	925,63	316,93
15 mm Middle Gap Case 6 Rows	173,60	95,46	26,46	69,00	1195,23	863,98	331,25
15 mm Middle Gap Case 12 Rows	171,33	95,84	25,68	70,16	1204,61	881,79	322,82

Calculation procedure for the values can be found in Appendix B.

3.3 Disturbance in Channels Case

In Figure 44, the base case, longitudinal vortices have been observed in the recirculating flow zones. In this case "Disturbance in Channels" 2 different shapes of disturbance creators have been installed in middle of the channels between fins to observe the effect of these disturbance creators on the flow and heat transfer and most importantly longitudinal vortices.

This case's aim is not to come up with a solution for providing air to recirculating flow zones of Base Case; this cases' aim is about observation of the effects of disturbance in channels to the flow behaviour in naturally cooled horizontal plate finned heat sinks. The details of the disturbance creators are explained below. Their material properties are the same as heat sink.

- Little plate fins of 3 mm thickness 5 mm height
- Little Pin Fins of 5 mm height and 1.8 mm radius
    - Entire Heat Sink
    - 6 Channels of the Heat Sink
    - 10 Channels of the Heat Sink

have been installed into middle of the heat sink.

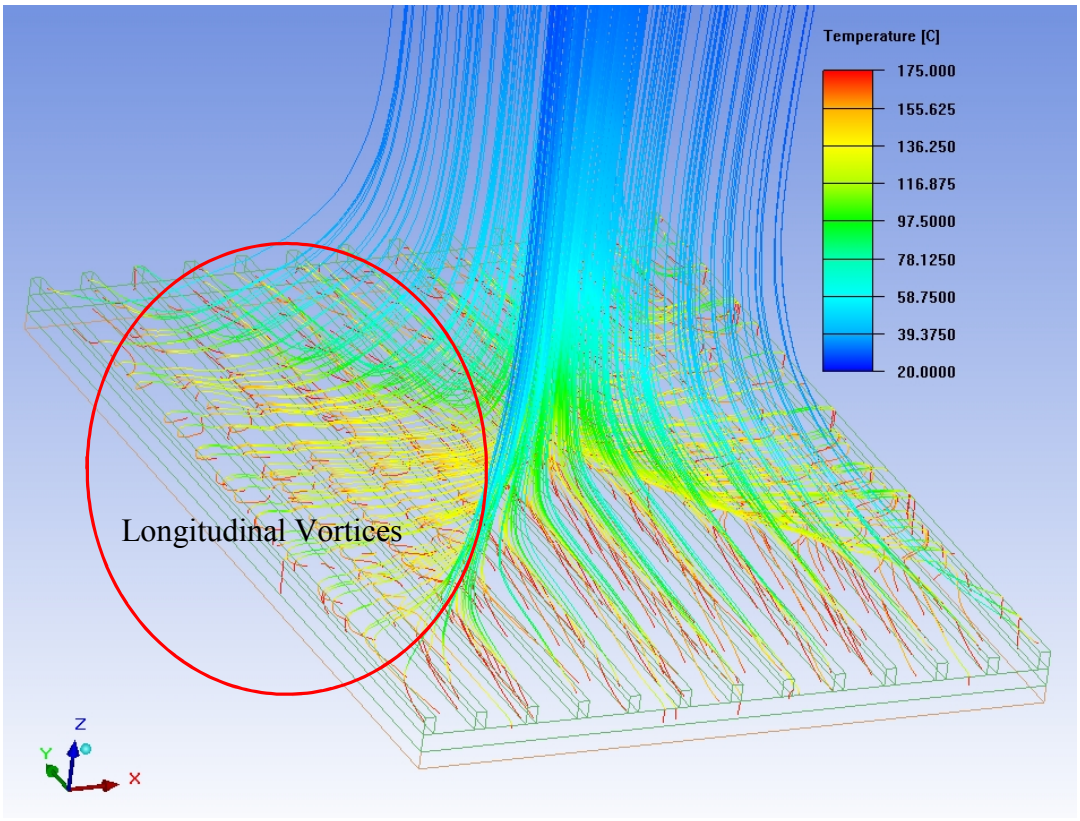

Figure 44: Pathlines of Base Case coloring based on fluid temperature

3.3.1 Plate Fin Disturbance Case

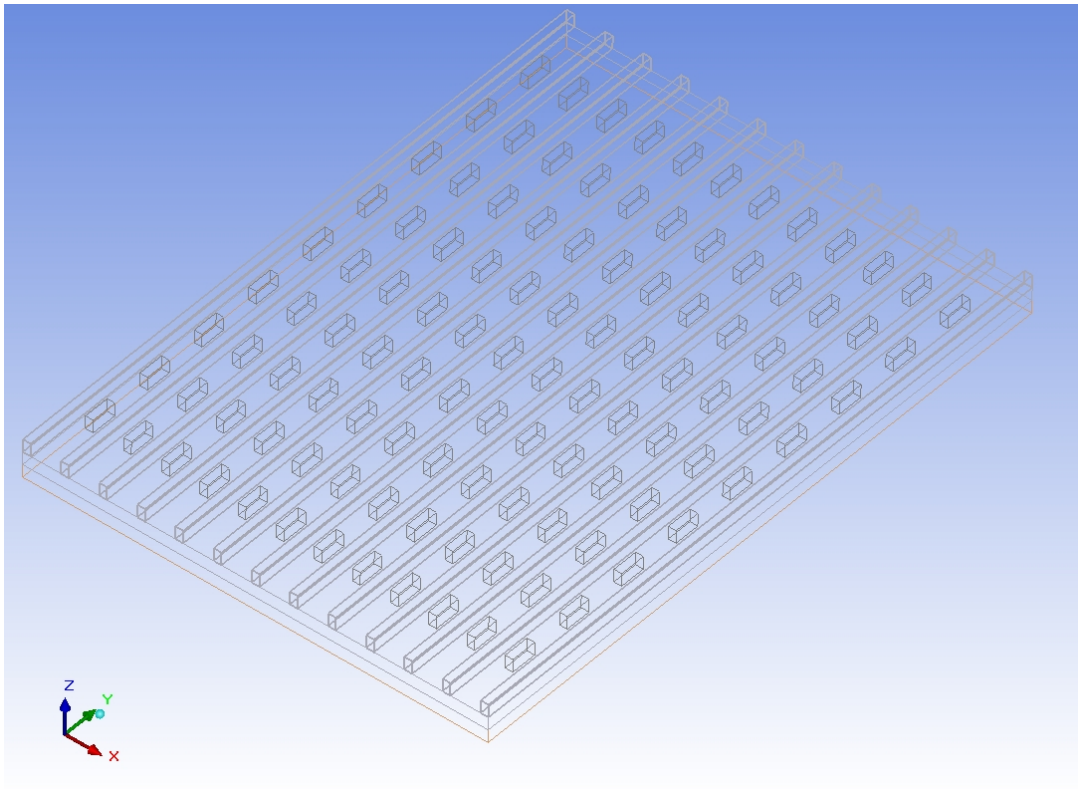

Figure 45 Heat sink with rectangular plate fins in the middle of the channels

In this case, little rectangular plate fins which has 3mm thickness,5 mm lenght and 5mm and 3mm height have been installed into the middle of the channels as it can be seen in Figure 45. 9 disturbance fins have been installed in each channel with 25 mm of distance with each other's center.

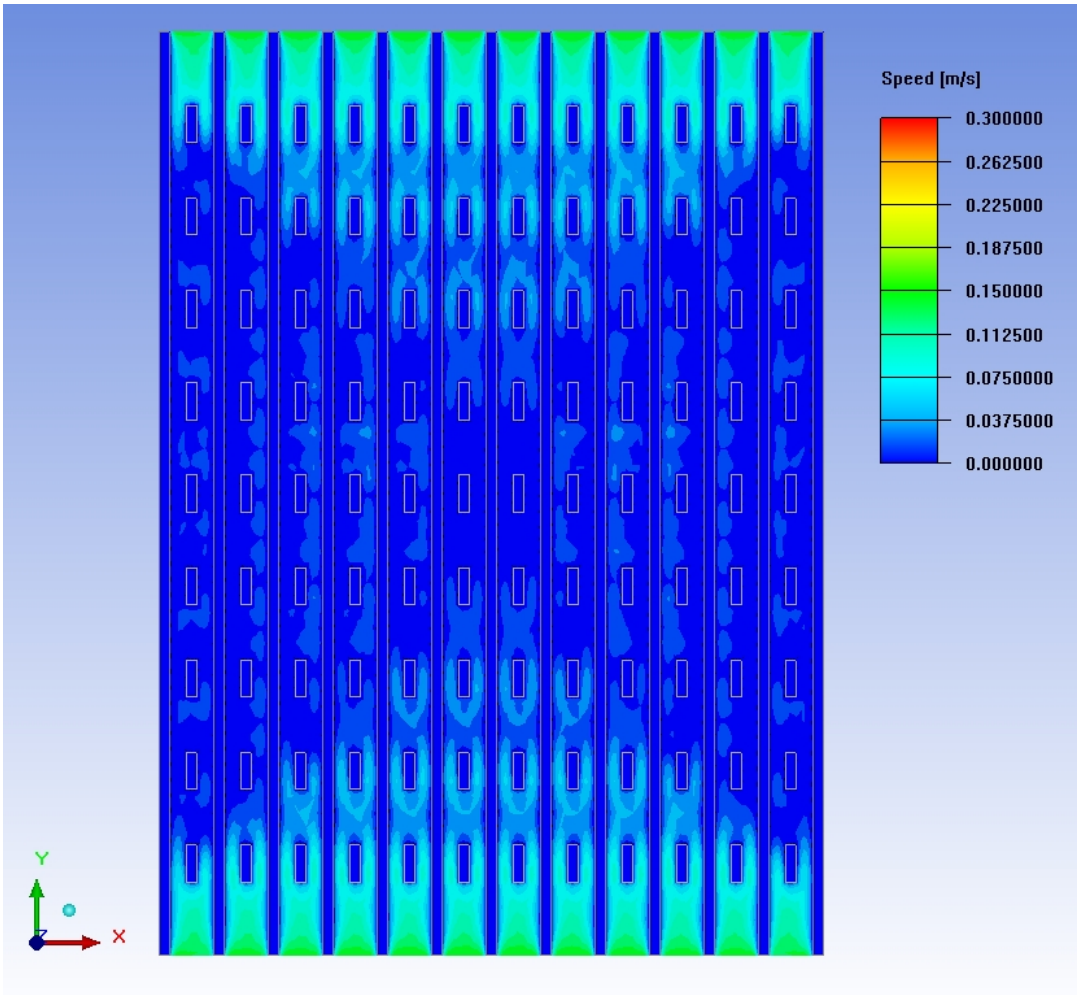

Figure 46 Speed contours above 2mm of the base plate of the heat sink with rectangular disturbance fins of height=5mm in the middle of the channels

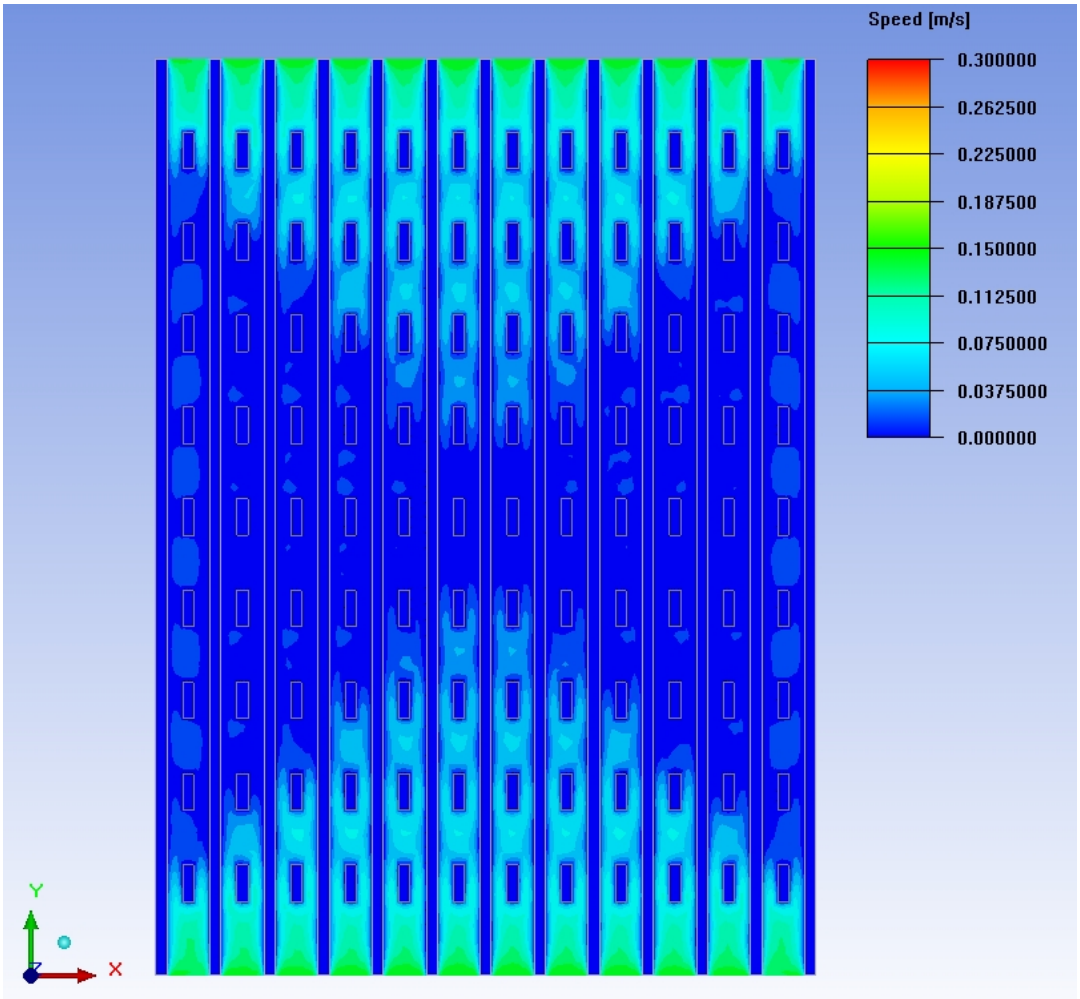

Figure 47 Speed contours above 2mm of the base plate of the heat sink with rectangular disturbance fins of height=3mm in the middle of the channels

From Figure 47 and Figure 48 it can be seen that this methodology only worsened the case because of the head losses it brought to the flow in the channels. Comparing Figure 47 with the Figure 18 shows that this solution increased the area of the recirculating flow zones in addition as it can be seen that the flow in the channels could not reach to the middle of the heat sink unlike in the base case. Comparing the flow visualizations for 5 mm and 3 mm disturbance fin heights; 5 mm case seems to have more recirculation zones compared to 3 mm case.

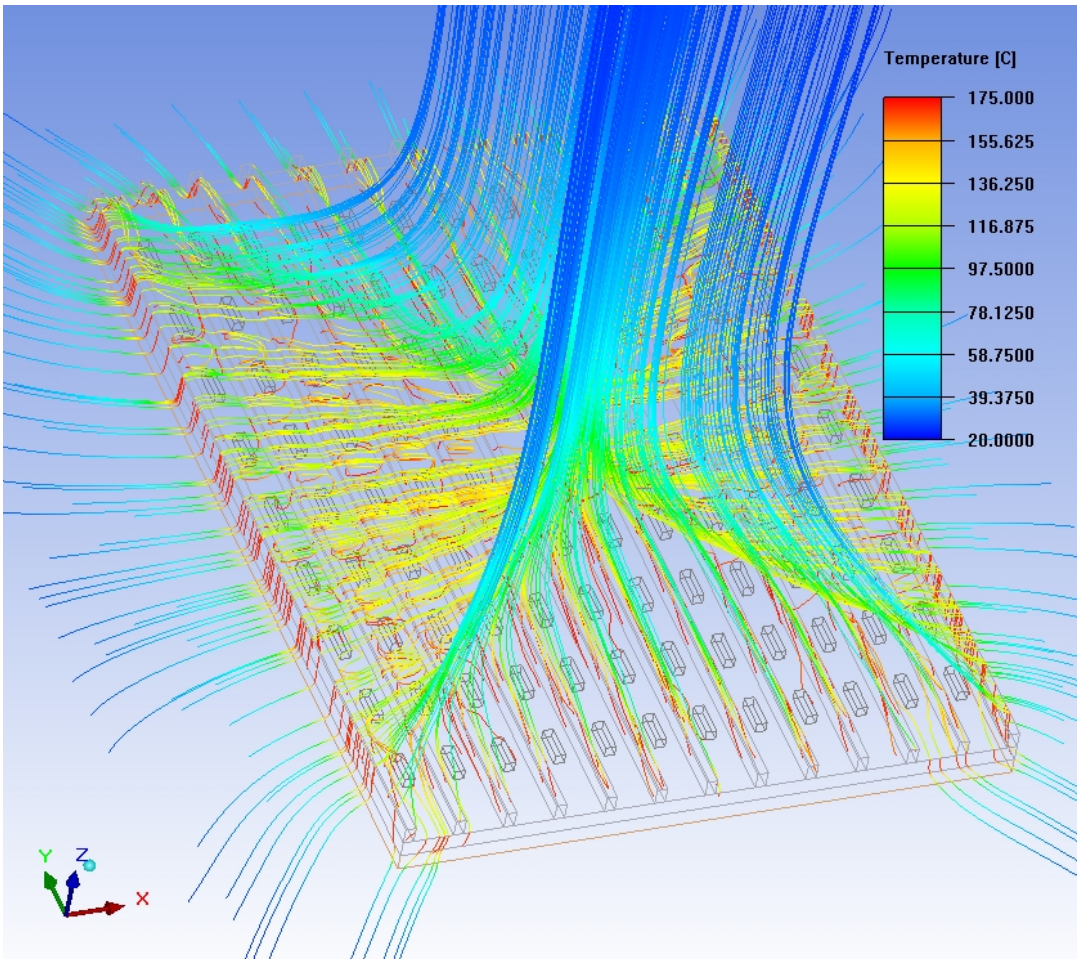

Figure 48 Plate fins disturbance case pathlines coloring based on fluid temperature

Figure 48 shows the pathlines of plate fins disturbance case it can be seen that vortices are still present in recirculating flow zones.

3.3.2 Pin Fins Disturbance Case

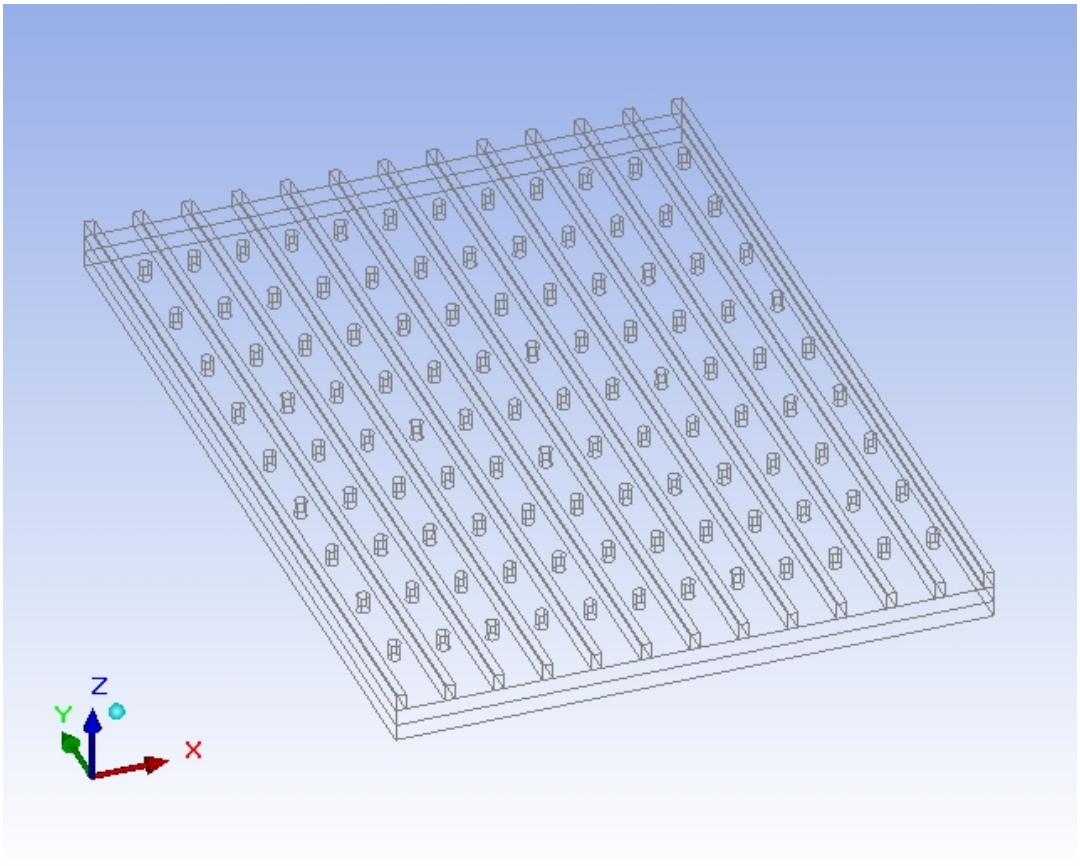

Figure 49 Heat Sink with 5mm Height Pin Fins in middle of the channels

In this case pin fins of 5mm height and 1.8 mm radius have been installed and three different cases has been analyzed for the pin fin case which are

- Pin Fins of 5 mm height and 1.8 mm radius
    - Entire heat sink (Figure 49)
    - 6 middle channels of the heat sink (Figure 50)
    - 10 channels of the heat sink (Figure 51)

9 pin fins have been installed in each channel with 25 mm of distance between their centers.

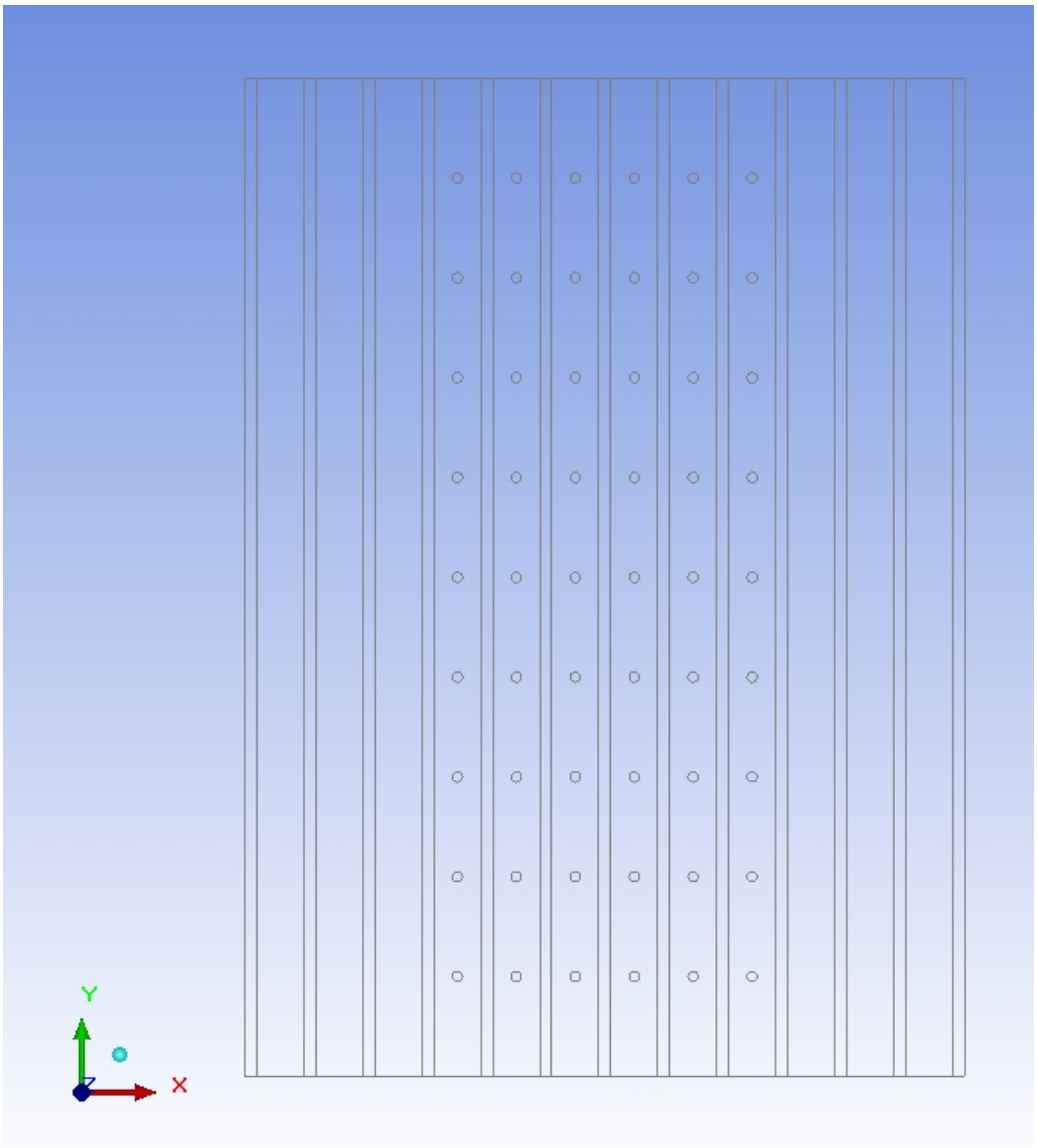

Figure 50 Pin Fins in 6 Channels of the Heat Sink

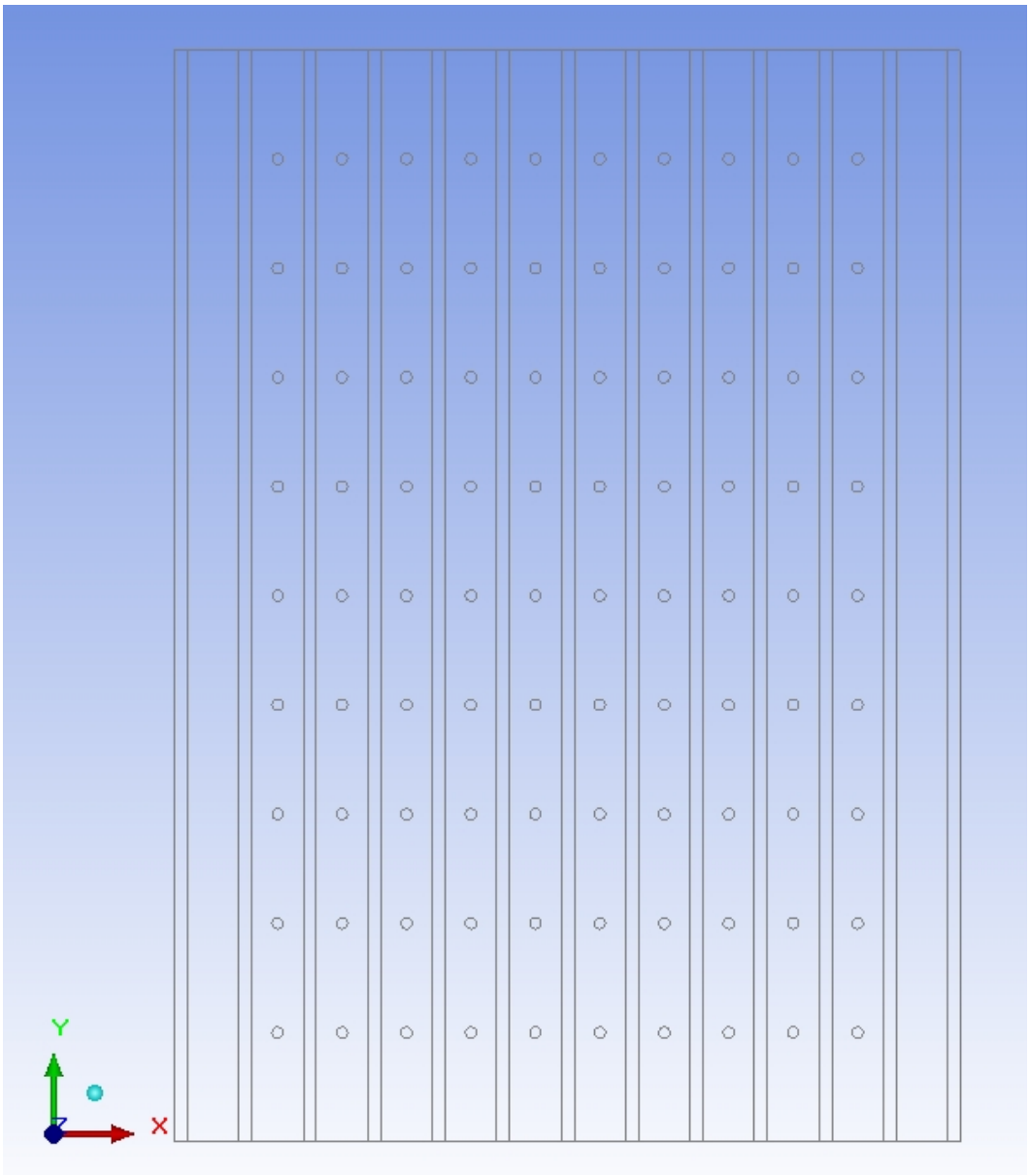

Figure 51 Pin Fins in 10 Channels of the Heat Sink

The flow visualization figures and figures of the enhanced heat sinks are shown in below.

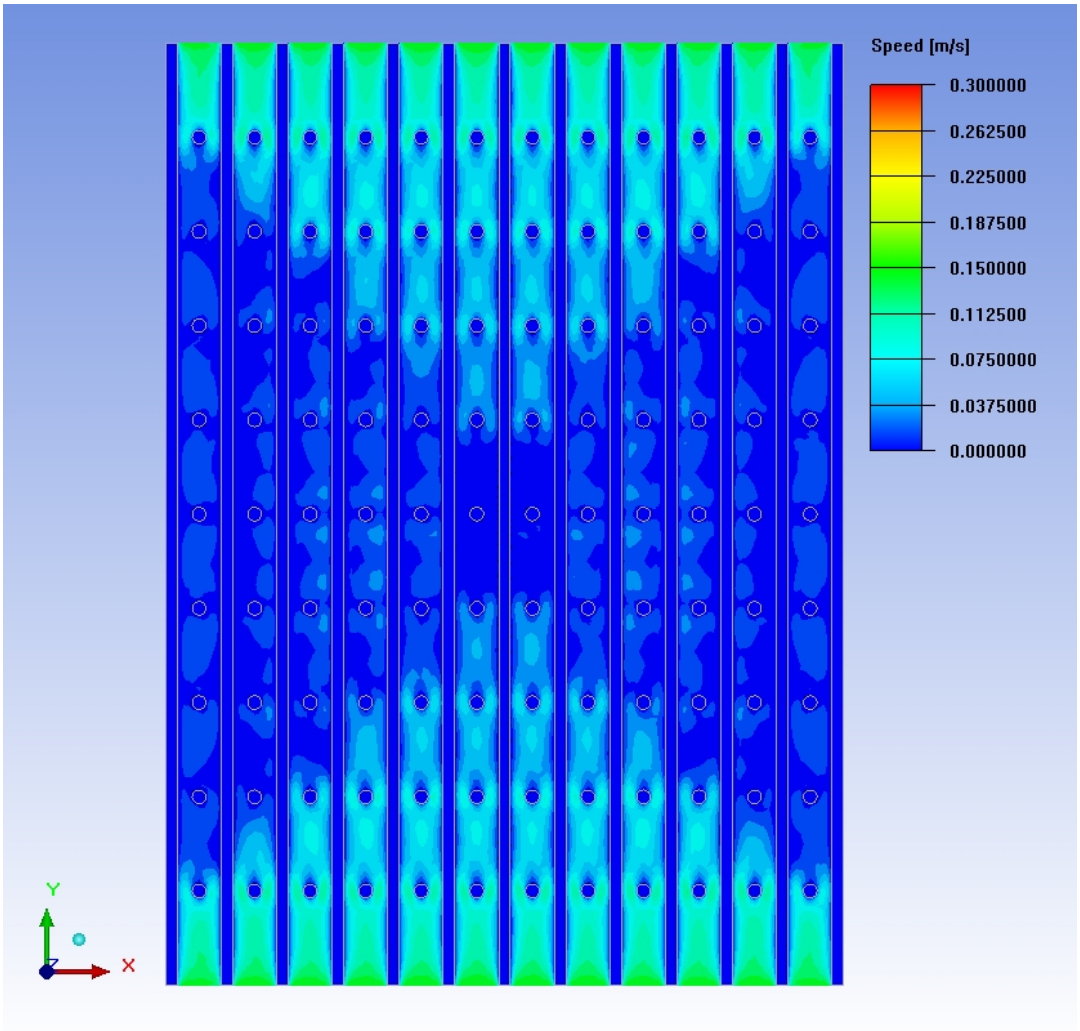

Figure 52 Speed Contours above 2mm of the Base Plate of the Heat Sink with Pin Fins in the Middle

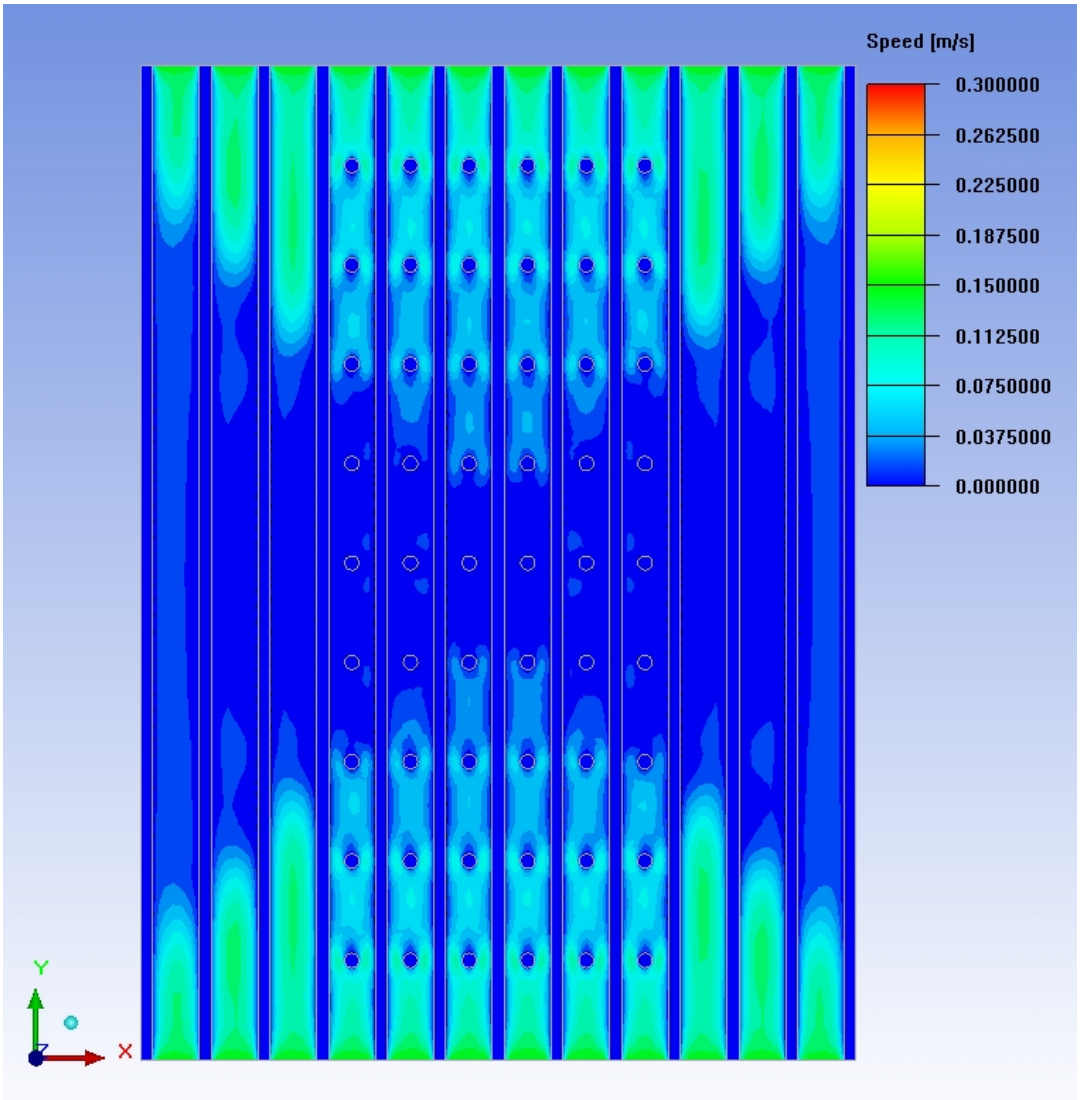

Figure 53 Speed Contours above 2mm of the Base Plate of the Heat Sink Pin Fins in 6 Channels of the Heat Sink

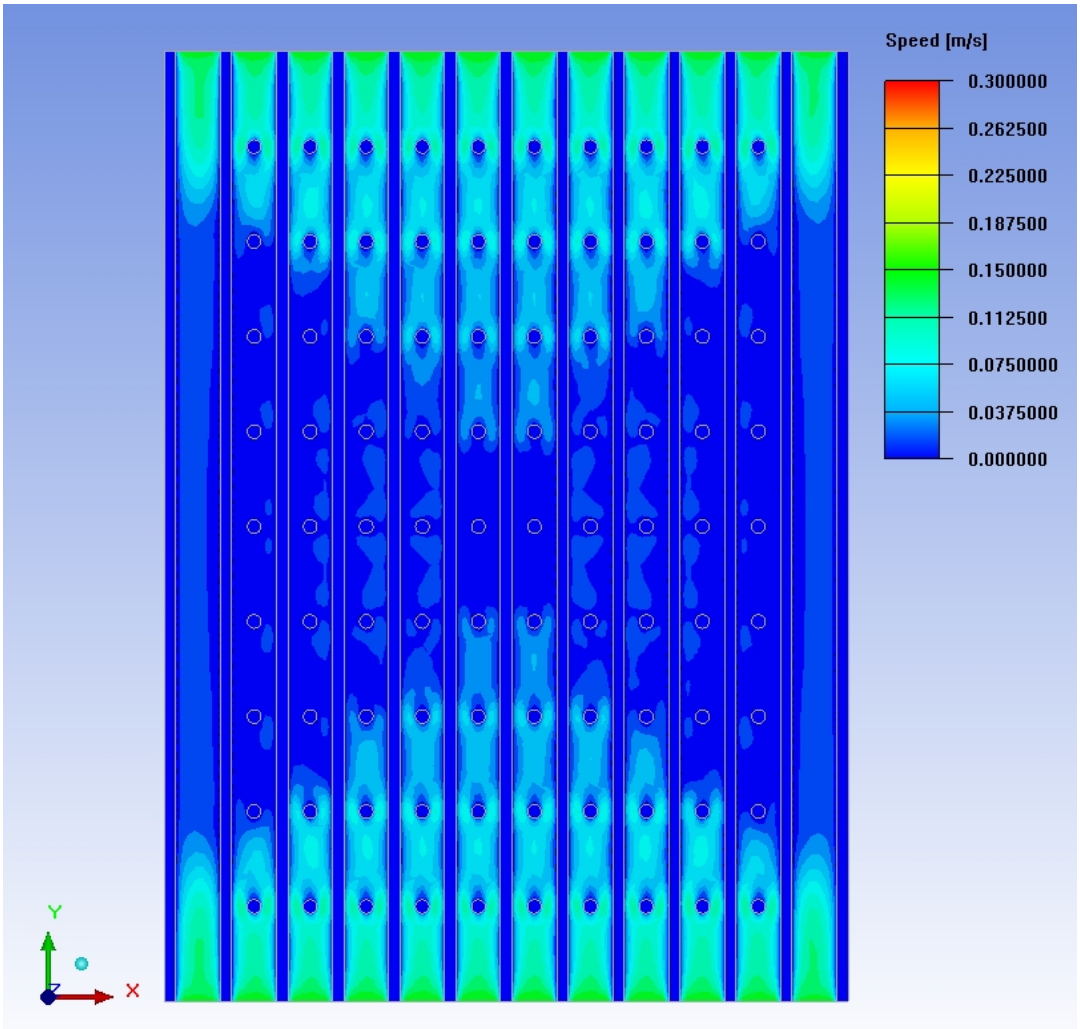

Figure 54 Speed Contours above 2mm of the Base Plate of the Heat Sink Pin Fins in 10 Channels of the Heat Sink

Observation of figures of speed contours above 2mm of the base plate from Figure 52 to Figure 54 shows the following consequences. Like in Plate Fin Disturbance Case, Pin Fin Disturbance Case also created head loss to flow in the channels. Also the area of recirculating flow zones seems to be increased.

Comparison of the results are given in Table 12.

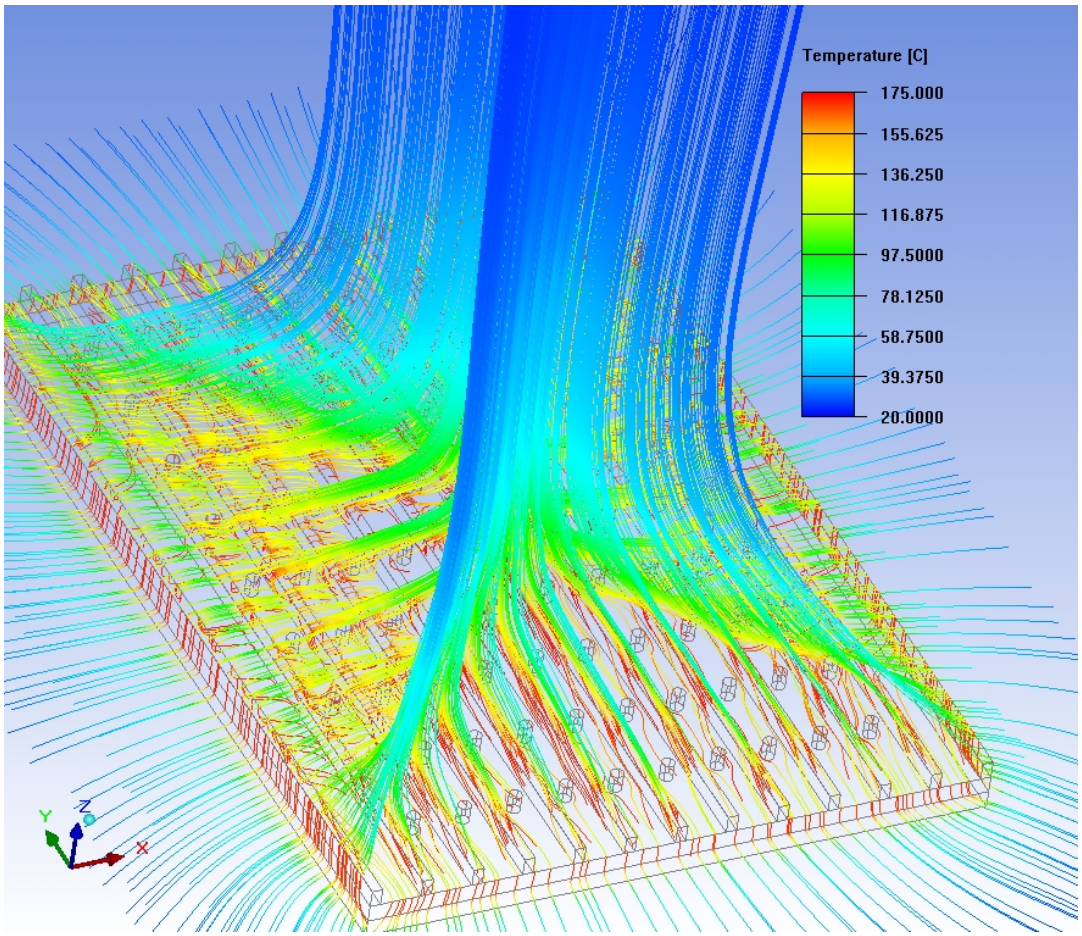

Figure 55 Pin Fin Disturbance Case (10 Channels) Pathlines coloring based on temperature of the air

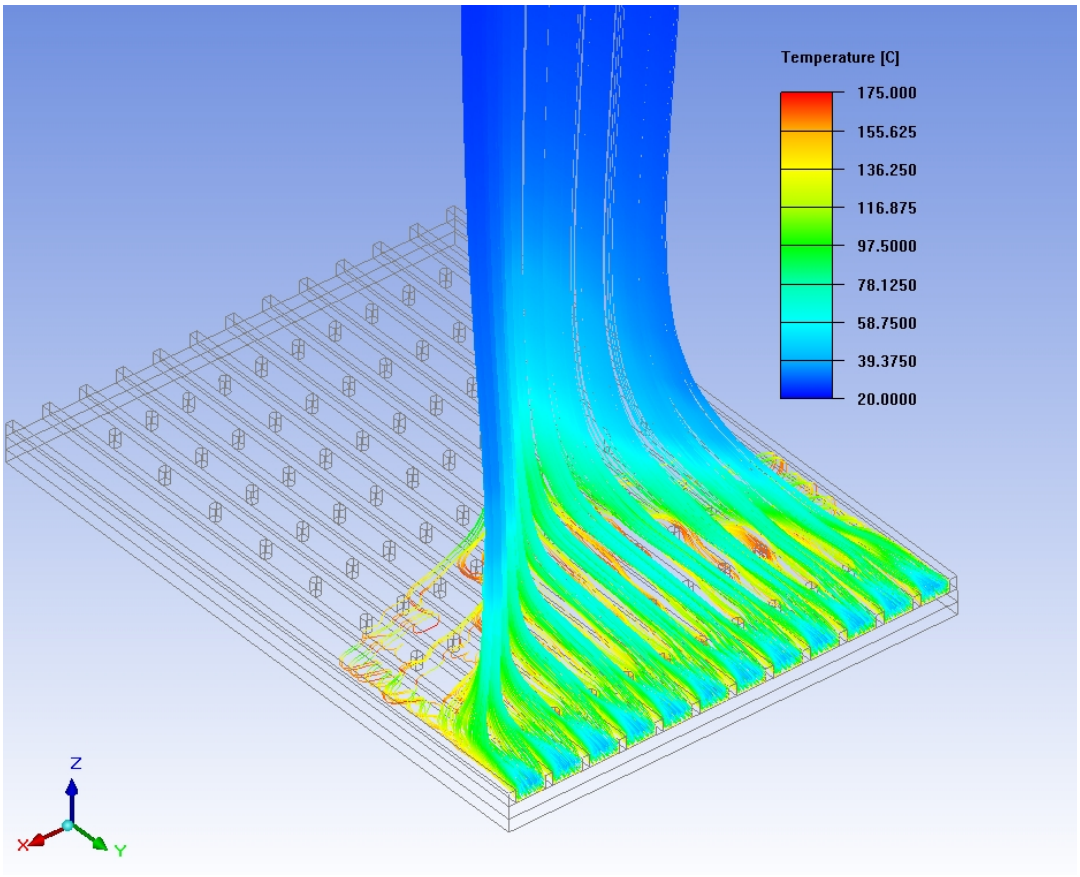

Figure 56 Pathlines of air entering into heat sink channels in Pin Fin Disturbance Case (10 Channels of Pin Fin) coloring based on temperature of the air

Figure 55 and Figure 56 shows the pathlines of the pin fin disturbance case. In the figure the longitudinal vortices in the recirculating flow zones are observed to be not hindered. Also from Figure 56 it can be seen that flow in the middle channels rises before coming to middle part of the heat sink. Speed contour figures also show this consequence. The loss of speed in channels is thought to be the reason for early rising of the fluid.

3.3.3 Results of Disturbance in Channels Case

From the figures of the speed contours of the heat sink it can be understood that this case did not affect the flow to be distributed over the overall flow zone. From

Table 12 it can be concluded that this case has nearly no contribution in heat transfer characteristics of the heat sink. q''_{conv} values have been reduced significantly due to the head losses that the disturbance creators caused. The base temperature has been reduced up to 3.6 °C in Pin Fin Disturbance in Entire Heat Sink case but this is explained by major increase in wet area of the heat sink.

Comparing the plate fins case: the 5 mm height disturbance fins reduced the base temperature more than 3 mm height case despite the flow structure seems worse than the 3 mm case. This can be explained by increasing the wet area of the heat sink more than 3 mm height disturbance case.

It is being thought that the disturbance creators case doesn't have a significant effect in low speed flows as in Natural Convection flows.

Table 12 The results of the Disturbance Creators Case

Case Name	T_{mean} Heatsink Base (°C)	Q_{Total} Heatsink into fluid (W)	Q_{rad} Heatsink (W)	Q_{conv} Heatsink (W)	q" (W/m^2)	q" $_{conv}$ (W/m^2)	q" $_{rad}$ (W/m^2)
Base Case	174,28	95,37	26,82	68,55	1186,36	852,69	333,67
Plate Fins in the Middle (3mm height)	171,18	95,82	27,48	68,34	941,79	668,12	273,68
Plate Fins in the Middle (5mm height)	167,98	96,50	27,56	68,94	898,86	642,15	256,71
Pin Fins in the Middle	170,68	95,91	26,98	68,93	1108,80	796,86	311,94
Pin Fins in the Middle 6 Rows	173,34	95,53	27,21	68,32	1144,88	818,75	326,13
Pin Fins in the Middle 10 Rows	171,52	95,86	27,05	68,81	1121,41	805,01	316,40

Calculation procedure for the values can be found in Appendix B.

3.4 Inspection of Base Case Recirculation Flow Zones

The three different sets of trials that have been explained before did not improve the flow structure. For this reason in order to solve the problem of recirculating flow

zones observed in [19]; first, deeper inspection of the Base Case needs to be performed.

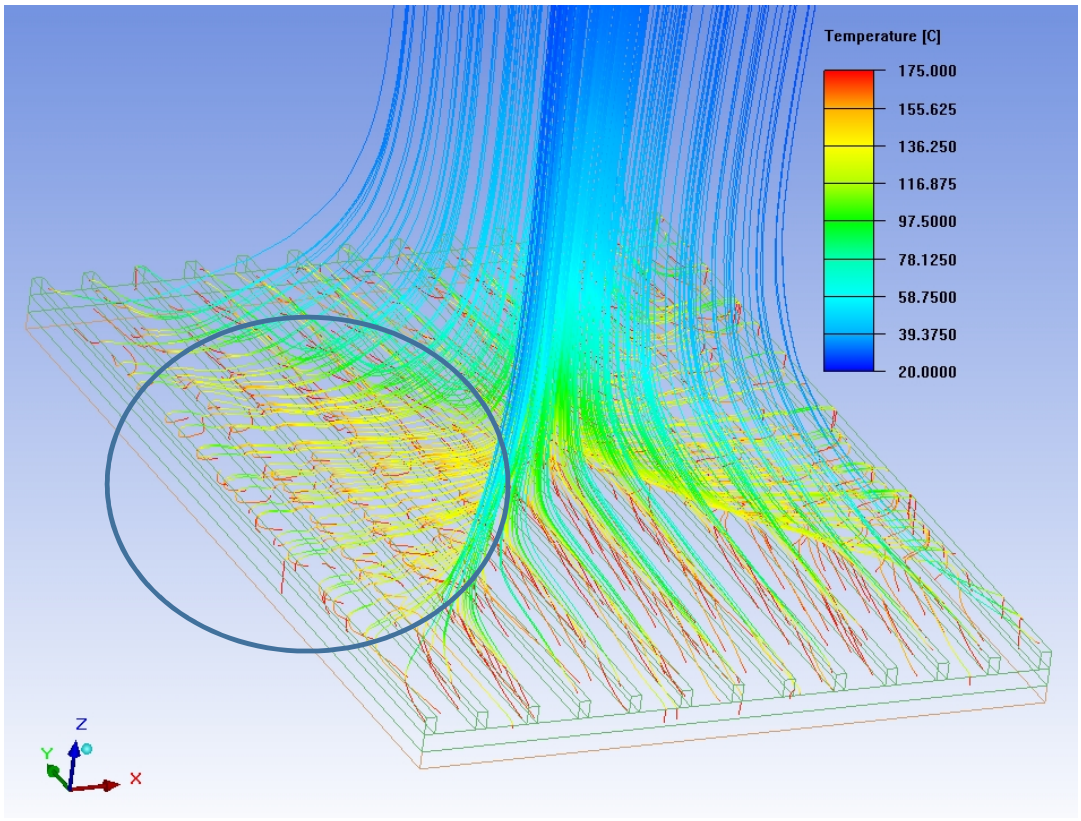

Figure 57 Pathlines of Base Case coloring based on temperature of the air

Examining the pathlines of the base case it was inferred that the X shaped flow in the heat sink is similar to the pathlines entered from the lateral sides of the heat sink as in Figure 57. Examining together Figure 58 and Figure 59 it has been observed that pathlines of air entering from the left side start where the flow stagnates in the channels, rises and joins the chimney structure. These figures resulted in a consequence that the X shaped recirculation flow is dependent on side air flow. For this reason, further inspection of side air flow has been conducted.

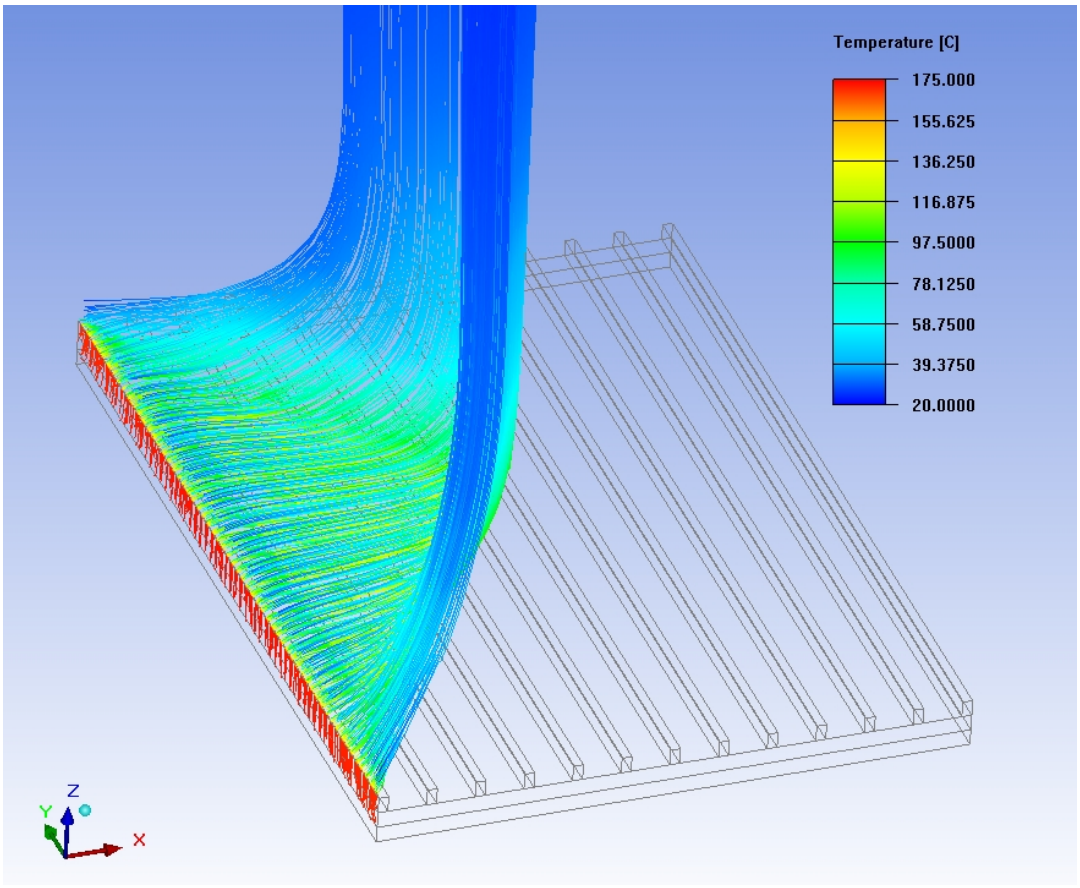

Figure 58 Pathlines of the air enters above the heat sink from left in Base Case coloring based on temperature of the fluid

Figure 58 shows the pathlines of air entering to the heat sink zone from the left side this figure shows that there is a secondary flow occurring above the heat sink.

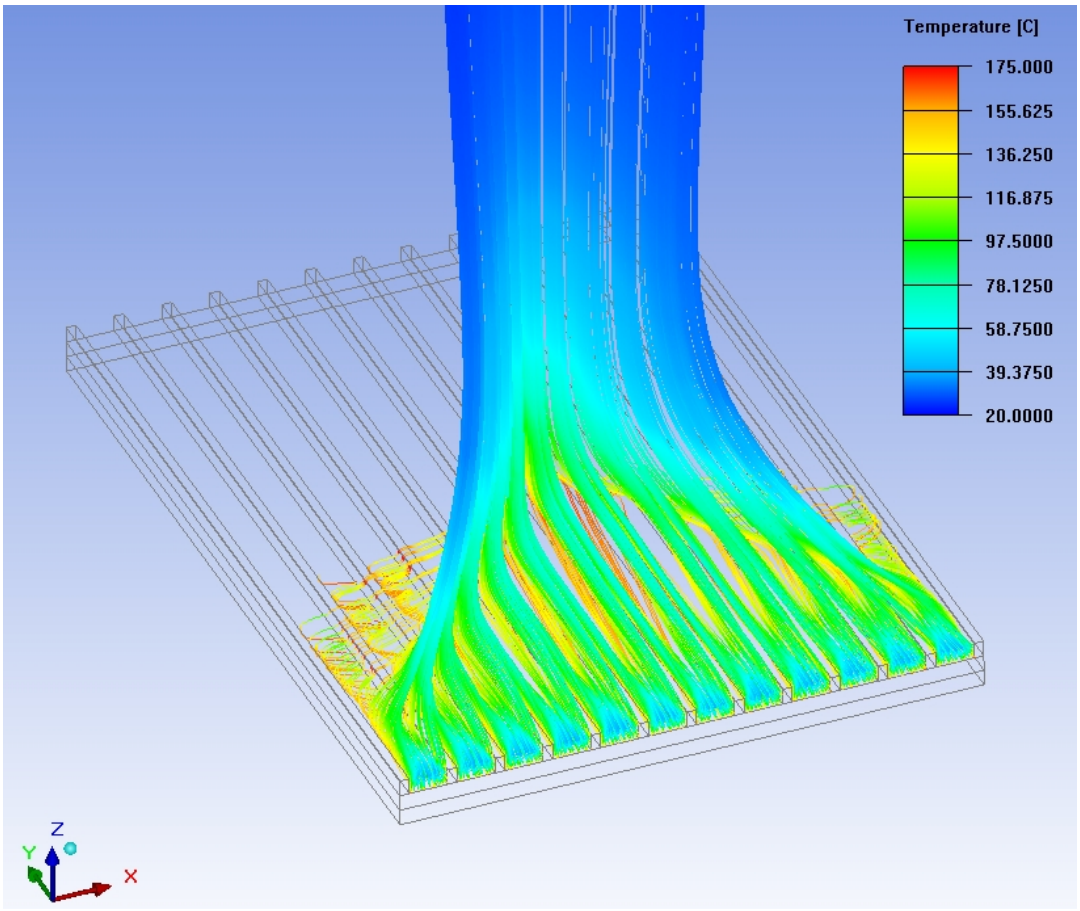

Figure 59 Pathlines of the flow enters into heat sink through the channels in Base Case coloring based on temperature of the fluid

Figure 59 shows pathlines of air entering into heat sink channels. Observing together Figure 58 and Figure 59 shows that the air rises in the channels when they mix with the side air flow.

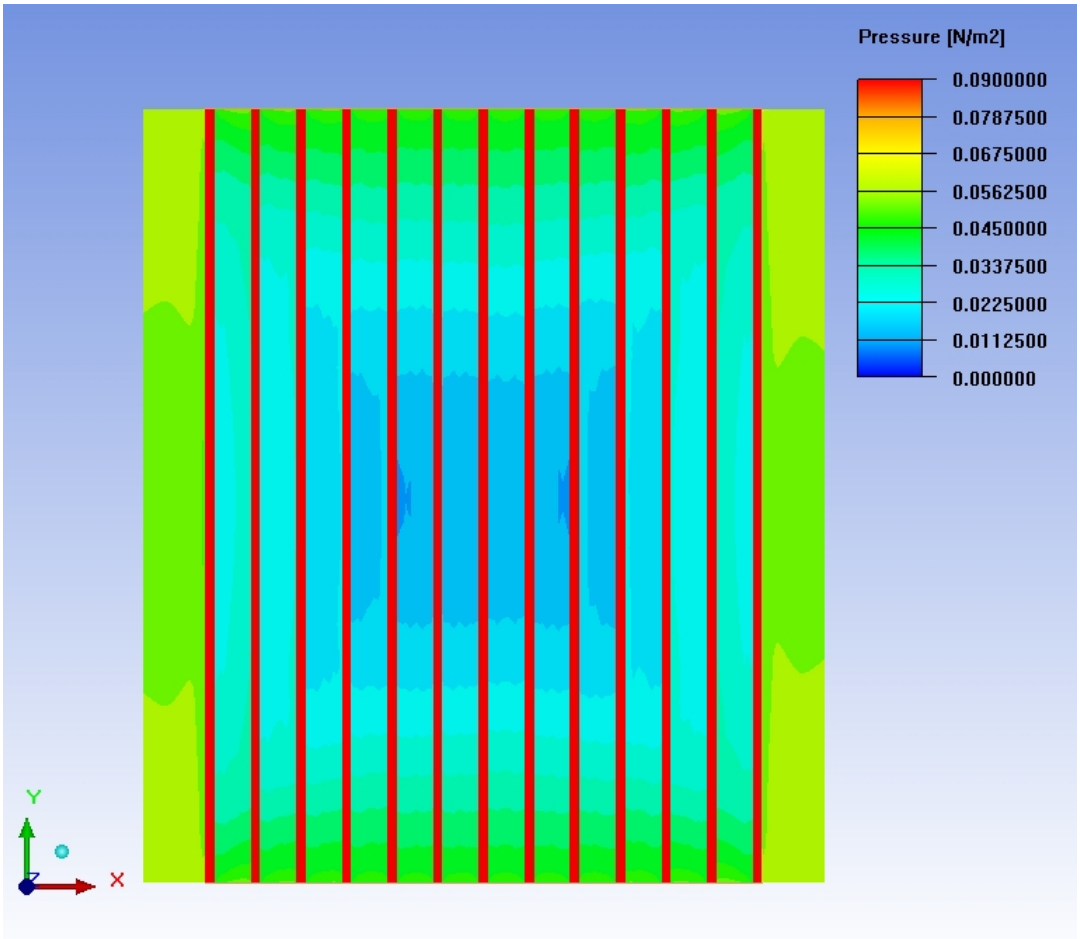

Figure 60 Pressure Contours at the tip of the fins of the Base Case (Red lines represent heat sink fins)

The reason for the dynamics of the side air flow needs to be examined. Observing Figure 60 shows that there is a low pressure zone in the middle of the heat sink. As it can be seen in Figure 58; the air enters from the left side of the heat sink tends to move to low pressure zone in the middle of the heat sink. This situation creates an additional air flow other than the flow in the heat sink channels.

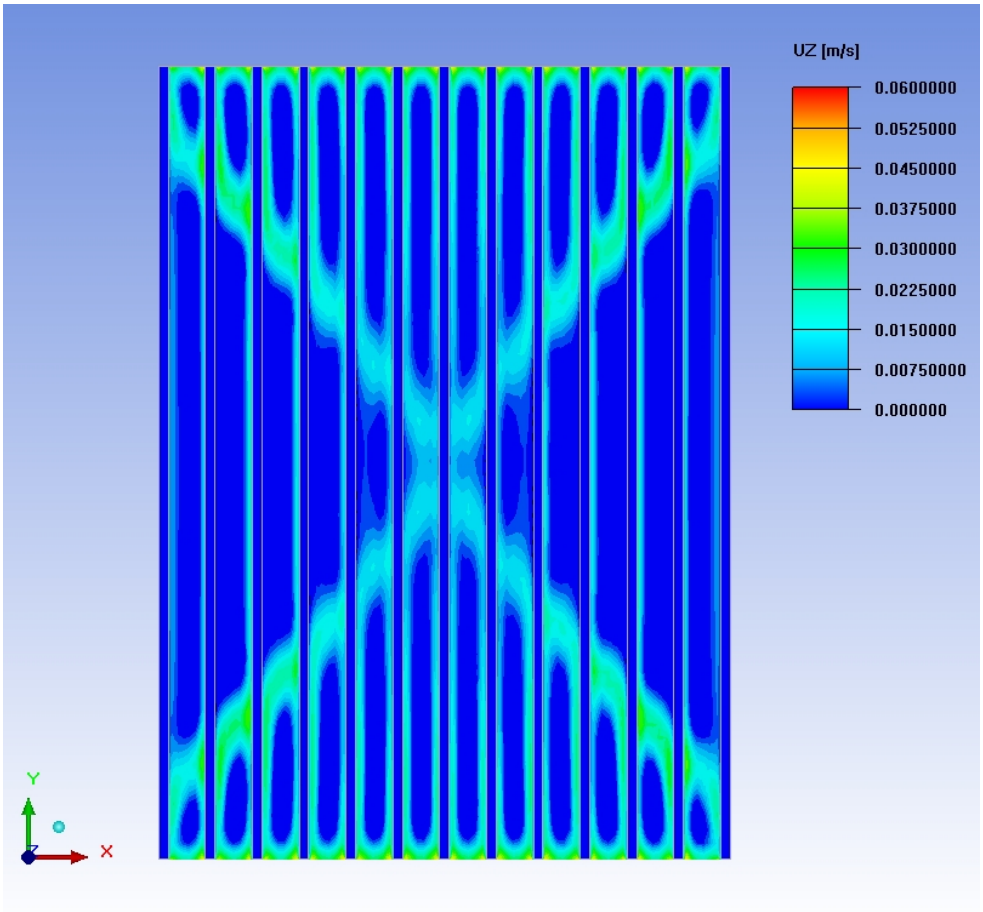

Figure 61 Contours of speed in +z direction at the tip of the fins of the Base Case (5 mm above the base plate)

The upper zone flow creates a suction force for the air that is moving in y direction in the channels. Figure 61 shows the speed in +z direction at the tip of the fins. This speed contour figure shows that the air in the channels is being sucked into the air flow in the upper zone of the heat sink which can be seen in Figure 58. This phenomenon causes the air in the channels to move upwards before reaching to the middle of the heat sink channels therefore causing ineffective natural convection cooling.

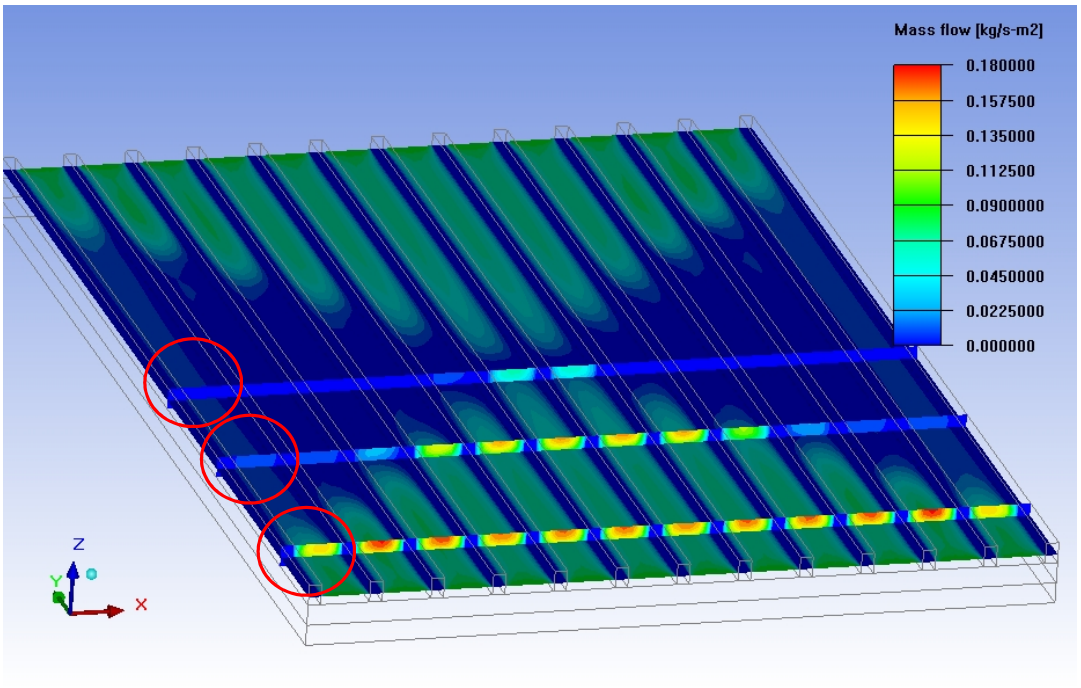

Figure 62 Contours of mass flow rates in the channels combined with speed above 2 mm of the base plate contours of the Base Case 10 mm, 50 mm and 100 mm away from the mid-plane respectively

Observing Figure 62 shows that there is nearly not a presence of air in the stagnated flow zones in the channels of the heat sink. Examining the marked channel in Figure 62, it can be understood that most of the fluid is being sucked by the upper flow; the remaining fluid in the channels first exhibits longitudinal vortex behaviour and then it also rises to join the chimney.

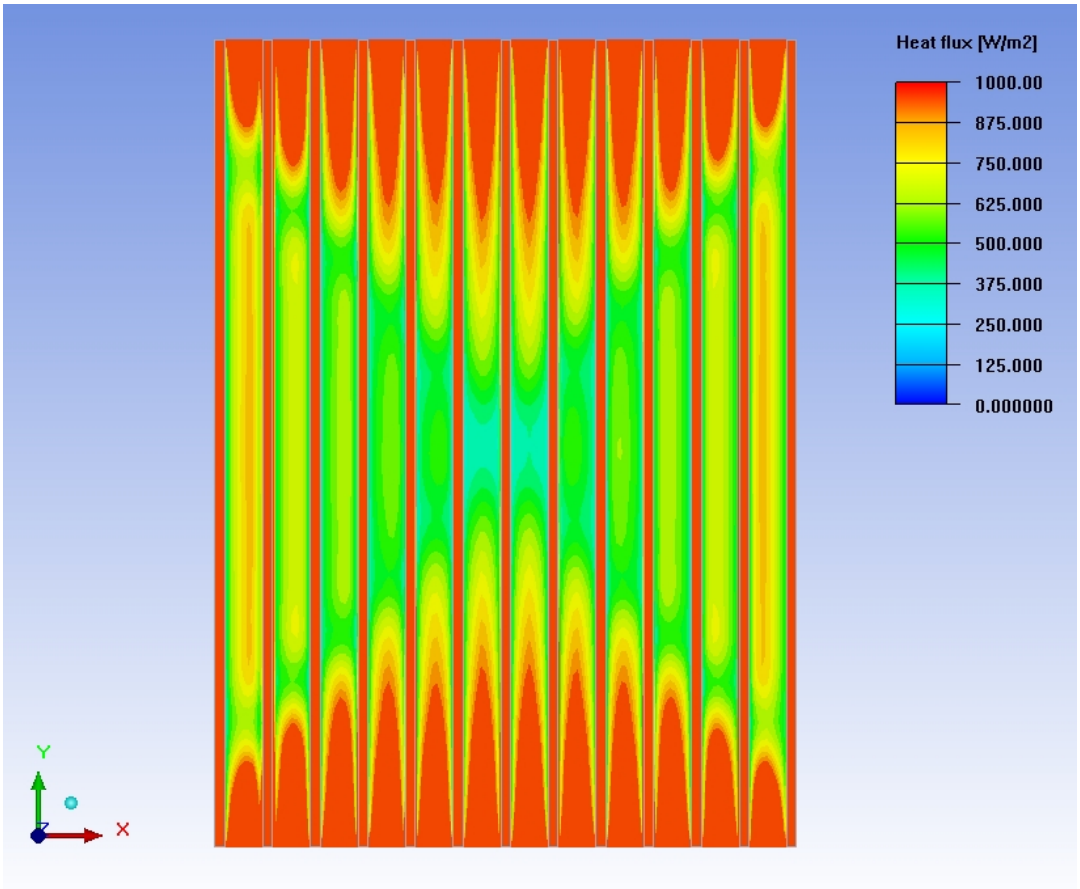

Figure 63 Heat flux contour of the heat sink base of Base Case (Red coloured zones yield higher heat flux values compared to green coloured zones)

Figure 63 shows the heat flux contours of Base Case base plate; in this figure it can be seen that heat flux values decrease nearly half of its values in the flow stagnated parts.

The longitudinal vortices that has been observed in [19] as in Figure 59 occur when the fluid enters into the suction zone which is created by the upper secondary flow. After entering into suction zone most of the fluid in the channels joins the upper secondary flow; the air that has been left in the channels exhibits longitudinal vortices due to the spoiled flow structure in the absence of the pressure driven flow.

Figure 64 shows the pressure distribution in the channels; it can be observed that the pressure is nearly constant after the flow stagnation points.

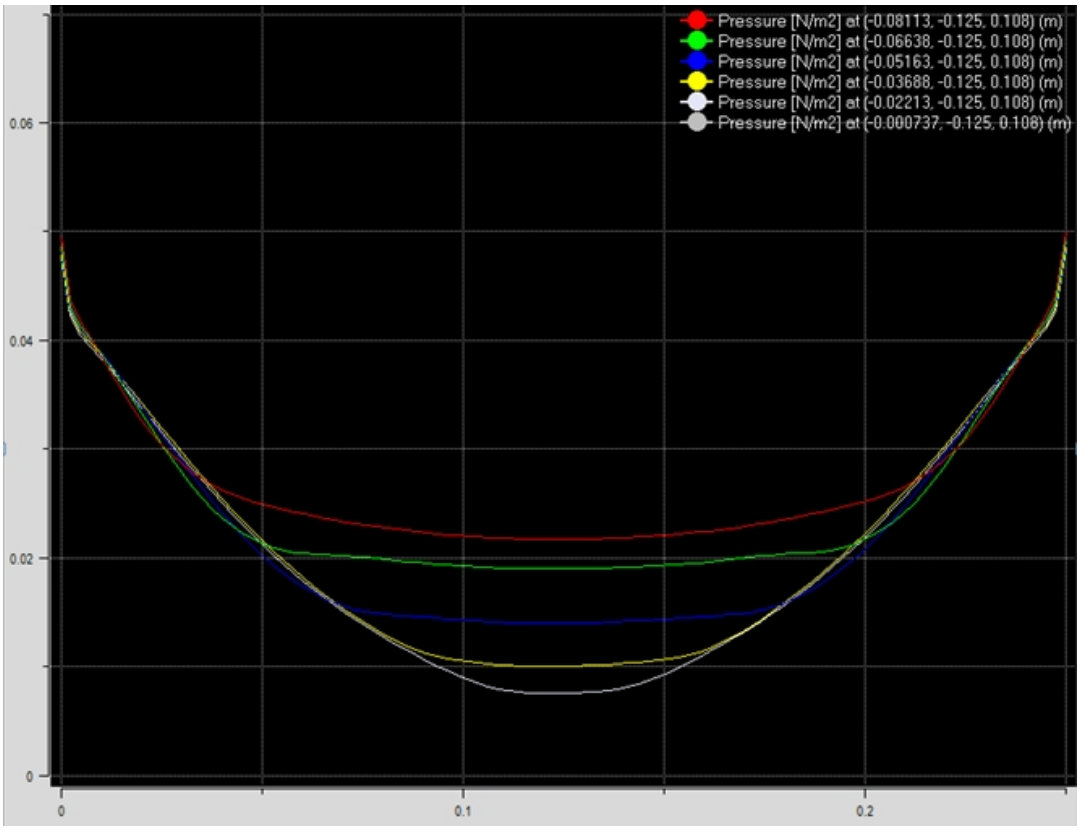

Figure 64 Pressure Variation in Channels of the Base Case, x axis represents heat sink channel length in mm while y axis represents pressure in the channels in N/m^2 (White Line: fifth channel from left side, Yellow Line: fourth channel from left side, Blue Line: third channel from left side, Green Line: second channel from left side, Red Line: first channel from the left side)

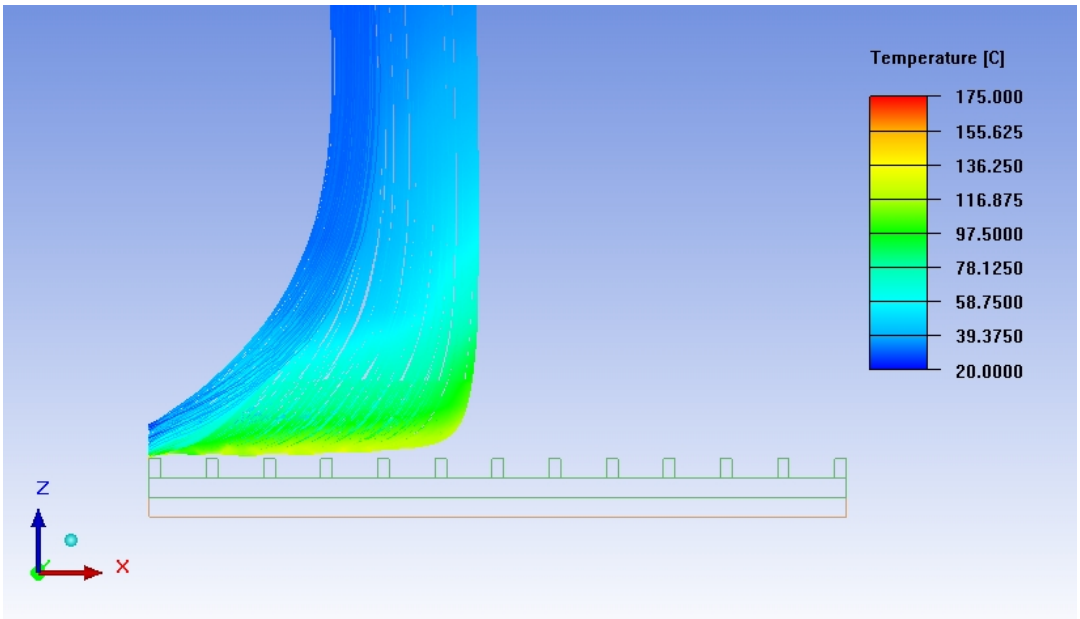

Figure 65 Pathlines of the air enters above the heat sink from left in Base Case coloring based on fluid temperature

The longitudinal vortices observed in Base Case are leftovers from the air entering into the channels, not the lateral air flow. Observation of Figure 65 shows that the lateral air flow does not come into the channels.

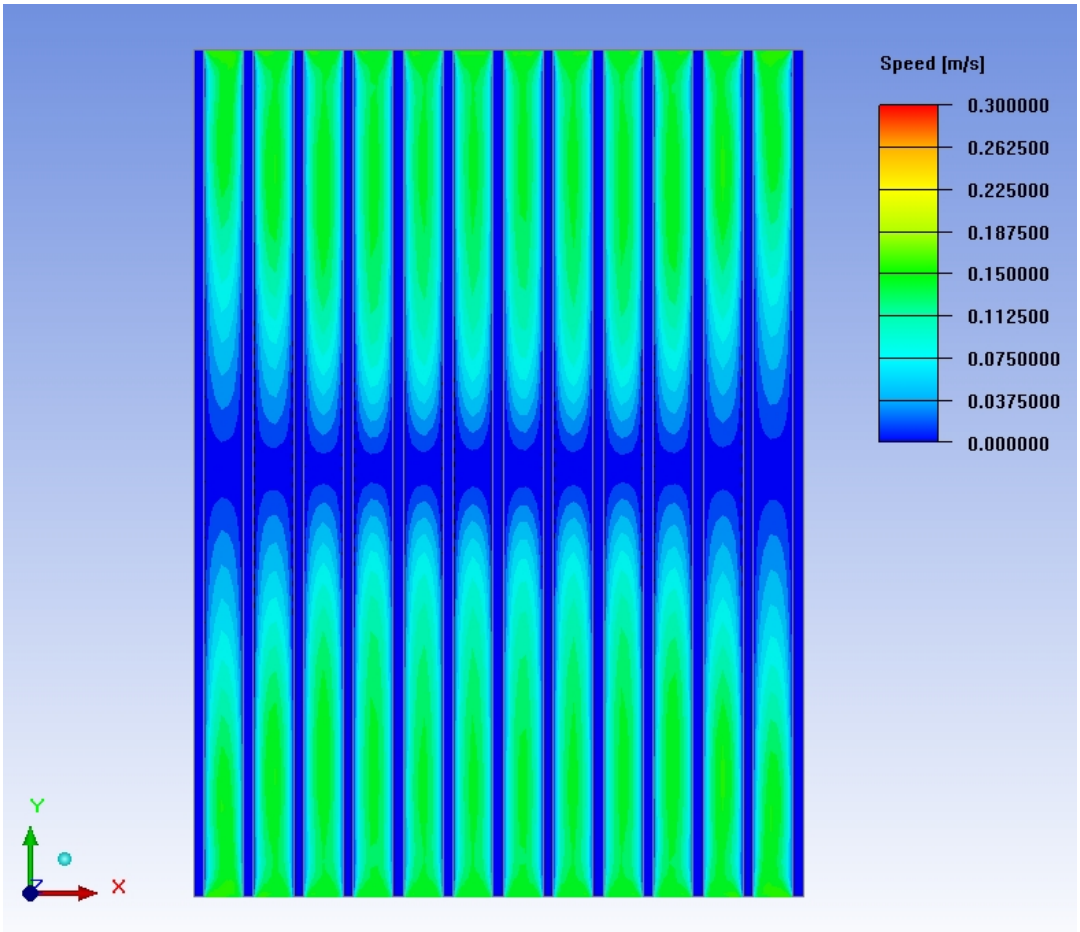

Figure 66 Speed contours above 2 mm of the heat sink base plate in Conventional 15 mm fin height heat sink

Figure 66 shows the speed contours above 2 mm of the heat sink base in 15 mm fin height conventional heat sink. From this figure it can be understood that this type of heat sink has regulated flow in the channels and do not exhibit recirculating flow zones.

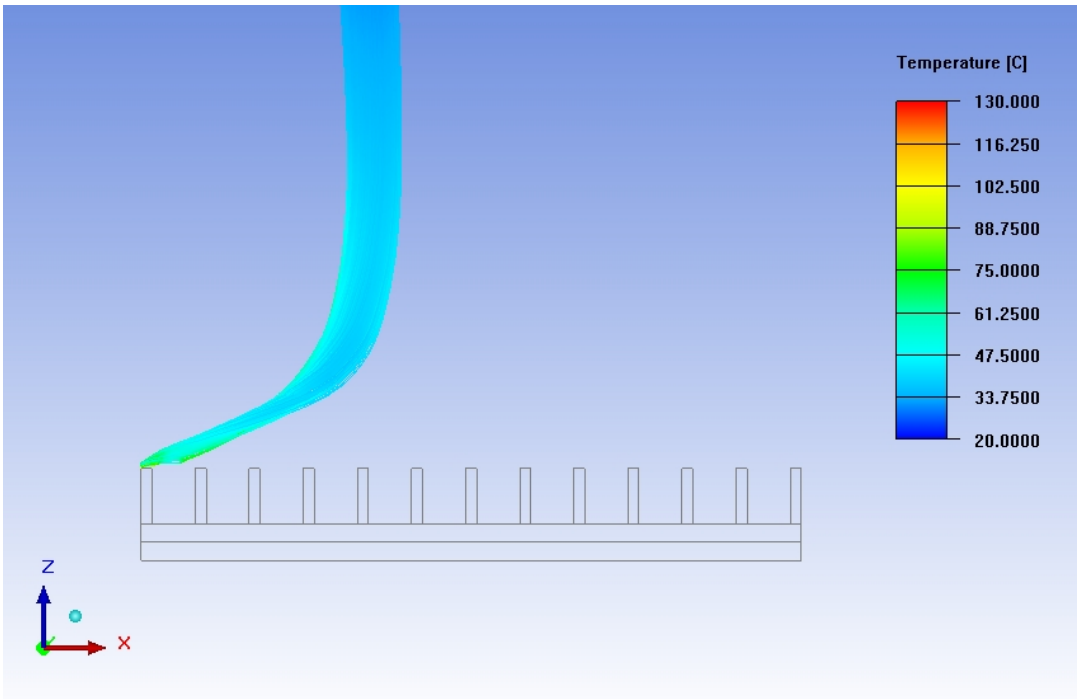

Figure 67 Pathlines of the air enters above the heat sink from left side in Conventional 15 mm fin height heat sink with all the other parameters are same as Base Case except Fin Height; coloring based on fluid temperature

Figure 67 shows the pathlines of air entering into heat sink zone from the left side for a conventional plate finned heat sink which has 15 mm fin height. Unlike the case in Figure 65 which shows the pathlines of air entering into heat sink zone from the left side for the Base Case the lateral air flow rises and do not follow a path touching the fins of the heat sink. Therefore for higher fin heights the interference of lateral air with flow in channels did not observed. For this reason the air in the channels is not being sucked by the lateral air flow in higher fin height heat sinks.

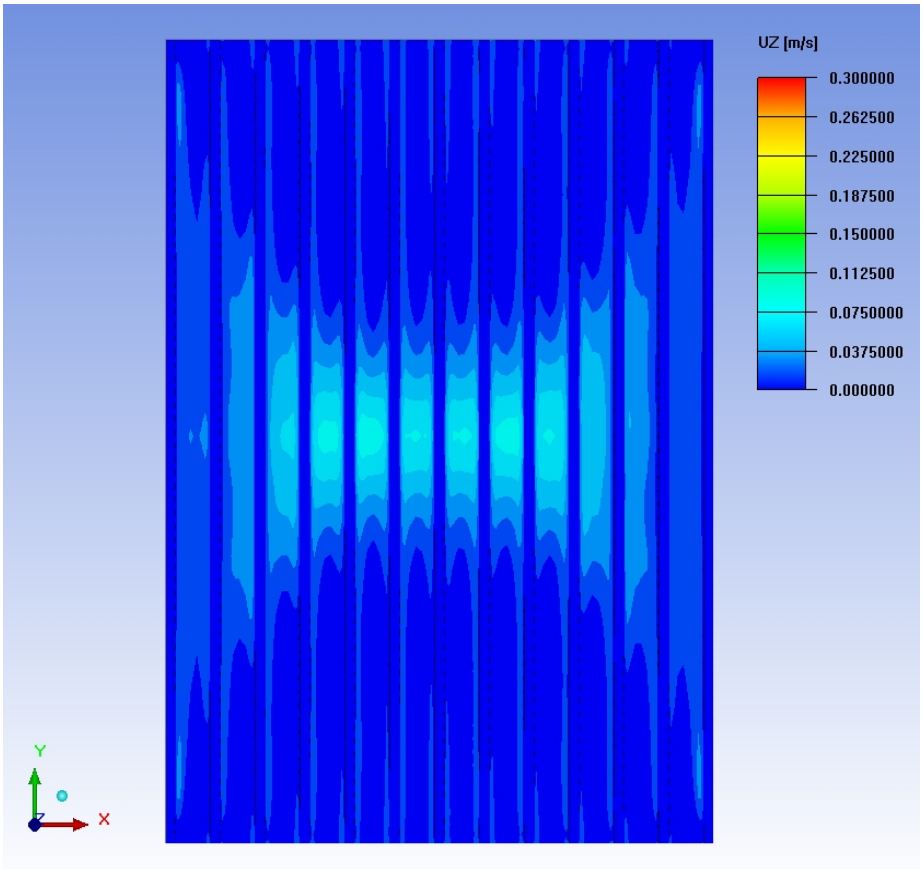

Figure 68 Contours of speed in +z direction at the tip of the fins of the Conventional Heat Sink with 15 mm fin height (15 mm above the base plate)

Figure 68 shows the speed in z direction figure at the tip of the fins in 15 mm fin height conventional heat sink. Comparing this figure with Figure 61 which shows the speed in z direction at the tip of the fins for Base Case. An X Shaped flow is not present here and this shows a single chimney type flow occurs for conventional 15 mm fin height heat sink.

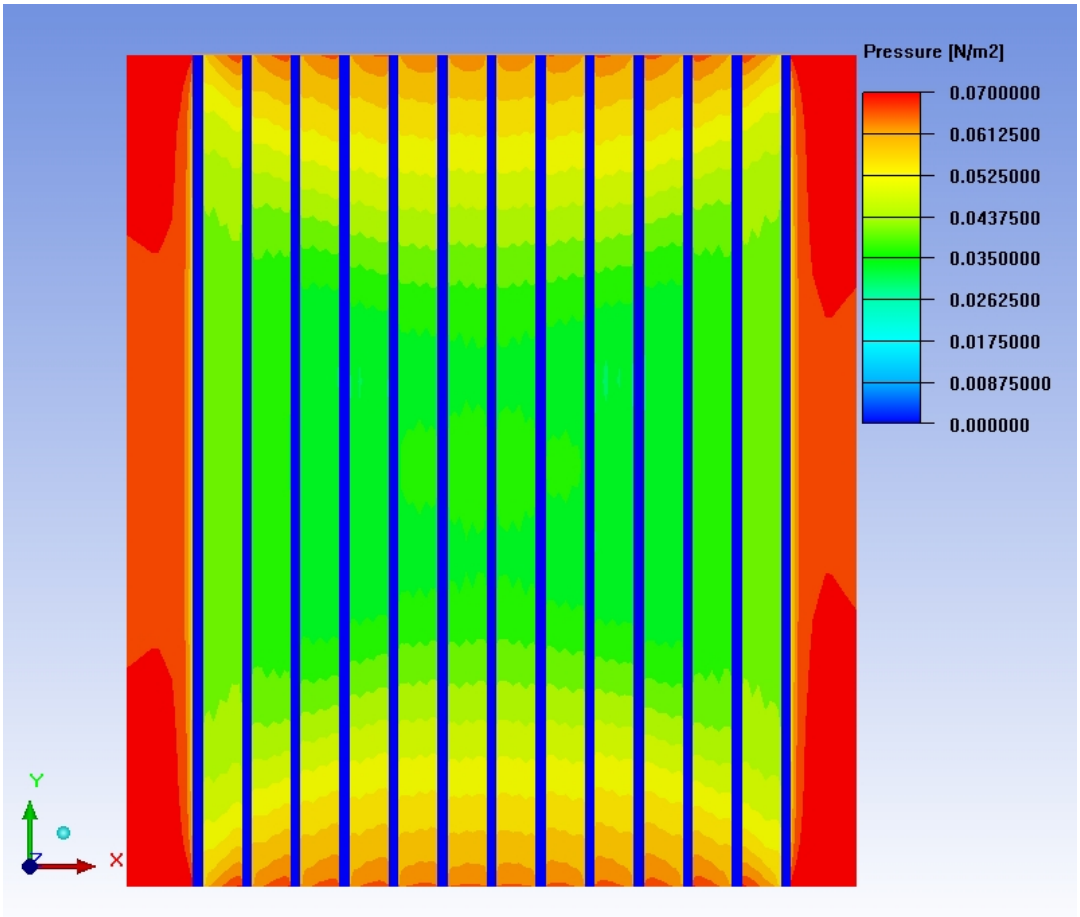

Figure 69 Pressure Contours at the tip of the fins in conventional 15 mm height finned heat sink (Blue lines represent heat sink fins)

Examining Figure 69 shows the pressure contours of a conventional 10 mm fin height heat sink. From this figure it can be observed that there is not a major low pressure zone at the middle of the heat sink unlike the base case. Therefore the air from the sides do not be forced to move to the middle part of the heat sink unlike in Base Case.

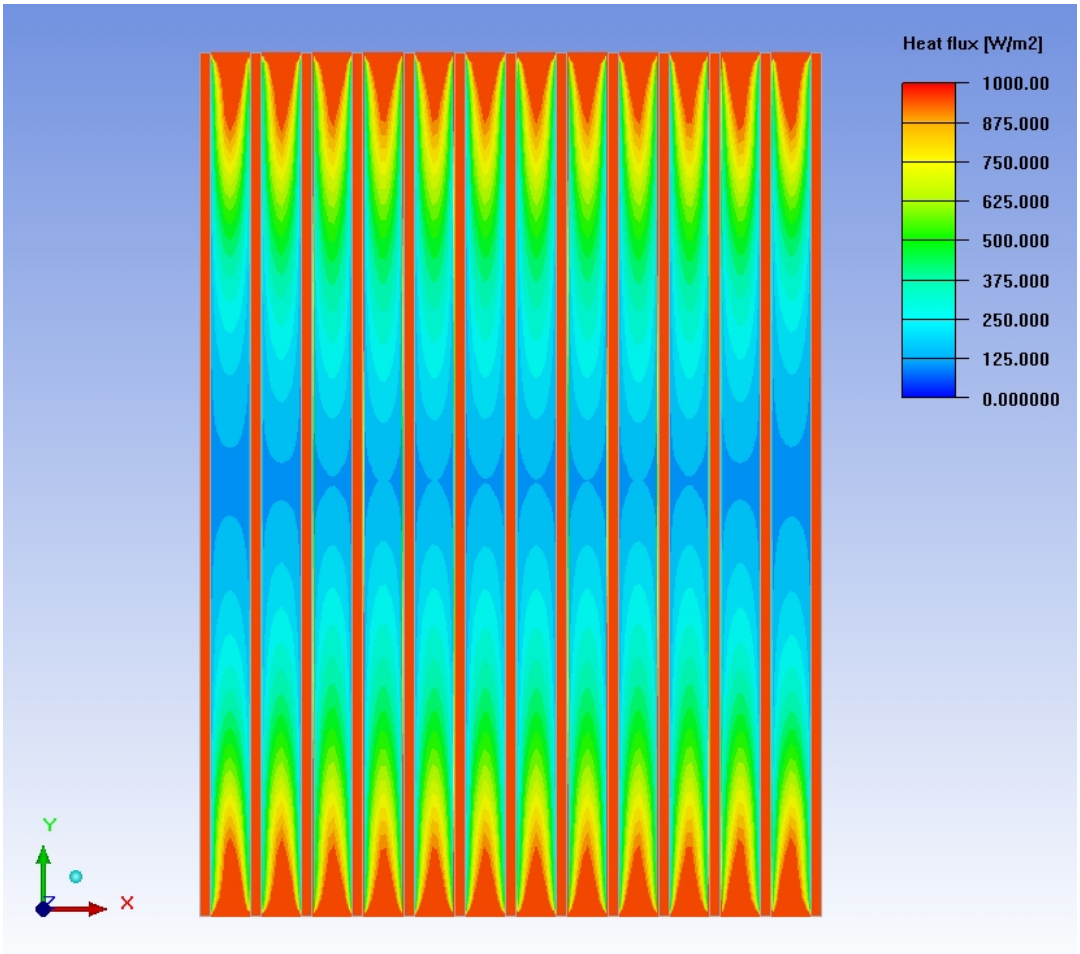

Figure 70 Heat flux contour of the heat sink base of 15 mm fin height conventional heat sink (Red and green coloured zones yield higher heat flux values compared to blue coloured zones)

Figure 70 shows the heat flux contours of the conventional 15 mm fin height heat sink's base. It uses the same scale as Figure 63 which yields the heat flux contours of Base Case's heat sink base. Comparing two of them using the same contouring scale makes it hard to understand the heat transfer difference between two cases since the flux values for the Base Case is higher than the conventional 15 mm fin height case. Therefore Figure 71 will be used for better understanding of comparison between two cases. Figure 71 represents the heat flux contours for the 15mm fin height conventional heat sink on a different contouring scale. It can ben seen that the

overal heat flux only reduces at the mid plane of the heat sink in which chimney occurs on top of it. However for the Base Case chimney structure occurs in a wider zone because of the lateral air flow coming from the sides this leads to increasing the area of recirculating flow zones and reducing heat transfer performance.

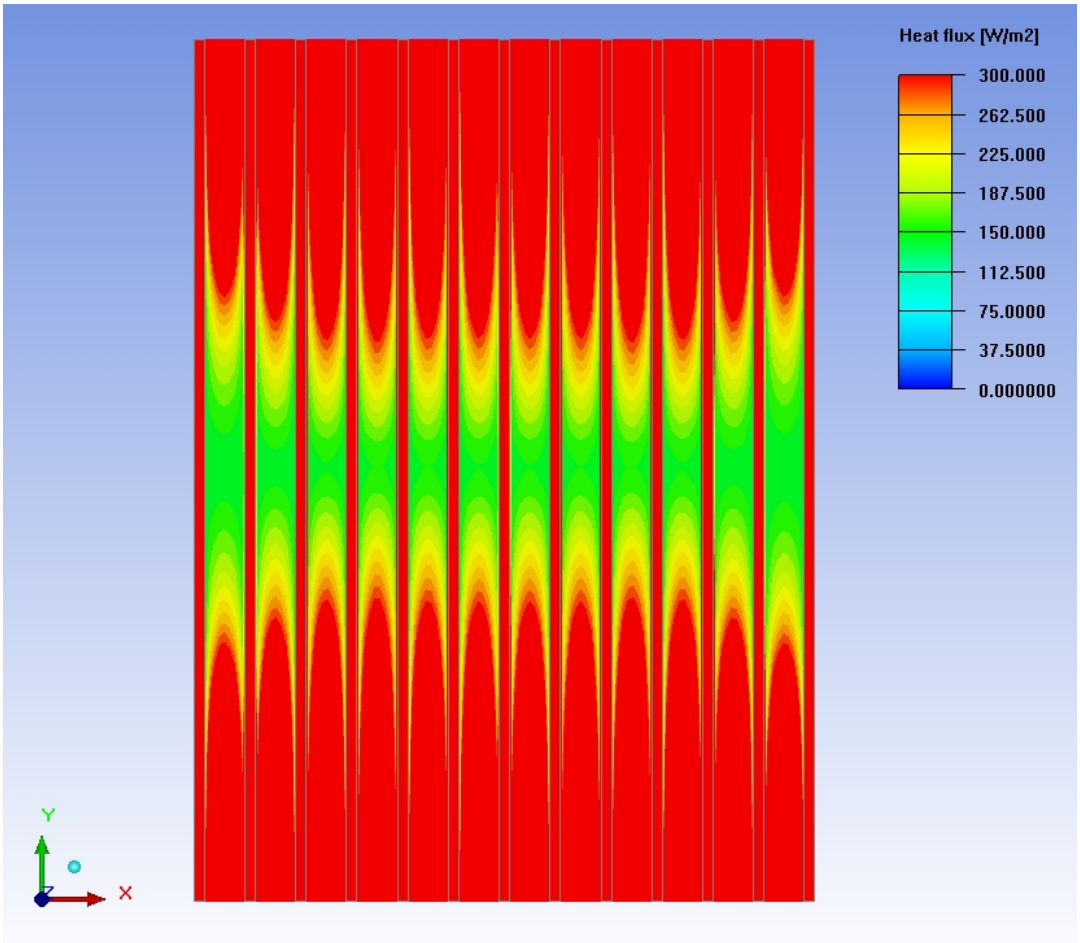

Figure 71 Heat flux contour of the heat sink base of 15 mm fin height conventional heat sink with a different contouring scale (Red coloured zones yield higher heat flux values compared to green zones)

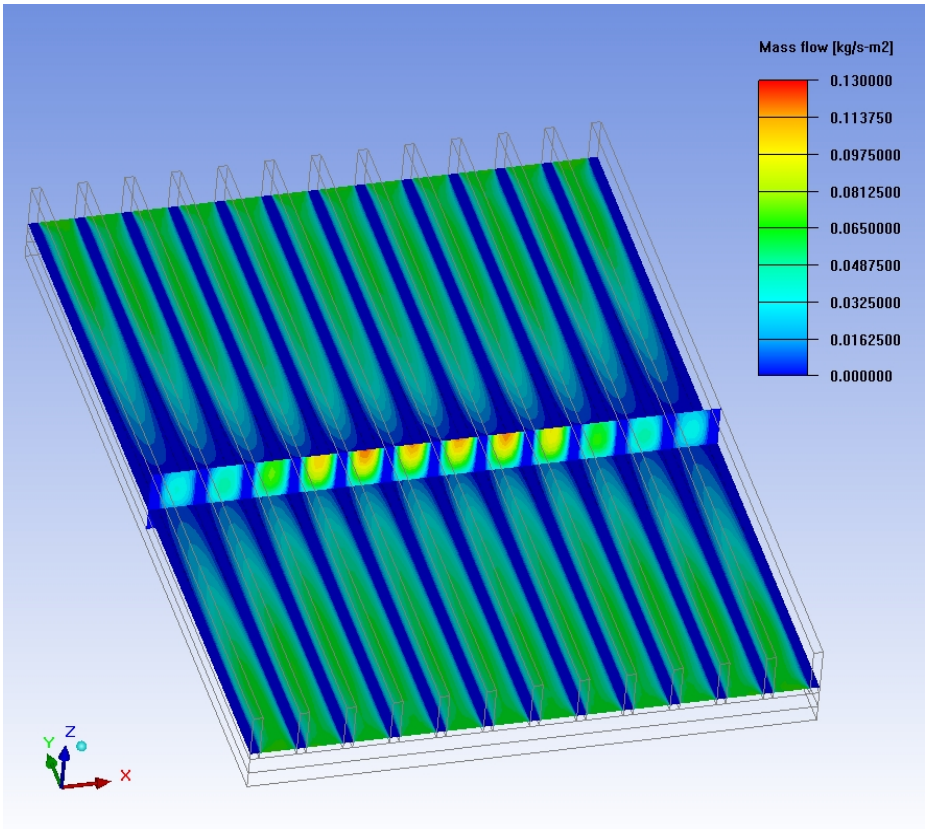

Figure 72 Contours of mass flow rates in the channels combined with speed above 2 mm of the base plate contours of the 15 mm fin height heat sink 10 mm away from the mid-plane

Figure 72 shows the mass flow rate in channels of the 15 mm fin height heat sink away from 10 mm of the mid plane. As it can be seen unlike the Base Case a major reduction in mass flow rate in channels has not been exhibited.

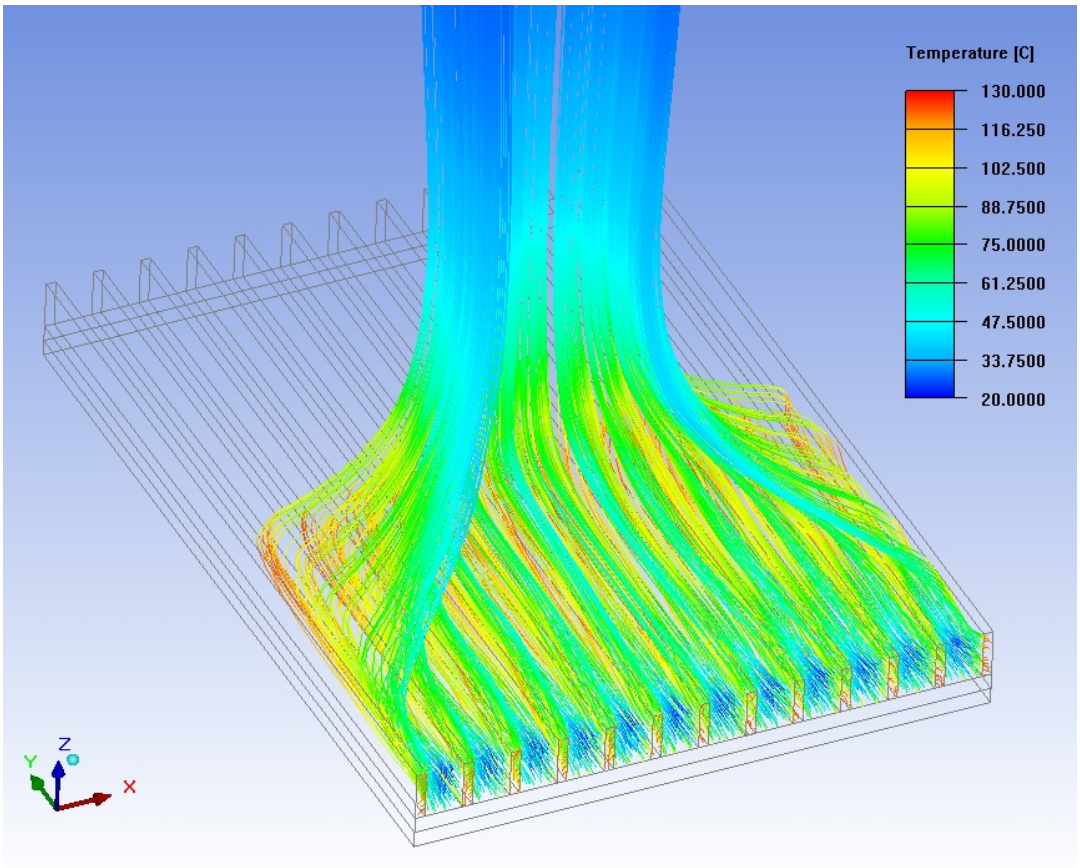

Figure 73 Pathlines of air entering into heat sink for 15 mm fin height conventional heat sink coloring is based on temperature

Figure 73 shows the pathlines of air entering into heat sink for 15 mm fin height conventional heat sink. There are some flow joining to chimney before coming to the middle of the heat sink. But from Figure 72 and Figure 68 we understand that this joining of the fluid is not major as the case in Base Case.

3.5 High End Fins Solution

Lateral air flow entering from the sides of the heat sink has been observed to disturb the flow in the channels by sucking the air in the channels to the upper secondary lateral flow. For this reason High End Fins Case has been analyzed. In this case the end fins on the left and right sides has been increased in order to observe the effect on high fins' effect on flow structure and heat transfer performance.

5 different end fin heights have been analyzed.

- HE=10mm End Fins
- HE=15mm End Fins
- HE=20mm End Fins
- HE=25mm End Fins

Figure 74 shows the figure of the 25 mm High End Fins Case. This figure illustrates the High End Fins Case. It can be observed that the end fins on the sides has been increased to 25 mm while middle fins' height has not been changed.

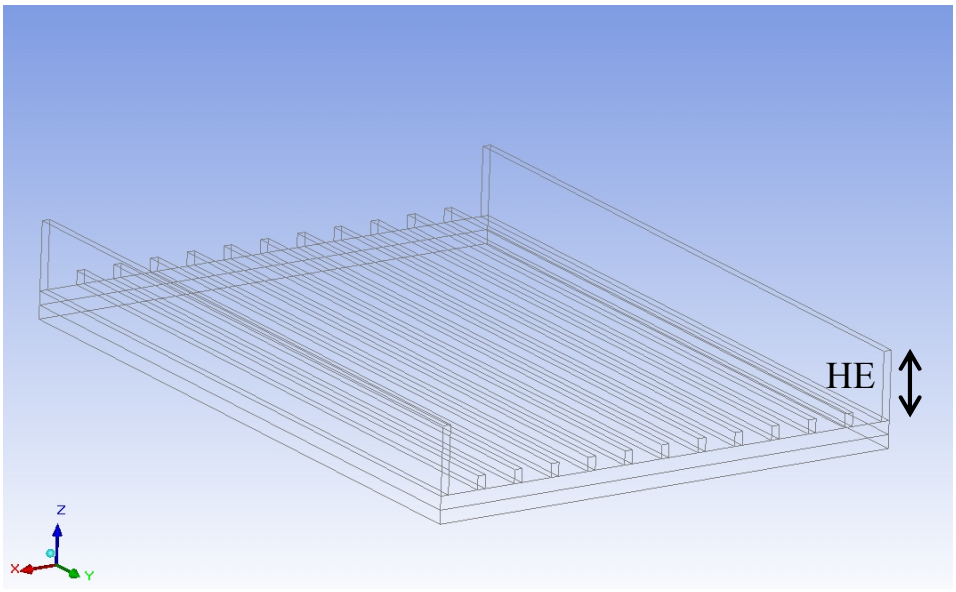

Figure 74 Heat Sink with 25 mm Height End Fins

3.5.1 Results of High End Fins Solution

Examining Figure 75 through Figure 78 it has been seen that this solution made the flow distribute all over the heat sink especially in higher end fins such as 25mm and 20mm cases. These results prove that the cause of the X shaped flow zone is caused by the lateral flow entering though flanks of the heat sink.

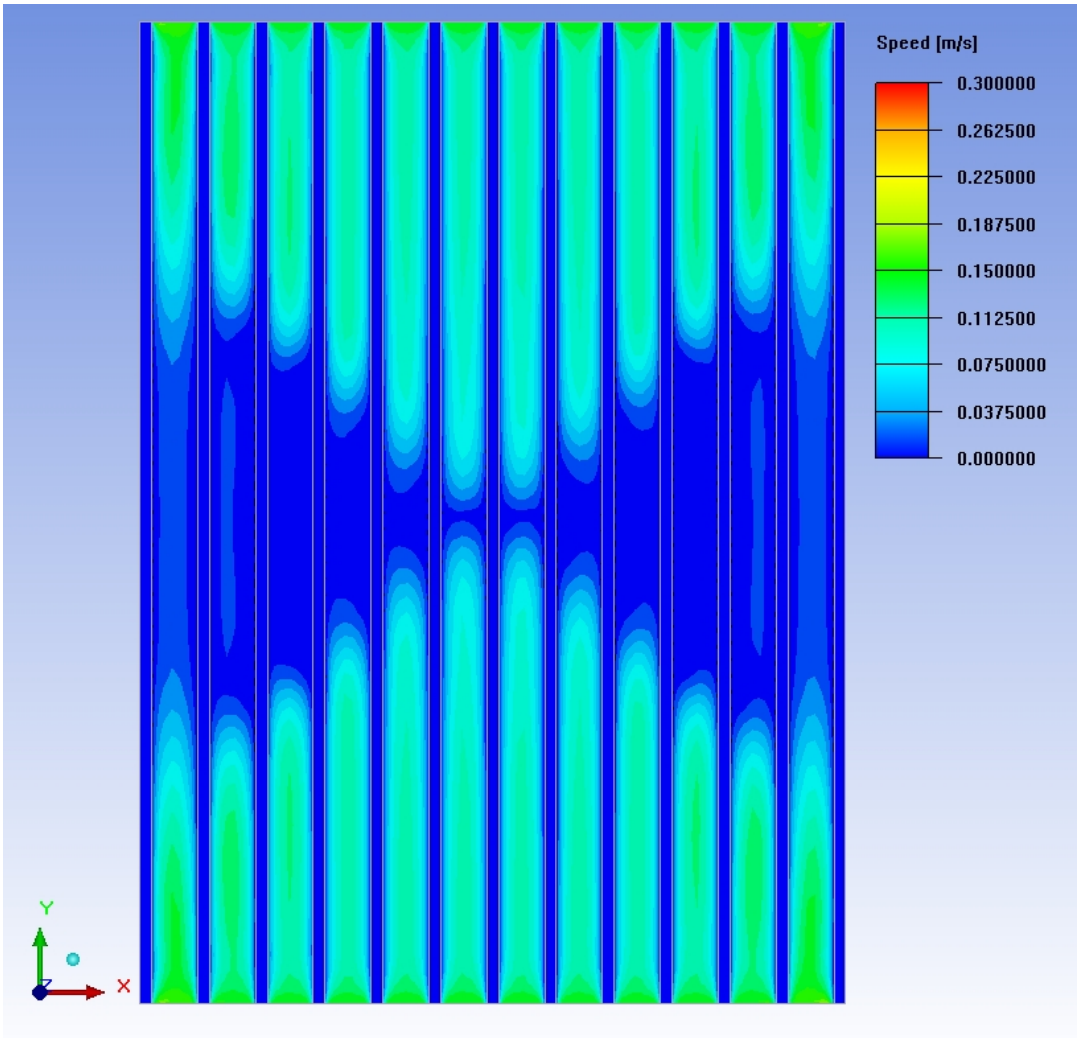

Figure 75 Speed Contours above 2mm of the Base Plate of the Heat Sink with 10 mm Height End Fins

Figure 75 shows the speed contour figures for 10mm High End Fins Case; it can be seen that this solution did not provide air flow to the entire heat sink zone however compared to the base case flow structure as in Figure 18, it may be stated that this solution reduced the area of recirculating flow zones.

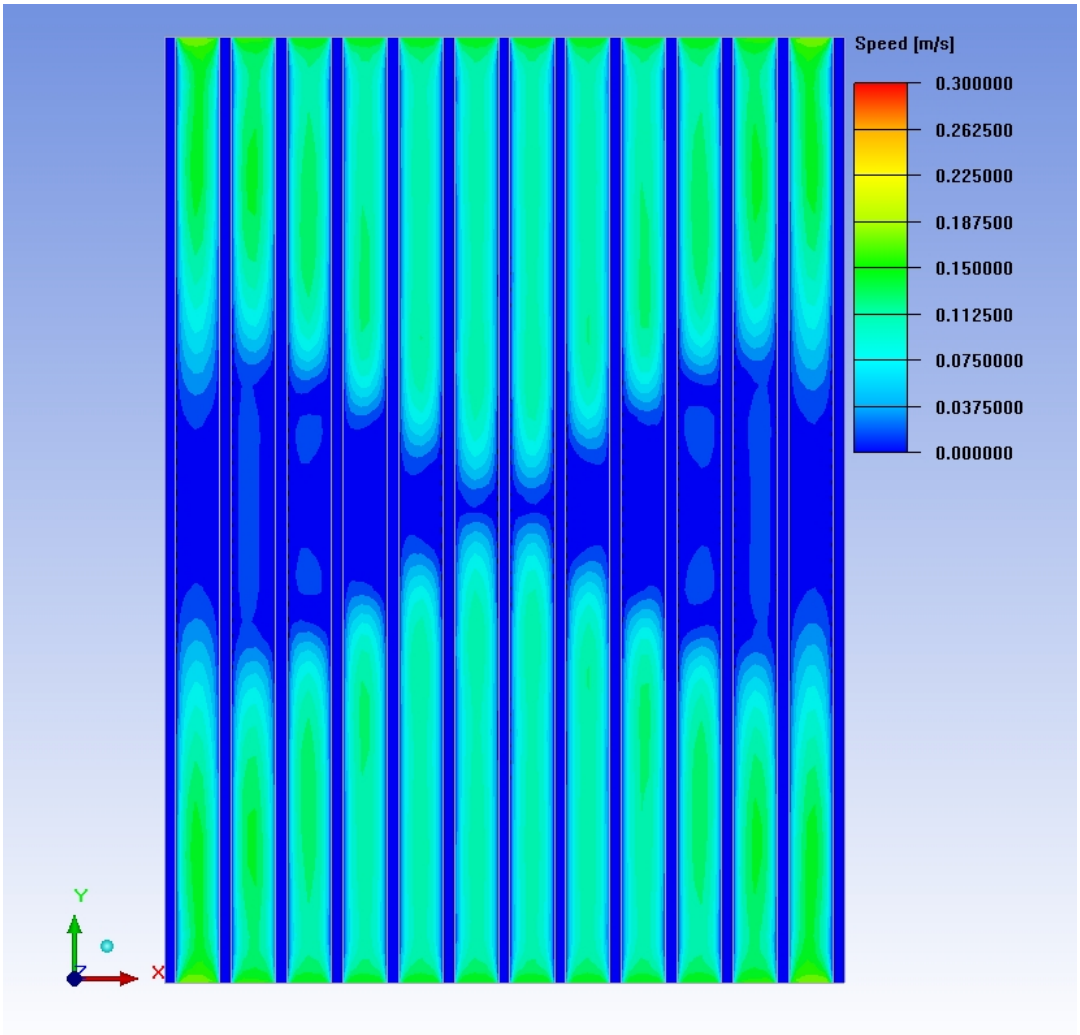

Figure 76 Speed Contours above 2mm of the Base Plate of the Heat Sink with 15 mm Height End Fins

By further increasing the end fin heights to 15 mm recirculating flow zones are observed to be reduced as it can be seen in Figure 76.

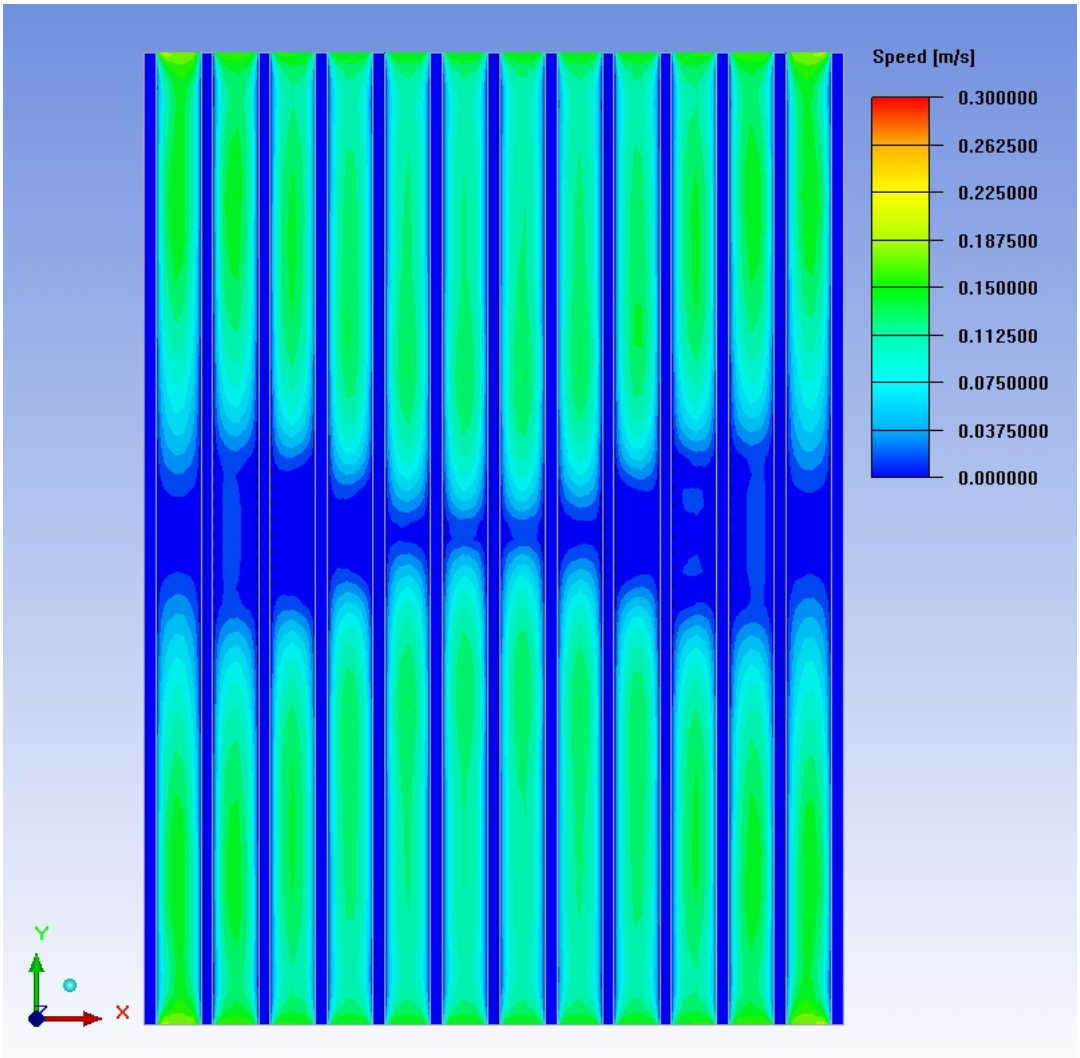

Figure 77 Speed Contours above 2mm of the Base Plate of the Heat Sink with 20 mm Height End Fins

With increasing the end fin heights to 20 mm the recirculating flow zones are nearly vanished except for a small region as it can be seen in Figure 77.

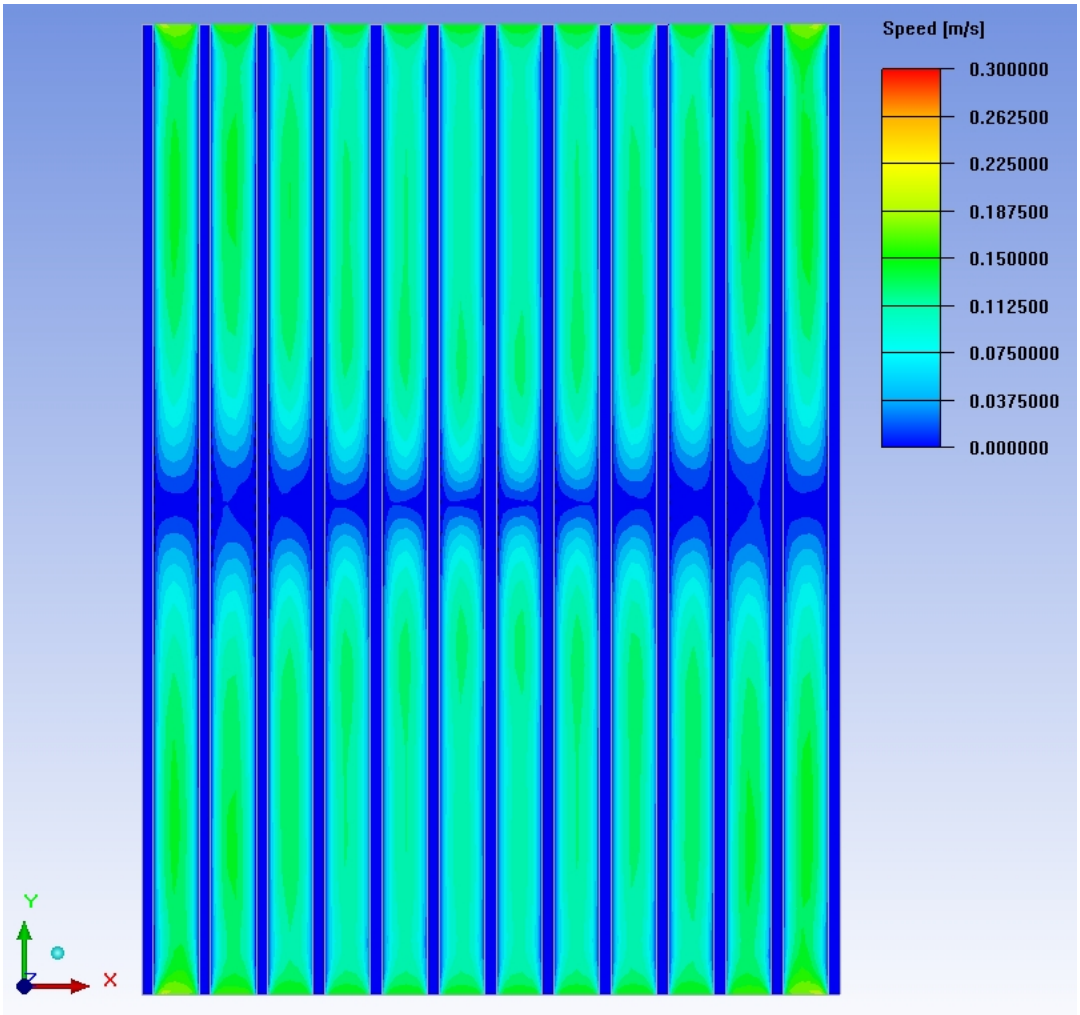

Figure 78 Speed Contours above 2mm of the Base Plate of the Heat Sink with 25 mm Height End Fins

When the end fin heights became 25 mm the recirculating flow zones vanished completely. Now all of the regions of the heat sink can have natural convection cooling.

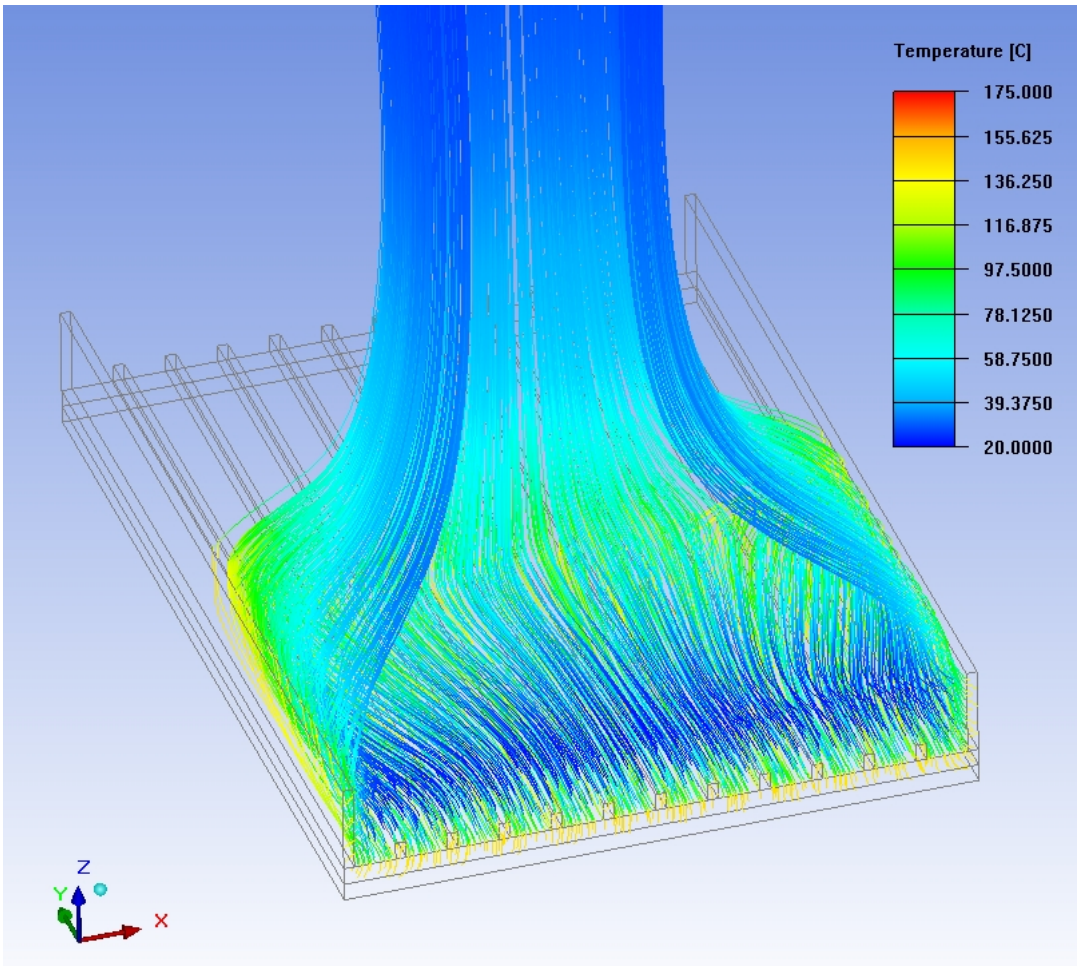

Figure 79 Pathlines of air entering to the channels of the heat sink of 25mm High End Fins Case coloring based on temperature of the air

Figure 79 shows that air entering to the channels of the heat sink. It can be observed that the longitudinal vortices structured flow do not exist for this case. And a single chimney type of chimney structure occurs which had been shown to dissipate more heat compared to other chimney types.[4]

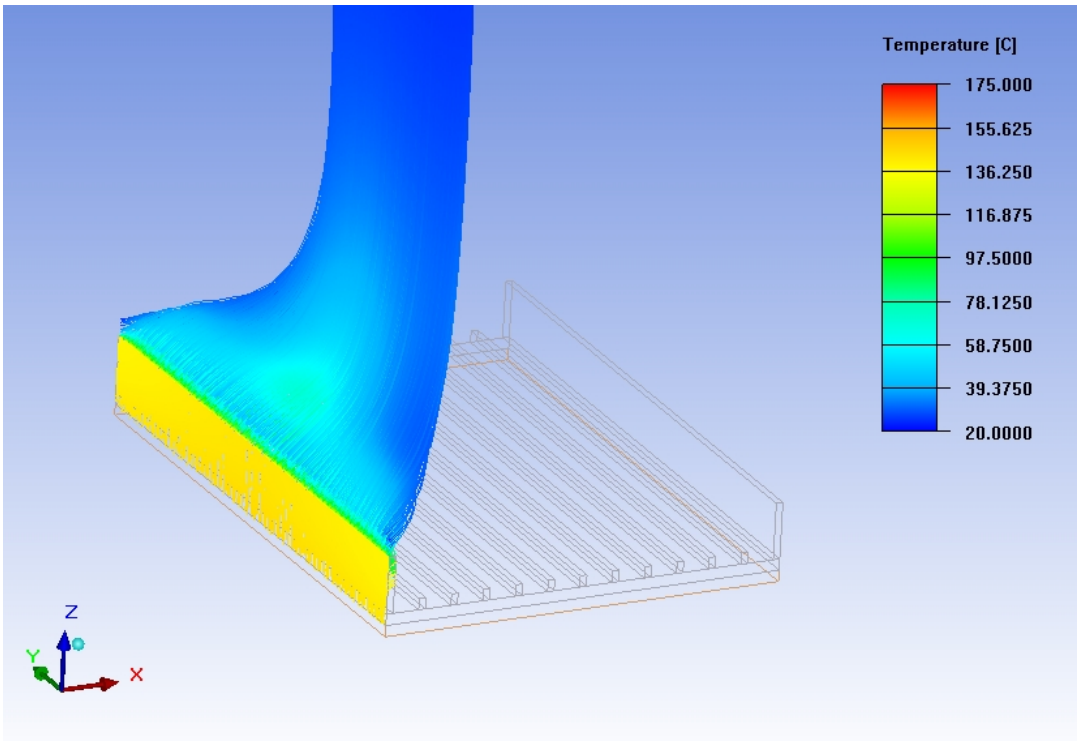

Figure 80 Pathlines of air entering to heat sink zone from left wall side in 25mm High End Fins Case coloring based on temperature of the air

Figure 80 shows the pathlines of air entering into heat sink zone from the left side in 25 mm high end fins case. Unlike in base case as it can be seen on Figure 65 in which the air from the sides do not rise; for the 25 mm high end fins case the the air coming from the sides rises. Therefore the interference of the lateral secondary flow with the flow in channels is reduced.

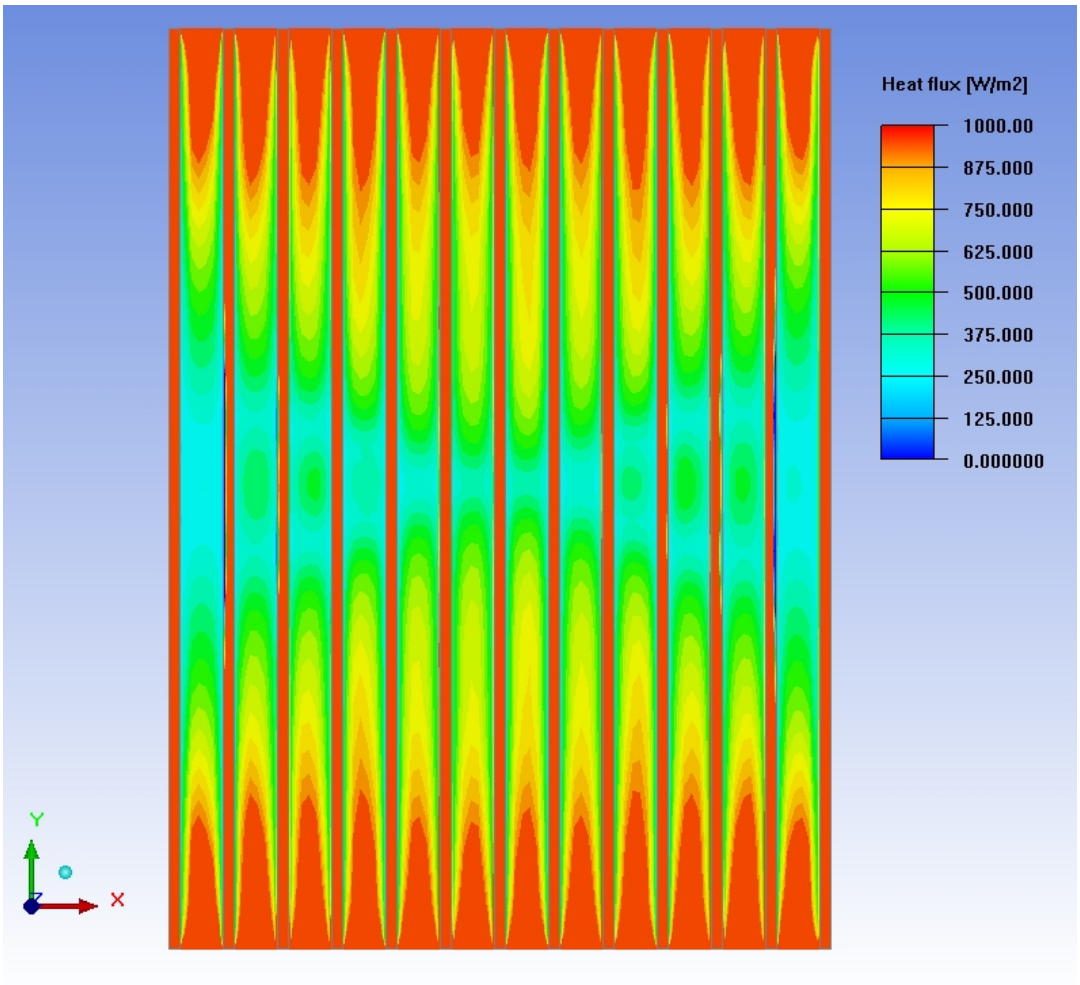

Figure 81 Heat Flux Values for 20 mm end fin height heat sink

Figure 81 shows the heat sink base heat flux values for the 20mm end fin height case. Comparing the figure with the Figure 63 which shows the heat flux values for the Base Case following observations can be made: the thermally in efficient zone has been decreased for the 20 mm end fin height case (blue zone in the middle), the flux values for the Base Case seems greater than the 20 mm end fin heights case but since the surface temperature of the Base Case is greater than the latter this was expected. By looking at this figures conclusion can be made that high end fins case reduced the thermally inefficient zone of recirculation.

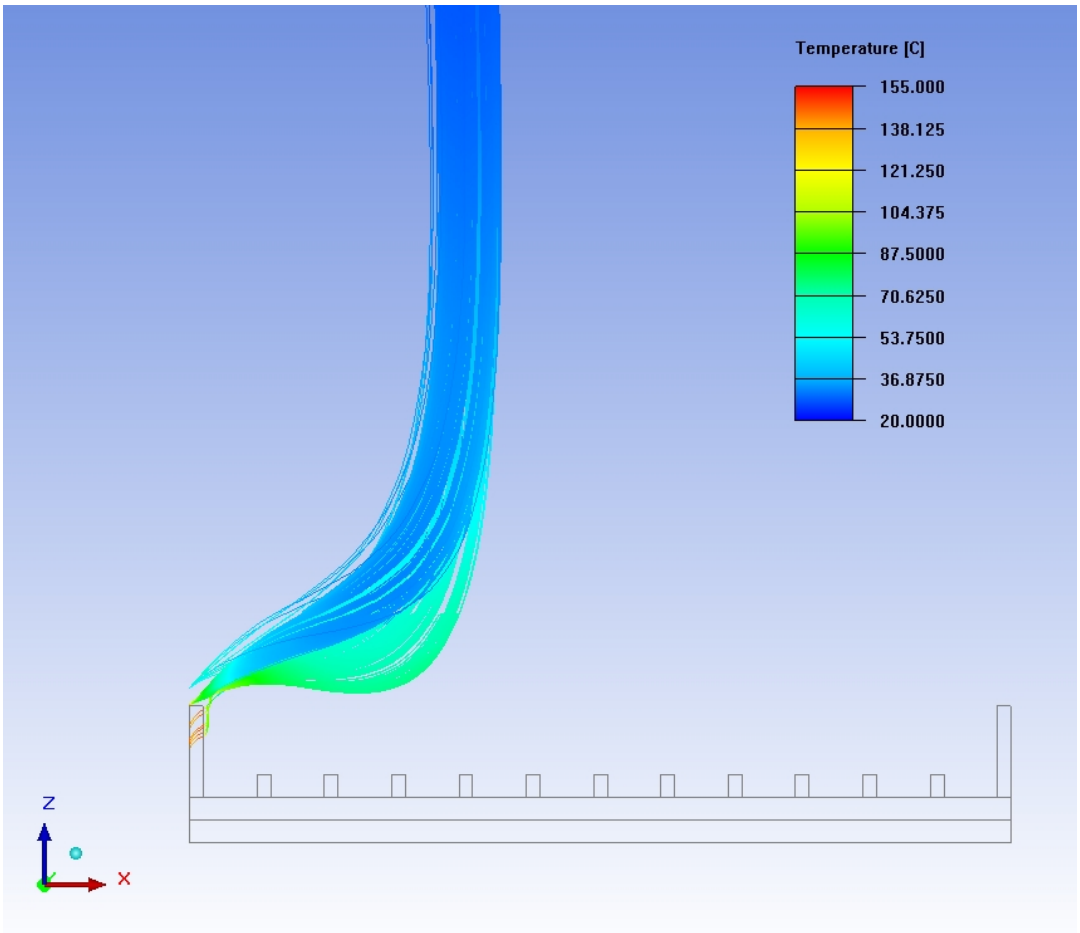

Figure 82 Pathlines of air entering into heat sink zone from the left side of the heat sink for 20 mm High End Fins Case (coloring based on temperature of the air)

Figure 82 shows the pathlines of air entering into heat sink zone from the left side in 20 mm High End Fins Case. Comparing the figure with Figure 65 it can be seen that unlike in Base Case the air from the sides does not interfere with flow in channels.

Examining Table 13 shows the high end fins case has dramatically increased the heat transfer performance of the heat sink. However, since the end fins are higher and have greater wet area; the comparisons of Table 13 are not enough. Therefore in order to understand the heat transfer effect of this solution. Middle fin heat transfer performance analysis has been made for each case. In which the heat transfer

coefficient of middle 11 fins has been compared with the Base Case's middle fin heat transfer coefficients.

Table 13 Results of the High End Fins Case

Case Name	T_{mean} Heatsink Base (°C)	Q_{Total} Heatsink into fluid (W)	Q_{rad} Heatsink (W)	Q_{conv} Heatsink (W)	q" (W/m^2)	q" $_{conv}$ (W/m^2)	q" $_{rad}$ (W/m^2)
Base Case	174,28	95,37	26,82	68,55	1186,36	852,69	333,67
10 mm High End Fins Case	167,33	96,75	26,19	70,56	1167,16	851,19	315,97
15 mm High End Fins Case	159,43	98,23	25,16	73,07	1150,35	855,69	294,66
20 mm High End Fins Case	151,17	99,79	23,89	75,90	1135,38	863,60	271,78
25 mm High End Fins Case	145,23	101,06	23,12	77,94	1118,09	862,30	255,79

Table 14 shows the middle fins' Convection Heat Transfer Coefficient values. Around 7% increase has been observed in middle fins. This was expected because of the diminishing of the recirculation flow zone.

Table 14 Middle Fin h Values of the High End Fins Case

Case Name	h (W/m^{2}K)	% variation in h
Base Case	6,12	0,00%
10mm End Fins Case	6,07	-0,83%
15mm End Fins Case	6,18	0,88%
20mm End Fins Case	6,39	4,42%
25mm End Fins Case	6,56	7,16%

It has been observed that High End Fins Case reduced the base temperature significantly. It may be wondered that whether the low base temperature regulated the flow or not. Since higher temperature differences leads to higher Gr.

Grashof Number is a non-dimensional term which defines the ratio of buoyancy forces to viscous forces. The flows which have higher Gr have higher buoyancy forces. Table 13 shows that the base plate temperature has been decreased to 145°C for 25 mm High End Finned Case from 174°C of Base Case which causes Gr to decrease for High End Finned Cases. This situation may cause the flow to rise due to high Gr before coming to the middle of the heat sink for the Base Case. For this reason additional cases has been analyzed in which the Q_{in} has been reduced to 25W and 75W respectively for the Base Case geometry heat sink. The flow visualization can be observed in Figure 83 and Figure 84. It can be seen that despite the low temperatures of the heat sink base, the flow characteristics is still the same or even worse for these cases. Therefore it is concluded that this type of flow is not being affected by the Q_{in} or Gr.

$$G = \frac{g\ (T_S - T_\infty) S^3}{\nu^2} \tag{3.1}$$

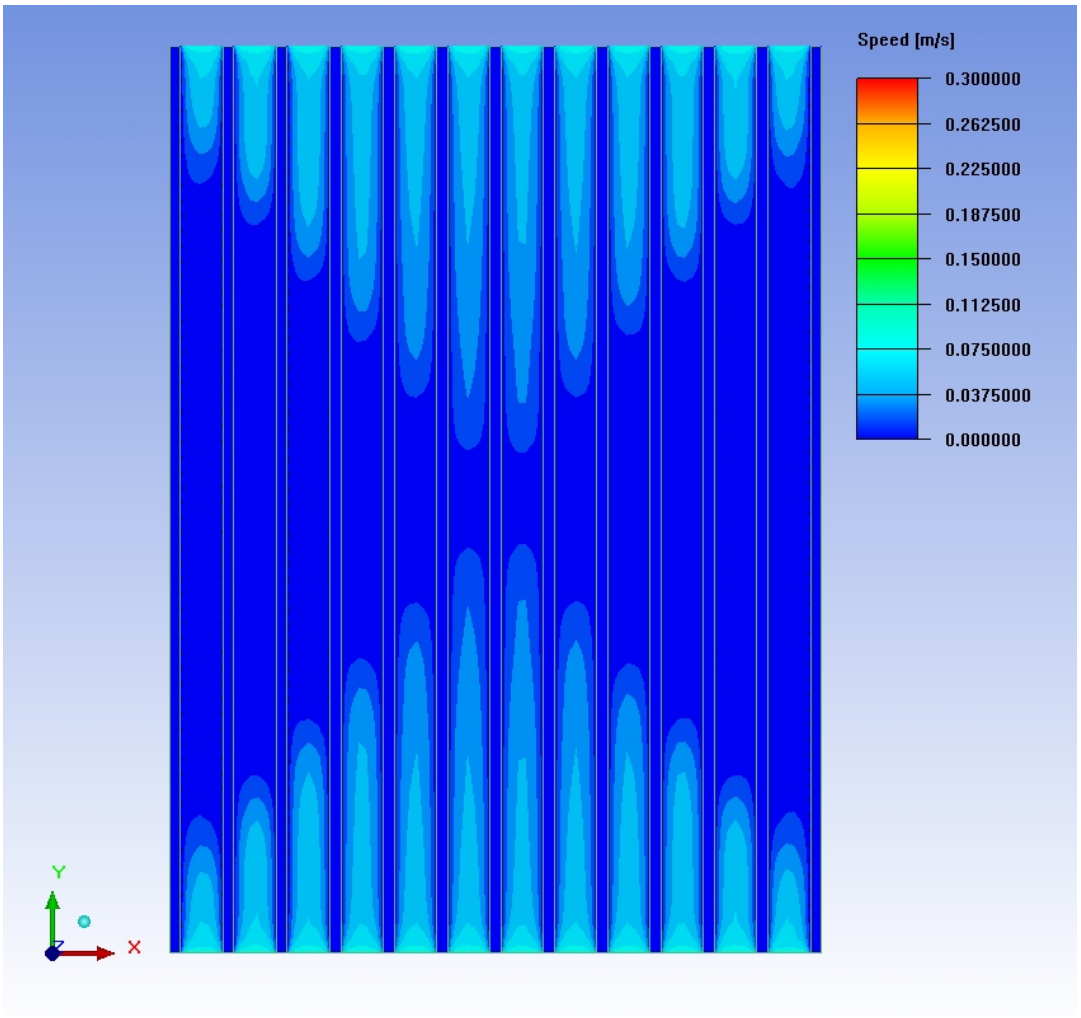

Figure 83 Speed Contours Above 2 mm of Heat Sink Base on Base Case with Q_{in}=25W (T_{mean} Heat Sink Base=61.06 ^{O}C)

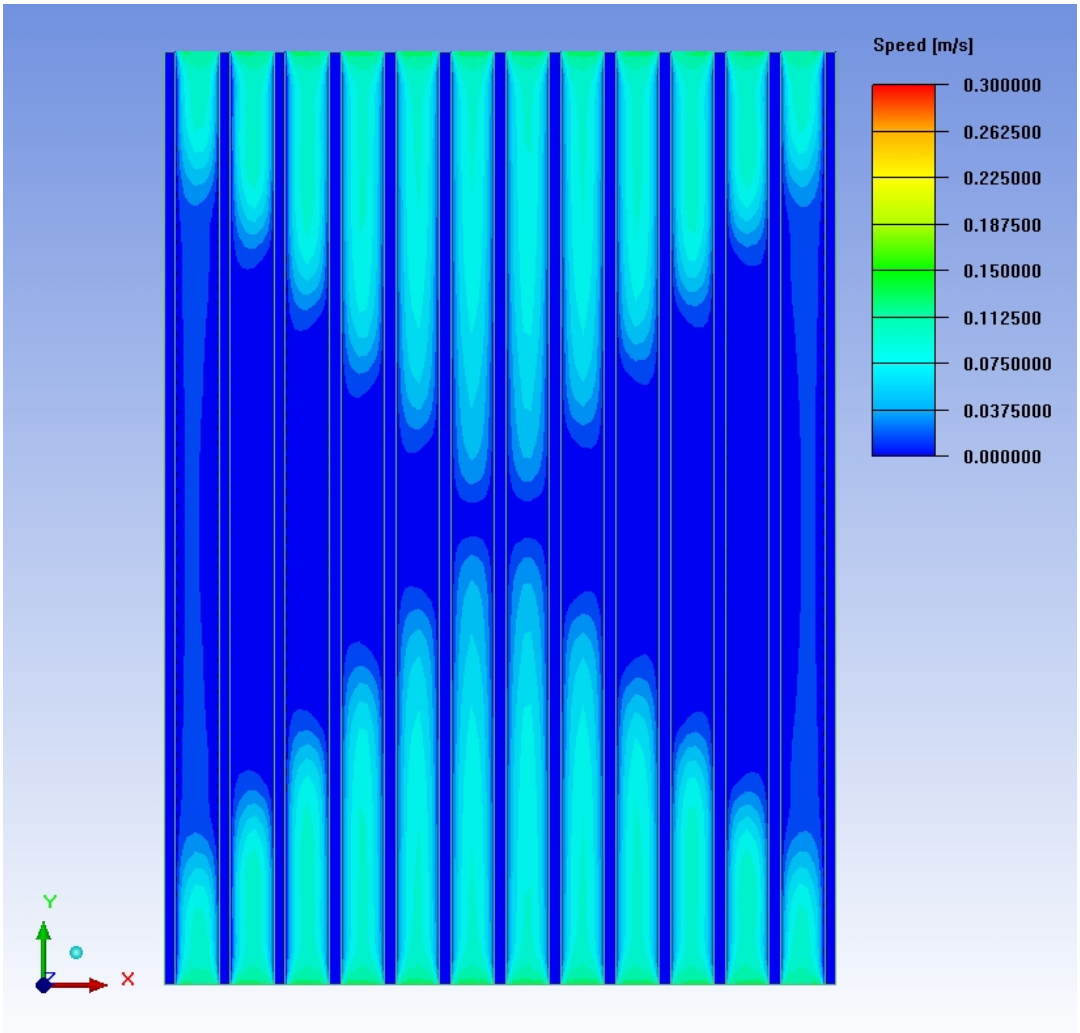

Figure 84 Speed Contours Above 2 mm of Heat Sink Base on Base Case with Qin=75W (T_{mean} Heat Sink Base=121.54 ^{O}C)

In addition to these, conventional heat sinks which have different fin heights have been analyzed and compared with the High End Fins cases. In Table 15 comparison of the High End Fins Cases and Conventional Heat Sinks can be seen. Since the Conventional Heat Sinks have higher wet area, higher Q_{conv} values are expected.

Table 15 Comparison of High End Fins Case with Conventional Heat Sinks with Higher Fins

Case Name	T_{mean} Heatsink Base (^oC)	Q_{Total} Heatsink into fluid (W)	Q_{rad} Heatsink (W)	Q_{conv} Heatsink (W)	**q" (W/m^2)**	**$q"_{conv}$ (W/m^2)**	**$q"_{rad}$ (W/m^2)**
Base Case	174,28	95,37	26,82	68,55	1186,36	852,69	333,67
10 mm High End Fins Case	167,33	96,75	26,19	70,56	1167,16	851,19	315,97
15 mm High End Fins Case	159,43	98,23	25,16	73,07	1150,35	855,69	294,66
20 mm High End Fins Case	151,17	99,79	23,89	75,90	1135,38	863,60	271,78
25 mm High End Fins Case	145,23	101,06	23,12	77,94	1118,09	862,30	255,79
Conventional Heat Sink with 10 mm Fin Height	148,00	100,56	24,82	75,74	887,75	668,64	219,11
Conventional Heat Sink with 15 mm Fin Height	126,30	104,81	21,81	83,00	717,05	567,86	149,19
Conventional Heat Sink with 20 mm Fin Height	109,63	108,03	19,14	88,89	603,33	496,42	106,91
Conventional Heat Sink with 25 mm Fin Height	99,73	109,35	17,85	91,50	515,90	431,69	84,21

Table 16 shows the heat transfer coefficients of middle fins in the heat sink. It can be seen that h values are lower in heat sinks with higher middle fin heights. These results show that the keeping the flow in the heat sink channels increases the heat transfer as expected.

Calculation procedure for the values can be found in Appendix B sample calculation.

Table 16 Comparison of *h* values of High End Fins Case with Heat Sinks with Higher Fins Cases' Middle Fins

Case Name	h (W/m^2K)	% variation in h
Base Case	6,12	0,00%
10mm High End Fins Case	6,07	-0,83%
15mm High End Fins Case	6,18	0,88%
20mm High End Fins Case	6,39	4,42%
25mm High End Fins Case	6,56	7,16%
10mm Fin Height	5,54	-9,55%
15mm Fin Height	5,52	-9,90%
20mm Fin Height	5,69	-7,05%
25mm Fin Height	5,57	-8,97%

Although lower temperatures and higher heat dissipation values can be achieved via conventional high finned heat sinks, from a weight to heat dissipation ratio point of view; the unconventional design high end finned case seems advantageous.

Table 17 shows the Q_{conv} to mass ratio of different heat sinks compared to the high end Fins cases. From the values it can be seen that lowering the base temperature with low weight heat sinks is possible.

Table 17 Q to mass comparison of High End Fins Case to Heat Sinks with Higher Fins

Case Name	$m_{Heat\ Sink}$ (kg)	Q_{conv} Heatsink/m (W/kg)
Base Case	0,74	92,74
10 mm High End Fins Case	0,76	92,91
15 mm High End Fins Case	0,78	93,82
20 mm High End Fins Case	0,80	94,89
25 mm High End Fins Case	0,82	95,04
10 mm Fin Height	0,87	86,99
15 mm Fin Height	1,00	82,81
20 mm Fin Height	1,13	78,39
25 mm Fin Height	1,27	72,29

Another case which has been analyzed in this study is Base Case Heat Sink with no end walls. The flow structure obtained in this study can be observed in Figure 85. It can be seen that this solution did not affect the flow in inner regions although the side channels has been supplied with air.

The results of this study can be seen in Table 18. It is seen that this solution does not have a significant effect on heat transfer although the sides have been supplied with air. The reduction in area led to minor increase in Heat sink base temperature.

Table 18 No End Walls Case Results

Case Name	T_{mean} Heat sink Base (^oC)	Q_{conv} heat sink
Base Case	174,28	68,55
No End Walls	176,86	68,25

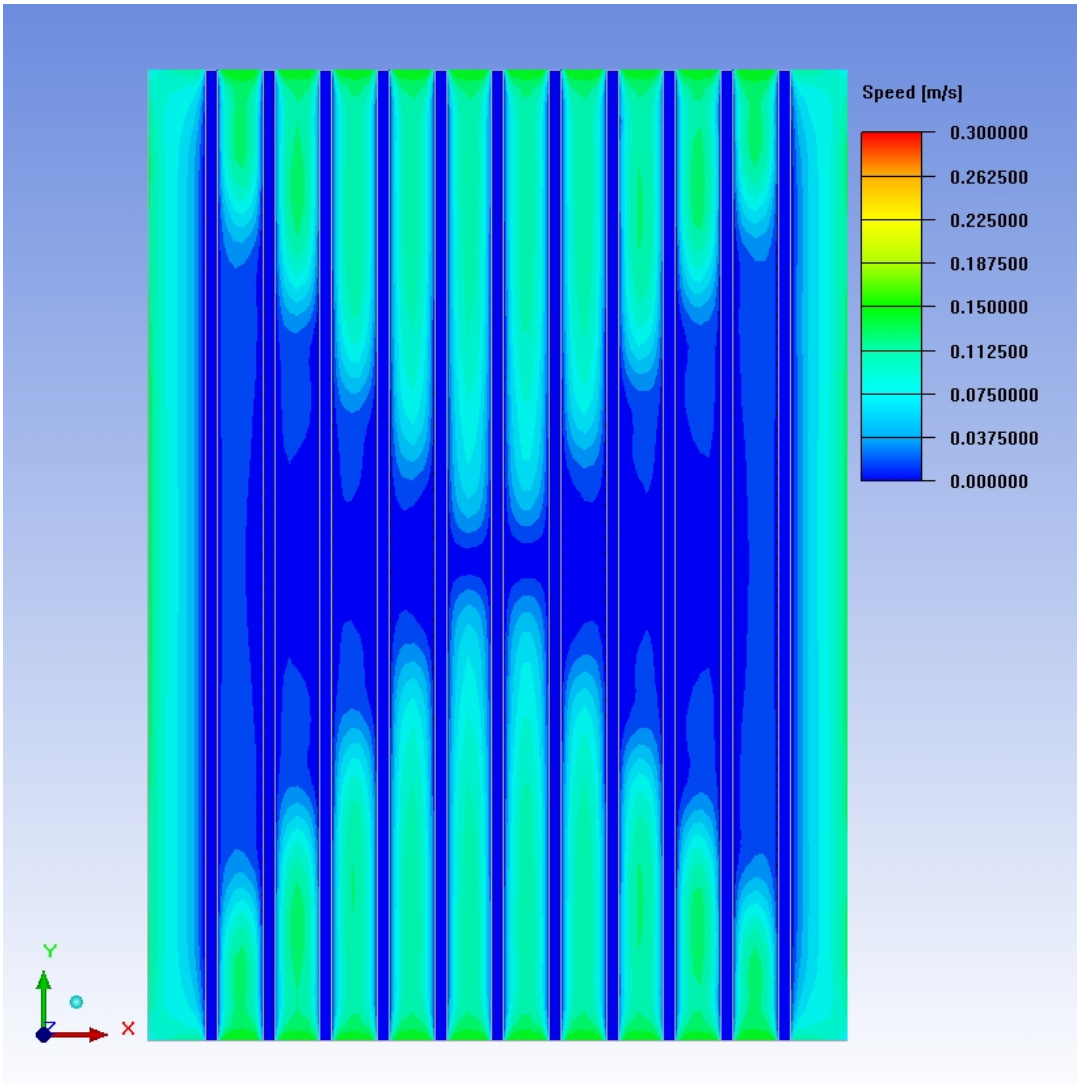

Figure 85 Speed Contours above 2mm of the Heat Sink Case with no end walls case

CHAPTER 4

CONCLUSION

4.1 Summary

In this study the flow problem for a small height plate finned heat sink has been analyzed. In [19] Tari and Mehrtash observed recirculating flow zones for a particular case. This study aimed to extend that work and aims to regulate the flow pattern in the heat sink channels and by this way the heat transfer performance. Many different methods have been analyzed in order to improve the flow structure. The cases that have been analyzed are.

- X Shaped Mixing Gaps Case
- Disturbance in Channels Case
- Middle Gap Case
- High End Fins Case

Table 19 shows the results which exhibits the lowest base temperature for each case.

Table 19 Comparison of all cases (Only the best result of each case has been shown on this table)

Case Name	T_{mean} Heatsink Base (°C)	Q_{Total} Heatsink into fluid (W)	Q_{rad} Heatsink (W)	Q_{conv} Heatsink (W)	q" (W/m^2)	q" $_{conv}$ (W/m^2)	q" $_{rad}$ (W/m^2)
Base Case	174,28	95,37	26,82	68,55	1186,36	852,69	333,67
25 mm High End Fins Case	145,23	101,06	23,12	77,94	1118,09	862,30	255,79
Conventional Heat Sink with 25 mm Fin Height	99,73	109,35	17,85	91,50	515,90	431,69	84,21
5mm X Shaped Cut	173,76	95,41	26,63	68,78	1192,75	859,81	332,93
G=25 mm Middle Gap Case	167,76	96,48	24,36	72,12	1235,16	923,30	311,86
Plate Fins in the Middle (5mm height)	167,98	96,50	27,56	68,94	898,86	642,15	256,71

The X shaped flow has been thought to be distributed to the recirculating flow zones by the help of mixing gaps which are implemented in the original flow stagnation points. This solution couldn't regulate the flow. The heat transfer performance of the heat sink has not been changed in this case study. Another trial which involves cutting gaps on the outmost fins has also been conducted and observation has been made that this solution also did not improve the flow structure or the heat transfer characteristics also. After understanding the reason behind the X shaped flow in the heat sink, which comes out to be the lateral flow. The X Shaped Mixing Gaps Case's reason for do not improving the flow structure has been concluded. In which since

the upper flow in the heat sink sucks the air in the channels the air could not be distributed to recirculating flow zones.

Disturbance in Channels Case aimed to observe the flow characteristics of longitudinal vortices structured flow pattern with the help of different fin shaped objects in the channels. From the visualization of the speed contours above 2mm of the heat sink base it has been observed that this method has worsened the flow because of the frictional losses it provided. For this reason, the heat transfer performance of the heat sink did not increase on the contrary it has decreased although the increase of wet area led to temperature drops of heat sink base. This type of disturbance in the channels concluded to be inappropriate for naturally cooled heat sinks. Combination of the Disturbance in Channels Case with Middle Gap Case or X Shaped Mixing Gaps case would not be successful neither because of the lateral air flow sucking the air from the channels.

Middle gap case provided some flow entering from lateral ends for this reason the flow in the middle has increased but it could not distribute to the entire recirculating flow zone of the heat sink. This method increased the heat transfer rate and showed the importance of supplying cooling fluid to recirculating flow zones. This solution reduced the base temperature by reducing wet area unlike the High End Finned Case and Disturbance in Channels case in which the wet area increases.

The reason of the X shaped recirculating flow has been found which is the lateral air flow in low fin height plate finned heat sinks. Also the reason for the longitudinal vortices observed in [19] has been found which is concluded to be the secondary lateral flow above the heat sink applying suction force to the flow in the heat sink channels and due to this interaction the flow pattern spoils and longitudinal vortices happen.

By finding the reason for X shaped flow pattern.High End Fins Case has been analysed. High end fins case greatly increased flow pattern which is being seen in

the speed contours flow visualizations. The convection heat transfer rate has been increased and the base temperature of the heat sink has been decreased dramatically. However in this case the wetted area of the heat sink increased compared to the base case. Therefore for examining the convection heat transfer performance of the heat sink, heat transfer coefficients of the middle fins have been compared and it has been seen that around 7% increase in heat transfer coefficient has been observed. Also this method has been compared by conventional high height finned heat sinks and an observation has been made that this solution is more advantageous in weight point of view.

It has been proved that the X Shape flow structure is independent of input power and temperature difference.

4.2 Conclusion

In this study a case which has been reported in [19] has been shown and improvising analyses to improve the flow conditions has been made. It is concluded that the lateral air flow affects the flow in the channels of the heat sink and therefore causing heat transfer performance loss. The lateral has shown to be sucking the air in the channels. The observed longitudinal vortices have been concluded to be occurred because of spoiled flow structure due to lateral air flow above the heat sink. It is concluded that in designing the horizontal plate finned heat sinks the lateral flow has to be considered also since it may spoil the flow structure and therefore heat transfer performance of the heat sink.

4.3 Future Work

It has been shown that the lateral air flow in short plate finned heat sinks affects the heat transfer performance of the heat sink in an unfavourable way. An observation has been made that the heat sink can also draw air from the sides of the heat sink. Heat sinks which enable cooling from all of the sides of the heat sink such as pin finned heat sinks or plate finned heat sinks with gaps are thought to not have this

kind of problem. On the other hand they have lower wet areas than the conventional plate finned heat sinks. A future work which compares different configurations of heat sinks can be conducted in order to find the best configuration for a specific application by the help of this study since this study shows the reason for recirculating flow patterns observed in low height finned heat sinks.

REFERENCES

[1] Zhang, M. T., Jovanovic, M. M., and Lee, F. C., 1997, "Design and Analysis of Thermal Management for High-Power-Density Converters in Sealed Enclosures", Proc. APEC 97—Applied Power Electronics Conference, Vol. 1, pp. 405–412.

[2] Elenbaas W., "Heat Dissipation by Parallel Plates by Free Convection", Physica 9 (1), 1-28,(1942).

[3] Starner K. E., McManus H. N., "An Experimental Investigation of Free Convection Heat Transfer from Rectangular Fin Arrays", Journal of Heat Transfer 85, 273-278, (1963).

[4] Harahap F., McManus H. N., "Natural Convection Heat Transfer From Horizontal Rectangular Fin Arrays", Journal of Heat Transfer 89, 32-38, (1967).

[5] Jones C. D., Smith L. F., "Optimum Arrangement of Rectangular Fins on Horizontal Surfaces for Free Convection Heat Transfer", Journal of Heat Transfer 92, 6-10, (1970).

[6] Fitzroy N.D., "Optimum Spacing of Fins Cooled by Free Convection", Journal of Heat Transfer, 462-463, (1971).

[7] Mobedi M., "A Three Dimensional Numerical Study On Natural Convection Heat Transfer From Rectangular Fins On A Horizontal Surface"., Ph D Thesis, Mechanical Engineering Department, METU (1994).

[8] Yüncü H. and Anbar G., "An Experimental Investigation on Performance of Rectangular Fins on a Horizontal Base in Free Convection Heat Transfer", Heat and Mass Transfer 33, 507-514, (1998).

[9] Baskaya S., Sivrioglu M., Ozek M., "Parametric Study of Natural Convection Heat Transfer from Horizontal Rectangular Fin Arrays", International Journal of Thermal Science 39, 797-805, (2000).

[10] Suryawanshi S.D., Sane N.K, "Natural Convection Heat Transfer From Horizontal Rectangular Inverted Notched Fin Arrays", Journal of Heat Transfer 131(8), 082501-082501-6, (2009).

[11] Huang G-J.,Wong S. C.,"Parametric Study on the Dynamic Behaviour of Natural Convection from Horizontal Rectangular Fin Arrays", International Journal of Heat and Mass Transfer 60,334-342,(2013).

[12] Huang G-J.,Wong S. C.,Lin C.-P., "Enhancement of Natural Convection Heat Transfer from Horizontal Rectangular Fin Arrays with Perforations in Fin Base",International Journal of Thermal Sciences 84,164-174,(2014).

[13] Yalcin H.G., Baskaya S., Sivrioglu M., "Numerical Analysis of Natural Convection Heat Transfer from Rectangular Shrouded Fin Arrays on a Horizontal Surface", International Communications in Heat and Mass Transfer 35, 299-311, (2008).

[14] Dogan M.,Sivrioglu M., Yilmaz O.,"Numerical Analysis of Natural Convection and Radiation Heat Transfer from Various Shaped Thin Fin Arrays Placed on a Horizontal Plate-A Conjugate Analysis", Energy Conversion and Management 77,78-88,(2014).

[15] Dialameh L., Yaghoubi M., Abouali O., "Natural Convection from an Array of Horizontal Rectangular Thick Fins with Short Length", Applied Thermal Engineering 28, 2371-2379, (2008).

[16] Dake T., Majdalani J.., "Improving Flow Circulation in Heat Sinks Using Quadrupole Vortices", 2009 ASME Summer Heat Transfer Conference.

[17] Yang K.-S..,Jhong J-H, Lin Y.-T., Chien K.-H., Wang C.-C.., "On the Heat Transfer Characteristics of Heat Sinks: With and Without Vortex Generators"., IEEE Transactions on Components and Packaging Technologies 2010;33(2):391-7.

[18] Mehrtash, M., "Numerical Investigation of Natural Convection from inclined Plate Finned Heat Sinks", M.S. Thesis in Mechanical Engineering, Middle East Technical University, Ankara, (2011).

[19] Tari, İ., Mehrtash M., "Natural Convection Heat Transfer From Horizantal and Slightly Inclined Plate Finned Heat Sinks", Applied Thermal Engineering 61, 728-736, (2013).

[20] Yazıcıoğlu B., "Performance of Rectangular Fins on a Vertical Base in Free Convection Heat Transfer", M.S Thesis in Mechanical Engineering, Middle East Technical University, Ankara (2005).

[21] Incropera F. P., Dewitt D. P., Fundamentals of Heat and Mass Transfer, John Wiley & Sons, New York, (1990).

APPENDIX A

MESH PARAMETERS

In the given example, mesh properties for the Base Case will be given.

In the cabinet:

- Mesh Type: Hexa Unstructured
- Max X Size: 27 mm
- Max Y Size: 75 mm
- Max Z Size: 20 mm
- Mesh Parameters: Normal
- Min Elements in Gap: 3
- Min Elements on Edge: 2
- Max Size Ratio: 2

In the Non-Conformal Mesh Assembly:

- Mesh Type: Hexa Unstructured
- Slack Settings:
    - Min X: 10 mm
    - Max X: 10 mm
    - Min Y: 20 mm
    - Max Y: 20 mm
    - Min Z: 0 mm
    - Max Z: 20 mm

- Max X Size: 2 mm
- Max Y Size: 5 mm
- Max Z Size: 10 mm

Object Parameters for the Heat Sink:

Base

- Z Count: 10
- High X Height: 0.5 mm
- Low X Height: 0.5 mm
- High Y Height: 0.5 mm
- Low Y Height: 0.5 mm
- High Z Height: 0.5 mm
- Low Z Height: 0.5 mm
- High X Ratio: 1.5
- Low X Ratio: 1.5
- High Y Ratio: 1.5
- Low Y Ratio: 1.5
- High Z Ratio: 1.5
- Low Z Ratio: 1.5

Fins

- X Count 5
- Y Count 60
- Z Count 10
- High X Height: 0.5 mm
- Low X Height: 0.5 mm
- High Y Height: 0.5 mm

- Low Y Height: 0.5 mm
- High Z Height: 0.5 mm
- Low Z Height: 0.5 mm
- High X Ratio: 1.5
- Low X Ratio: 1.5
- High Y Ratio: 1.5
- Low Y Ratio: 1.5
- High Z Ratio: 1.5
- Low Z Ratio: 1.5

Number of nodes: 2961185

Number of elements: 2881608

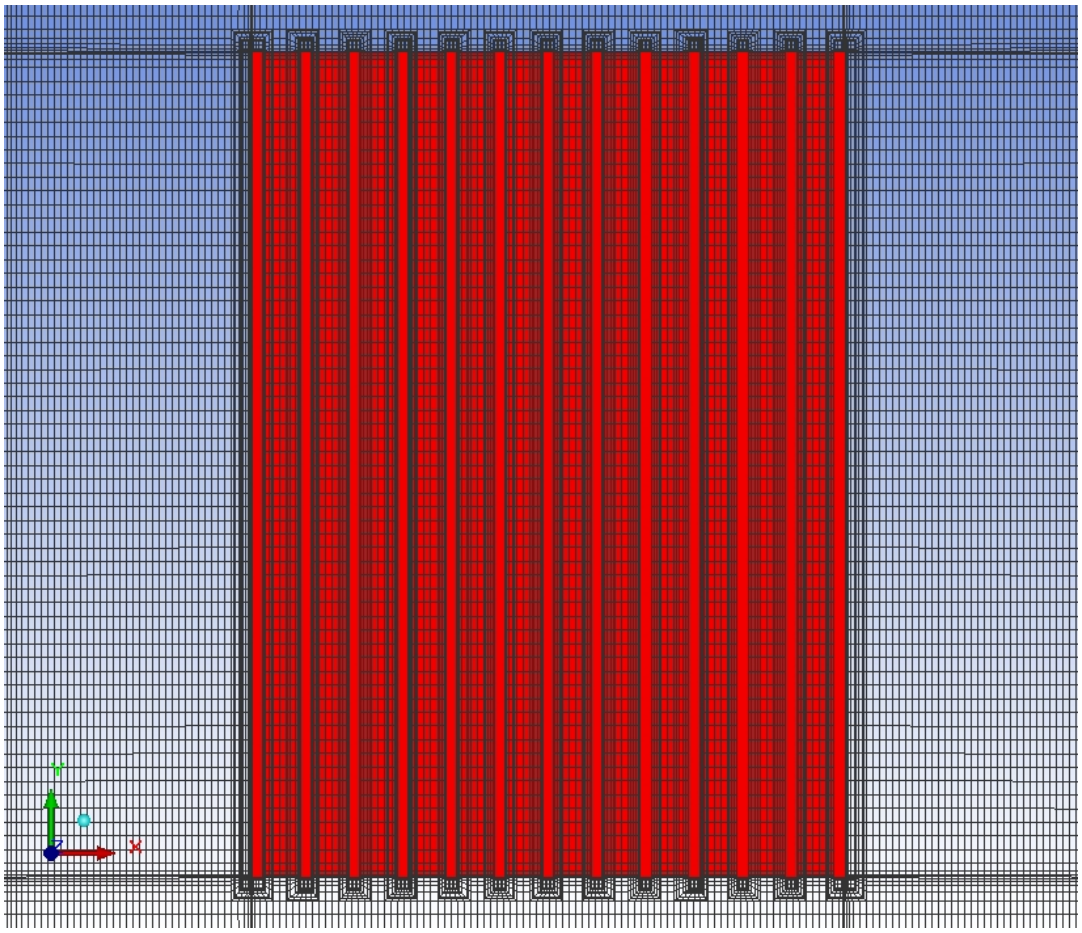

Figure 86 Mesh of Base Case (+z direction)

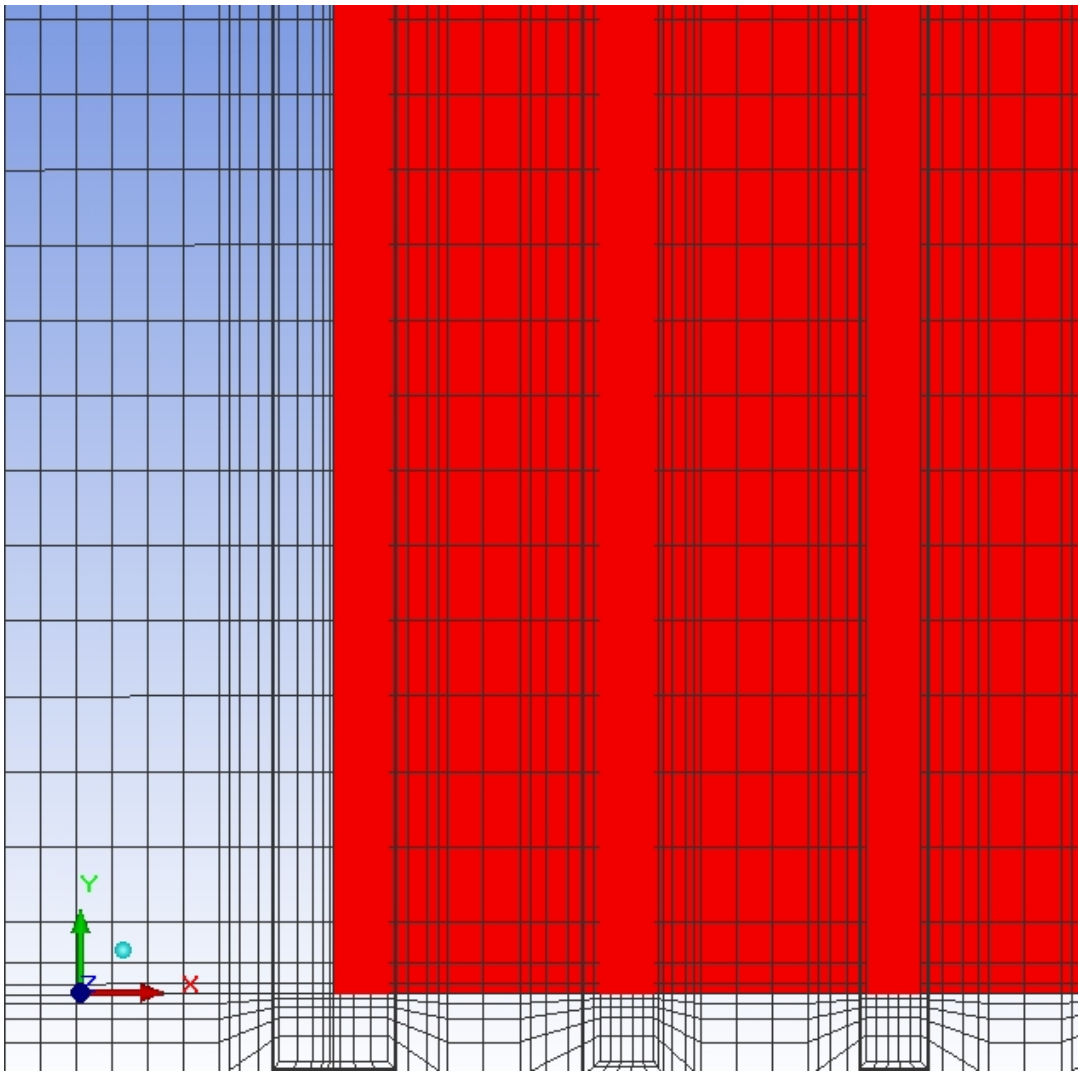

Figure 87 Mesh Around Fins in Base Case (+z direction)

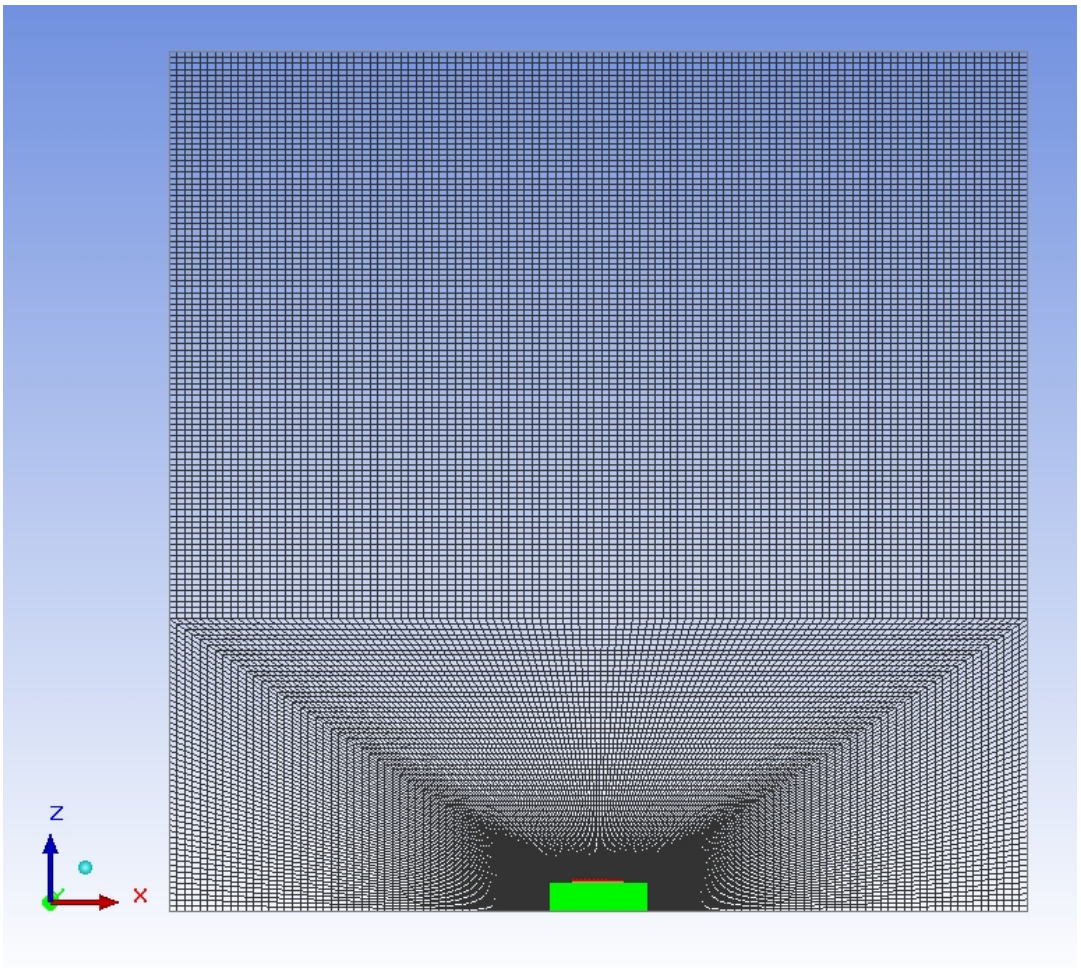

Figure 88 Mesh of the Entire Domain (+y direction)

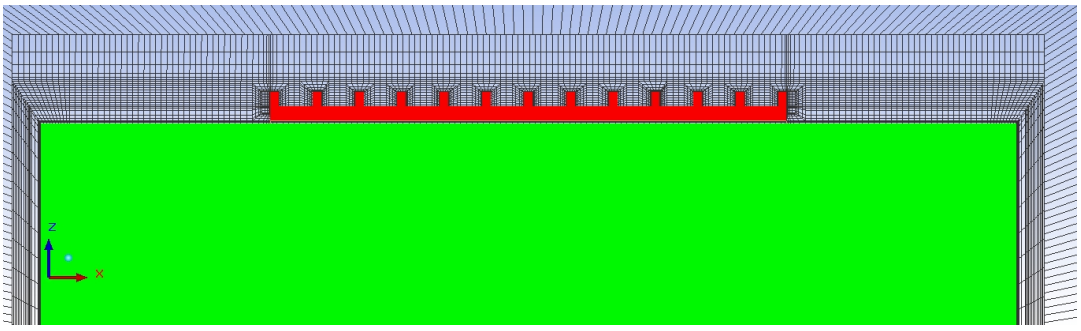

Figure 89 Mesh of the Non-Conformal Mesh Assembly (+y direction)

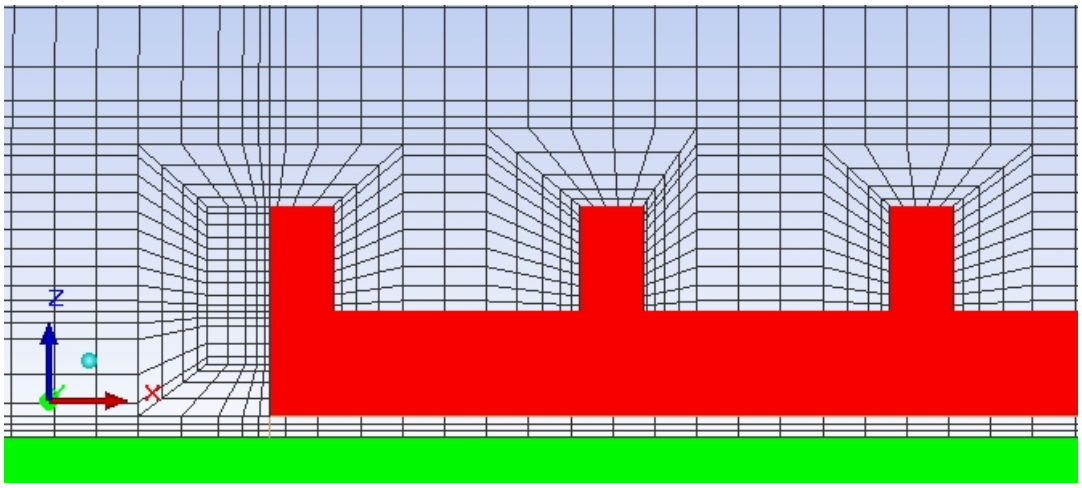

Figure 90 Mesh around Fins (+y direction)

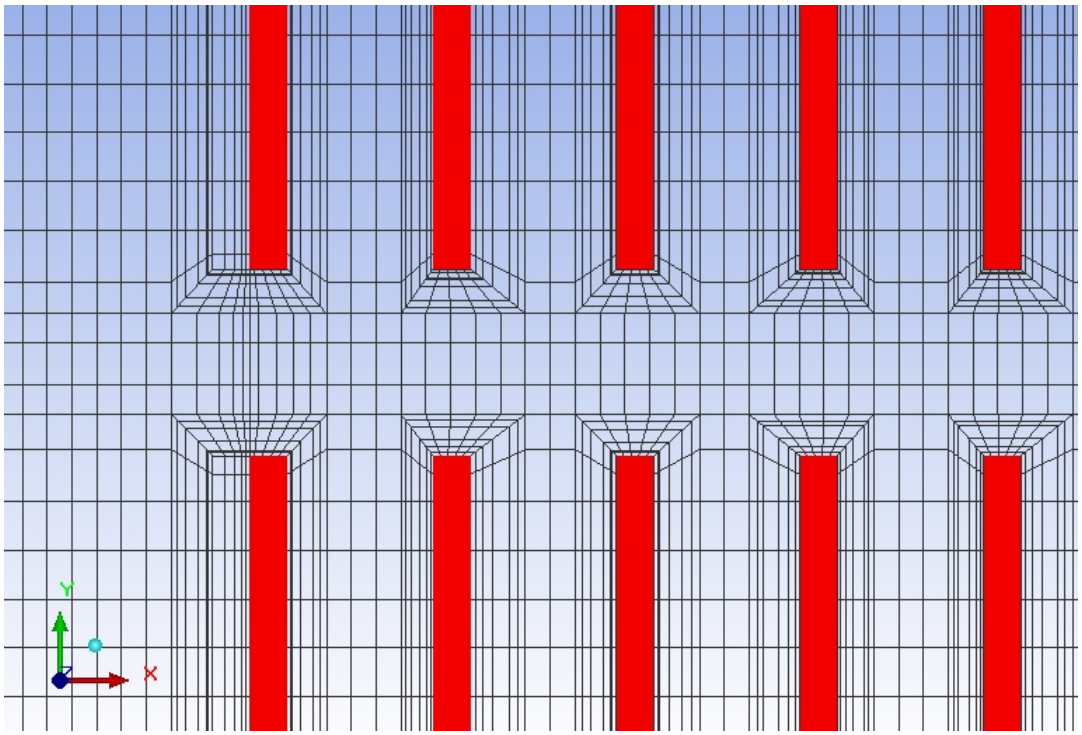

Figure 91 Mesh in gaps in 15mm Middle Gap Case

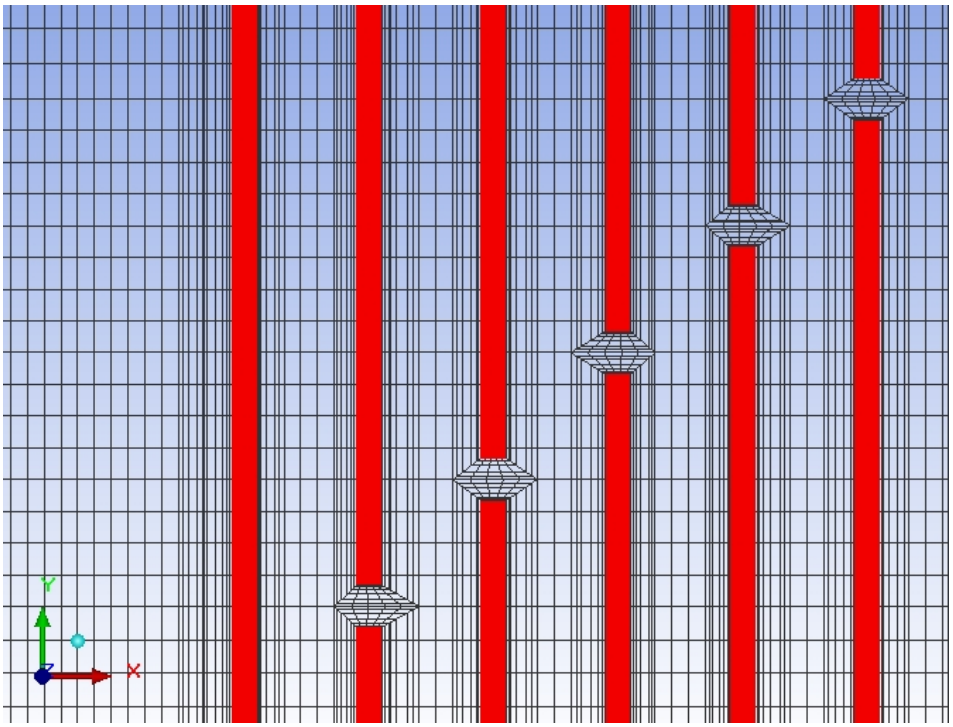

Figure 92 Mesh in gaps in 5mm X Shaped Gaps Case

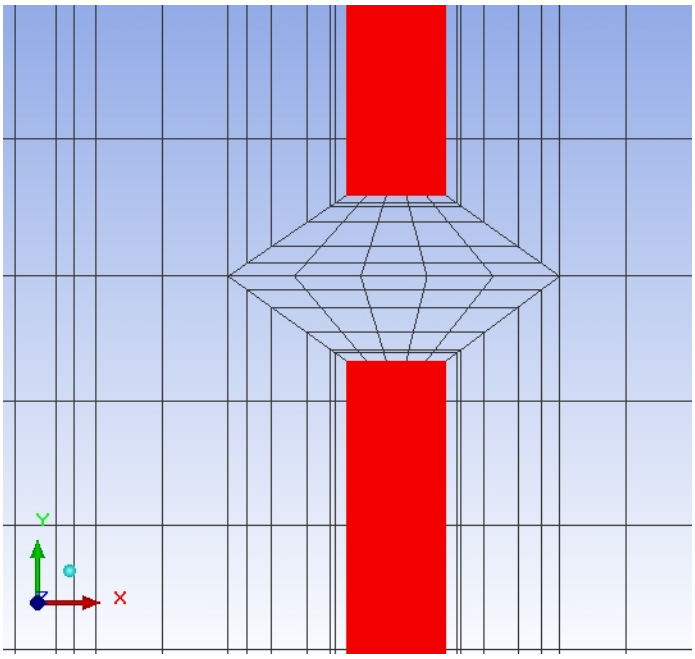

Figure 93 Mesh in gaps in 5mm X Shaped Gaps Case

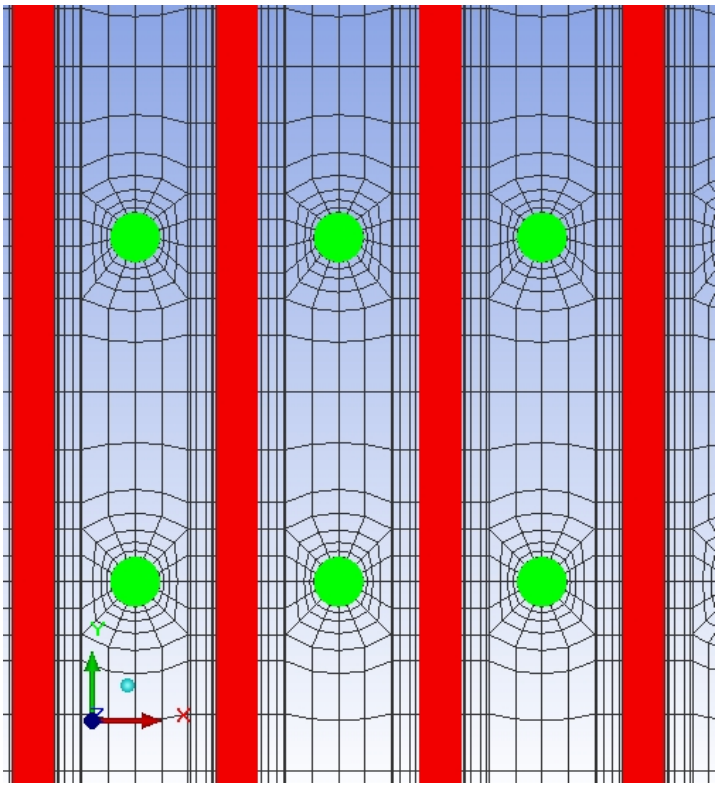

Figure 94 Mesh in Pin Fin Disturbance Case

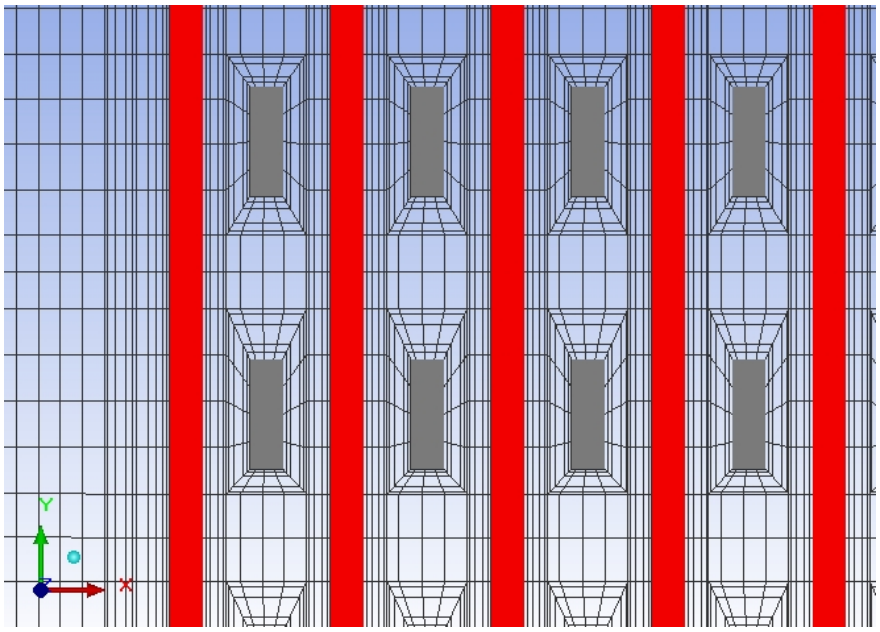

Figure 95 Mesh of Plate Fin Disturbance Case

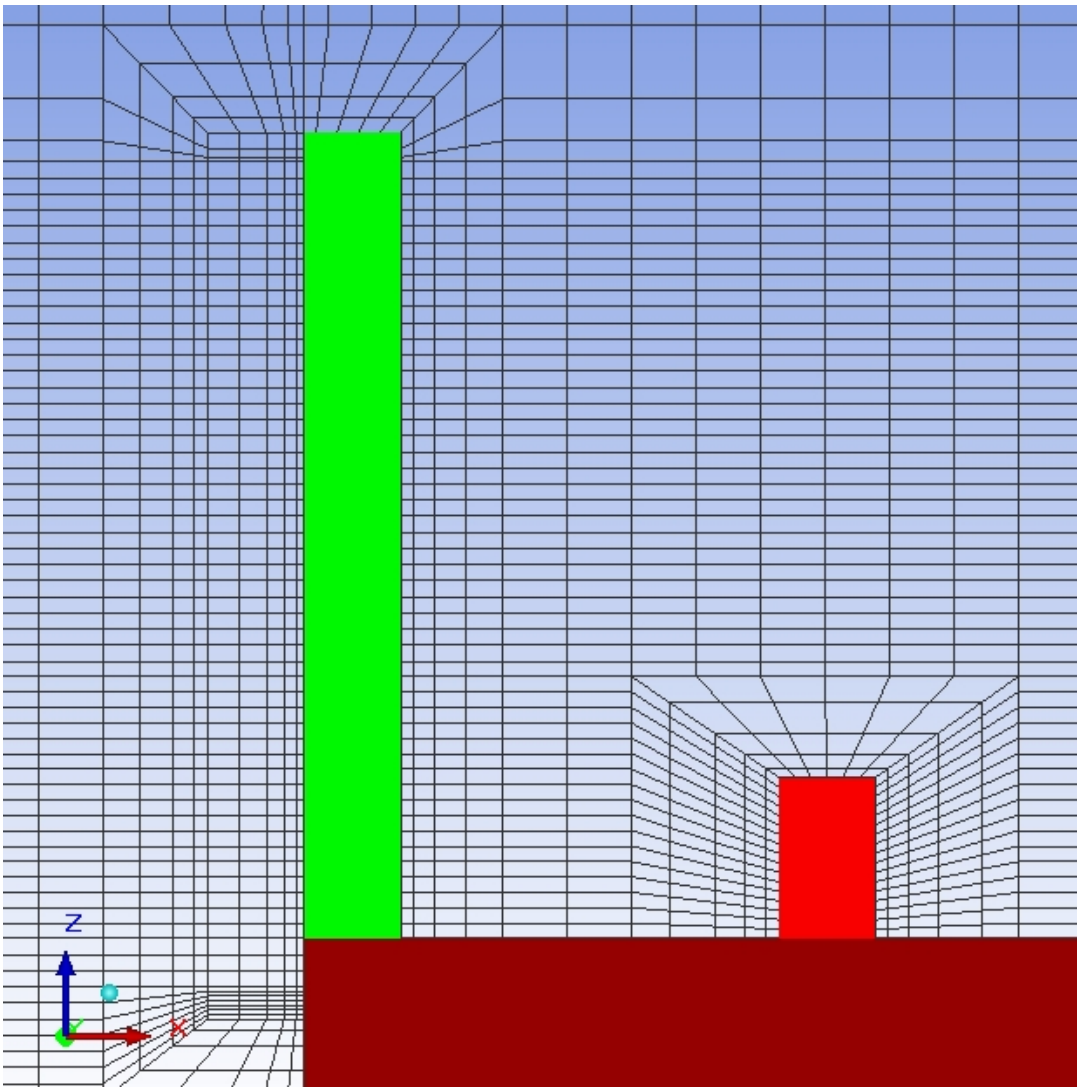

Figure 96 Mesh of 25mm High End Fins Case

APPENDIX B

SAMPLE CALCULATION

Sample calculation for the 20 mm High End Fins Case.

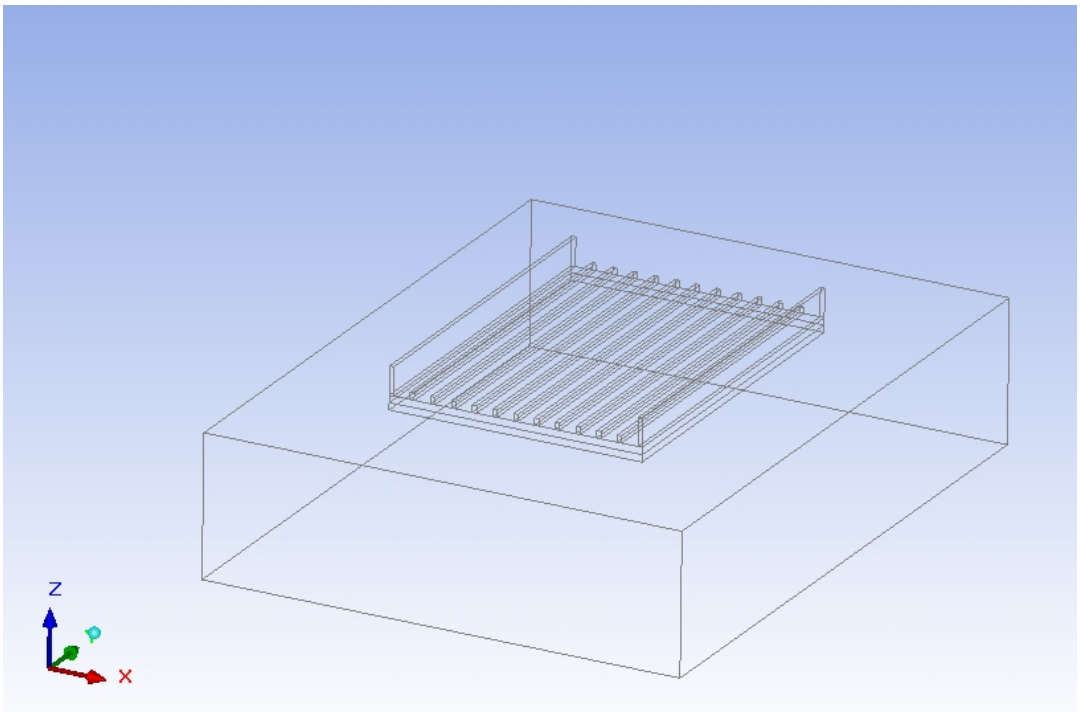

Figure 97 20 mm High End Fins Case

- Q_{source} to Concrete Block=24.857 W
- Q_{source} to Heat sink Base=99.7551 W
- Q_{Total} to Fluid of Heat sink= 99.7889 W
- Q_{rad} of Heat sink= 23.8868 W
- Q_{Total} to Middle Fins to Fluid= 38.8082 W
- Q_{rad} of Middle Fins= 8.54108 W
- T_{Mean} of Middle Fins= 151.241 ^{O}C
- A_{wet} Middle Fins= 0.03608 m^2
- A_{wet} Heat sink= 0.08789 m^2

Convection Heat Transfer from Heat Sink

Q_{conv} Heat sink =Q_{Total} - Q_{rad} = 99.7889-23.8868= 75.90 W

Heat Flux Values of Heat Sink

$q'' (W/m^2) = Q_{Total} / A_{Wet}$ = 99.7889 / 0.08789 = 1135.38 W/m^2

$q''_{conv} (W/m^2) = Q_{Conv} / A_{Wet}$ = 75.90 / 0.08789 = 863.60 W/m^2

$q''_{rad} (W/m^2) = Q_{Rad} / A_{Wet}$ = 23.8868 / 0.08789 = 271.78 W/m^2

Heat Transfer Coefficient of Middle Fins

Q_{conv} Middle Fins =Q_{Total} - Q_{rad} = 38.8082 – 8.54108= 30.27 W

$h = Q_{conv} /(A_{wet} .(T_{Mean} - T_{\infty})) = 30.27 / (0.03608 * (151.24 - 20) = 6.392 W/m^2K$